EVALUATION OF A METHODOLOGY FOR DETECTING RAILROAD TRACK GEOMETRY ANOMALIES AND DETERMINING RAIL VEHICLE FATIGUE LOADS

by

Brandon A. Schwarz

B.S., Mechanical Engineering
Northeastern University, 1987

Submitted to the Department of Civil and Environmental Engineering in partial fulfillment of the requirements for the degree of

MASTER OF SCIENCE
in Transportation

at the
Massachusetts Institute of Technology

May 1993

Signature of Author _____
Department of Civil and Environmental Engineering
May 7, 1993

Certified by _____
Carl D. Martland
Senior Research Associate
Department of Civil and Environmental Engineering
Thesis Supervisor

Accepted by _____
Eduardo Kausel
Chairman, Departmental Committee on Graduate Studies
Department of Civil and Environmental Engineering

EVALUATION OF A METHODOLOGY FOR DETECTING RAILROAD TRACK GEOMETRY ANOMALIES AND DETERMINING RAIL VEHICLE FATIGUE LOADS

by

Brandon A. Schwarz

Submitted to the Department of Civil and Environmental Engineering on May 7, 1993 in partial fulfillment of the requirements for the degree of Master of Science in Transportation

Abstract

An analytical methodology was developed by Allen (1992) for identifying track anomalies that can cause significant fatigue loads and estimating a freight car's dynamic response to those anomalies. The motivation for the studies described in Allen (1992) and in this report is the desire to predict freight car fatigue loading while the car is still in the design stage. The methodology finds all the track geometry anomalies that could cause significant fatigue loads, extracts these anomalies from the track data, uses them as the track input in computer simulations of the car response, and then determines the resulting fatigue loads. Mechanically, the methodology consists of six steps: vehicle modelling, track data analysis, threshold amplitude analysis, anomaly extraction, dynamic simulation, and fatigue load analysis. Studies were conducted with the purpose of evaluating and further developing the methodology. The work performed in these studies improves upon the second through fourth steps; track data analysis, threshold analysis, and anomaly extraction.

The ability to detect anomalies in a large set of track geometry data and the adequacy of the anomaly extraction technique were demonstrated. Detailed analysis was performed on three sets of track geometry data, totalling 328 miles. Case studies were performed utilizing two rail car models, a 70-ton box car called the paintspotter car and a three-platform articulated flat car.

These investigations identified several weaknesses in the original methodology. First, the technique for extracting the anomalies from the track data (called the threshold extension factor technique) did not guarantee that the anomaly segments were long enough to ensure accurate vehicle dynamic simulations. Second, the original methodology lacked a rational technique for determining the minimum anomaly amplitude that can cause significant fatigue loads. Third, the computer programs which embody the methodology were not adequate for processing large data sets. And, finally, the documentation of the methodology was incomplete.

As a result of these findings, several improvements were made to the methodology and computer programs. The anomaly extraction technique was changed to allow the user to prescribe the exact length of adjacent track to add to the anomaly segment. The technique also will automatically lengthen the anomaly, if necessary, to ensure that the geometry deviations at the end points of an anomaly segment are less than a specified

maximum. This technique guarantees that the dynamic simulation is not contaminated by fictitious transients. A rationale and a methodology was developed for determining the minimum anomaly amplitude that can cause significant fatigue loads. All the computer programs were modified to make them compatible with large scale data processing. And finally, the documentation was enhanced, including an update to the PFILT computer programs user's guide and a description of the filter used to determine the locations of the peaks in the track data, which was mentioned but not described in Allen (1992).

The methodology was found to have potential applications for track surface maintenance. Using the anomaly identification capability along with the ability to find the track location of the anomalies, a track maintenance schedule can be developed which guarantees that nowhere on the track does the car or track experience a load above a prescribed limit. Since only the anomalous length of track needs to be resurfaced, the cost savings over current resurfacing practice is potentially large. The technical benefits of this method are also potentially great since the larger loads which cause fast track and car component degradation are eliminated. Thus track maintenance scheduling cycles become longer.

Thesis Supervisors: Carl D. Martland
Title: Senior Research Associate

Professor David N. Wormley
Title: Professor of Mechanical Engineering

Acknowledgements

The work described in this thesis was made possible through the generous grants provided by the Association of American Railroads in their ongoing support for the MIT Affiliated Laboratory in the Center for Transportation Studies. I especially wish to thank Som Singh of the AAR technical staff at Chicago for all the support he provided.

I would like to thank the railroad, and the two people at that railroad, for providing us with all the track data which made this report possible.

I am very grateful to Professor David Wormley for giving me the opportunity to work on this project. It was because of this project that I was able to continue with my studies at the Center for Transportation Studies. I wish him all the best at his new position at Penn State University.

I am thankful for all the assistance and guidance John Allen provided during his transition from and my transition onto the project.

The most help in making this report possible was given by Carl Martland. Thank you Carl for everything that you have done. It was more than I ever would have asked for, and more than I ever would have expected. I am forever grateful.

Mom and Dad, my thanks are so great I can't possibly express them. Don't go anywhere, I still need you. (Oh, did I mention that I love you.)

To the clients and consultants from beautiful mountain I would like to express my gratitude for all the help, especially to George S., Juliette G., and Dr. Rubin.

I give extra special thanks to my friends in the dungeon: NikNikNikNik, Cheezhed, Dan, Camille, John, Scottie, E-Dub, Doc, and Duff. The two years we spent together at MIT was very special.

And now, Damn the anomalies - full speed ahead!

Table of Contents

Table of Figures

Table of Tables

1 Introduction

Freight cars must be designed to withstand the forces generated under normal operating conditions. Fatigue loads in freight cars are generated by the response of the cars to track irregularities and by train control actions. Large fatigue loads can cause component failure and possibly derailments, and well as rapid track deterioration. Field tests have shown that car and component fatigue lives are strongly influenced by a small number of discrete events which generate severe fatigue loads (Kalaycioglu and Tajaddini, 1988). This finding provides opportunities for prediction of car and component fatigue life, for better design of components, and for improvements in maintenance of track geometry.

An analytical methodology was developed by Allen (1992) for identifying track geometry anomalies that can cause significant fatigue loads and estimating a freight car's dynamic response to those irregularities. The motivation for the studies described in Allen (1992) and in this report is the desire to predict freight car fatigue loading while the car is still in the design stage. The methodology finds all the track geometry anomalies that could cause significant fatigue loads, extracts these anomalies from the track data, uses them as the track input in computer simulations of the car response, and then determines the resulting fatigue loads. The methodology is capable of detecting lateral and vertical track geometry anomalies. Using a mathematical model of a 70-ton box car, referred to as the paintspotter car in Kalaycioglu and Tajaddini, (1988), the methodology was verified by Allen (1992) over a small set of carefully chosen track anomalies.

Mechanically, the methodology can be broken up into six steps: vehicle modelling, track data analysis, threshold analysis, anomaly extraction, simulation, and fatigue load analysis. The work performed in this study focused on the second through fourth steps: track data analysis, threshold analysis, and anomaly extraction.

The methodology was implemented in PC-based computer programs. The NUCARS program (Blader and Klauser, 1989) is used to model the freight cars, to perform dynamic simulations of the vehicle-track interaction, and to predict fatigue loads. The three steps of the methodology focused upon in the research documented in this report are embodied in three computer programs, collectively called the PFILT programs (pronounced 'pea-filt').

A systematic method for identifying and extracting anomalies from a set of track data is presented in Allen (1992). The routine for identifying track geometry anomalies which can cause significant fatigue loads is referred to as threshold-based anomaly identification. The procedure searches through the data seeking the peaks which are associated with large variations of track geometry, then the data around the peaks are extracted. The extracted data is called an anomaly segment.

In Hamid, et al (1983) a track geometry anomaly is described as a displacement in track geometry lasting between 20 and 100 feet. But it is clear that not all of these variations are anomalies. To be an anomaly, a variation must deviate markedly from the common value, i.e. it must be a rare occurrence. Unfortunately this definition is loose since there is no agreement on what is rare and what is merely uncommon. Usually, the parameter which is measured and thus used as a criterion is the amplitude of the geometric variation of the track surface because it is easiest to measure and most obvious.

Indeed, other methods of attempting to classify, such as the shape functions proposed by Hamid, Owings, and Kenworthy (1982) or families proposed by Allen (1992), have proven too limited or cumbersome when attempting to apply the techniques to large numbers of anomalies taken from actual track data.

Considering the effects of vehicle dynamics, an anomaly has sometimes been defined as the smallest amplitude variation that can cause significant fatigue loads. This, of course, only substitutes the subjective "rare" for the just-as-subjective "significant." All track surface variations greater than this amplitude are then called anomalies, and those of lesser amplitude are just harmless irregularities. However, because the dynamic response of any one vehicle does not determine the boundary between "rare" and "not rare" for all vehicles, the track data analysis should be independent of vehicle dynamics.

Hence, there is no clear line between an anomaly and irregularity. In this report the term anomaly is applied to all the track surface variations that exceed a specified amplitude threshold, for simplicity and to indicate the type of variation we are looking for, i.e. the rare one. The value of the threshold is based upon the best judgement of the analyst.

The purpose of the research described in this report is to evaluate and enhance the overall fatigue load methodology. The ability of the methodology to adequately identify and extract anomalies from an extensive set of track data was demonstrated. The PFILT programs were evaluated and improved to allow the methodology to be applied to large volumes of track data.

Two major improvements to the methodology were realized: 1) A new anomaly extraction technique was developed and 2) a rational methodology for determining the

minimum anomaly amplitude that can cause significant fatigue loads was developed . These improvements were demonstrated in the analysis of 328 miles of track surface profile data and three case study applications of the methodology utilizing two sets of vehicle characteristics. This report also contains a complete description of the threshold-based anomaly identification methodology with detailed documentation of the discrete-time differentiating filter. This is an integral part of the threshold-based anomaly identification routine mentioned, but not documented, in Allen (1992).

There are components of the methodology which can be used to improve current track surface maintenance practices. Currently, railroads use statistical track surface roughness indexes to determine the condition of the track. These indexes typically measure the variance of track surface from the mean over a short segment of track of arbitrarily chosen length. The value of the variance is called the track quality index (TQI) (Roney and McIveen, 1991). When the TQI of a segment of track exceeds some limit determined by experience, the track surface has degraded. But, only when the TQI of a number of contiguous segments exceed the limit is the track resurfaced. The track segments are typically 500 ft long. Special track features such as switches, bridges and grade crossings are taken out of the data. There are limitations inherent in the current practice and costly surface maintenance practice is required to compensate for it. Track surface maintenance planning based on anomaly identification offers the possibility of improved track conditions at lower cost.

The new anomaly extraction technique and the rational methodology for determining the minimum anomaly amplitude that can cause significant fatigue loads are presented in Chapter 2. In Chapter 3, improvements to the PFILT programs are documented. These improvements include new abilities in data processing and reporting,

and implementation of the new anomaly extraction technique. The three track data analyses are presented in Chapter 4, and the three case study applications of the overall methodology are in Chapter 5. Conclusions and discussion follow in Chapter 6. Also in Chapter 6 is a discussion of the limitations of current maintenance practice and the applications and benefits of track surface maintenance based upon anomaly identification.

The work presented in Chapters 4 and 5 led to the developments presented in Chapters 2 and 3. The initial efforts were to apply the original methodology to a limited set of track data. Then, from the results of this study, the methodology was improved. Subsequent efforts used the improved methodology on a larger set of data. This cycle was repeated three times. Thus, the analyses and methodology evolved together. It was decided to present all the improvements to the methodology and the PFILT programs prior to presentation of the data analyses and case studies that led to these improvements so that the reader is familiar with the entire set of tools referred to in these chapters.

2 Improvements to the methodology

Significant improvements to the overall methodology were made in two areas: The development of a threshold amplitude analysis and a new technique for augmentation and extraction of anomalies.

The threshold amplitude analysis is the third step in the methodology, following the vehicle modelling and track data analysis. Threshold amplitude is defined as the smallest amplitude anomaly on the track that can cause significant fatigue loading in the rail car. Thus, the threshold amplitude is an essential relation between the vehicle and the track. Accurately determining its value is critical to finding all the anomalies that can cause significant fatigue loads, without including a great many anomalies that can not cause significant fatigue loads. In the Section 2.1 a methodology is presented for determining the threshold amplitude. It is a general procedure that ties together a specific vehicle traversing a specified track segment.

A new technique for augmenting and extracting anomalies was developed which replaces the previous technique. The new technique ensures that extracted anomalies are of sufficient length such that the transients associated with the start of a simulation settle down before the simulation reaches the anomalous track variation. The new technique is presented in Section 2.2.

2.1 A rational methodology for determining the threshold amplitude

The threshold amplitude is the critical link between the track data and the vehicle model. Threshold amplitude is defined as the smallest amplitude track anomaly that can cause a significant fatigue load. The threshold amplitude is neither a vehicle parameter

nor a track parameter, but a vehicle-track interaction parameter. To determine its value requires knowledge of the track anomalies, vehicle parameters, and the nature of the interaction between them. Finding the threshold amplitude is critical; a value too large and some anomalies that could cause significant fatigue loads may be missed; and an amplitude too conservative requires a large number of simulations over anomalies with no potential of causing significant fatigue loads. But amplitude of geometric variation is not the only concern. A factor which must be considered is the potential for repeated geometric variations within an anomaly. The stumbling block has always been measuring the repetitiveness, or potential repetitiveness, of the anomaly. The new methodology determines this potential.

2.1.1 Other methodologies proposed for determining the threshold amplitude

In Allen (1992), the threshold amplitude was chosen iteratively, i.e. by running simulations over a number of anomalies and finding the amplitude corresponding to the first occurrence of a significant fatigue load, or alternatively, by choosing a conservative value of threshold amplitude. Though the first approach requires many simulations and consumes much time and effort to identify a threshold value, it does not guarantee that anomalies of lesser amplitude will not cause significant fatigue loads. The second approach, choosing a conservative threshold amplitude, can guarantee that no anomalies which can cause significant loadings are missed, but the price of using this method is also high. For each 0.1 inch the chosen threshold amplitude is less than the maximum

allowable value, the number of anomalies increases by a factor of two. Given the time and effort required to extract anomalies and to run NUCARS, there is a strong incentive to select the threshold amplitude carefully.

Allen (1992) proposed a third methodology, whereby anomalies were arranged by family shape functions in an attempt to classify them. With vehicle response histories due to each family of anomalies known a priori, anomalies from new track anomalies could be classified by family shape, thus revealing the potential response. Unfortunately this method did not work, primarily because the shape of an anomaly depends heavily on the location of the end points. Many anomalies looked similar in the middle but different near the ends, and it was not possible to generalize the significance of these differences. Furthermore, many anomalies are similar in gross shape with small variations superposed. Again, it was not possible to measure the significance of these differences. This method of anomaly classification also requires that every anomaly be reviewed and classified, which becomes a lengthy procedure as the data sets increase in length. For these reasons, the family of anomalies classification system is not used.

2.1.2 The methodology for determining the threshold amplitude

A general methodology is presented below to determine the minimum anomaly amplitude that can cause fatigue loads in a car component to exceed a defined limit. The goal of applying this methodology is to reduce the number of anomalies that must be used in simulations to *only* those that could cause significant fatigue loads. The methodology eliminates the need to analyze 90 percent or more of all the anomalies and still ensures conservative results. The seven steps of the methodology are:

1) Identify the fatigue loads on the component.

2) Determine the car actions that cause fatigue loads.

3) Determine the worst-case scenario for the car actions, i.e. those situations that lead to the largest car actions and, hence, largest fatigue loads.

4) Identify and determine the values of the car and track parameters that put the car in the worst-case scenario.

5) Set up a parametric study of the worst-case scenario as a function of anomaly amplitude.

6) Run simulations on worst case scenarios to determine the peak fatigue load on the component until the results predict that the defined load limit was exceeded.

7) Define the threshold amplitude as that anomaly amplitude that first caused the load to exceed the defined limit.

Steps 1-4 are presented in order. Then an explanation of the rationale for steps 5-7 is presented. The remainder of the threshold amplitude analysis, steps 5-7, then continues with an example application.

STEP 1: The first step is to determine the type of fatigue loading that occurs on the component in revenue service. For example, a bolster transmits vertical loads between the car body centerplate and the truck spring groups. It carries no appreciable lateral or longitudinal loads nor any torques. It is susceptible to fatigue due to large vertical loads.

STEP 2: The next step is to identify the car actions which lead to fatigue loads. Continuing with our example, vertical loads on the bolster are caused primarily by bounce and pitch motions of the car body.

STEP 3: Sinusoidal track inputs produce harmonic bounce and pitch motions of the car body (Hartog, 1984). Increasingly large fatigue loads on the bolster occur as the response to a sinusoid grows at resonance. This is the worst-case scenario.

STEP 4(car): Next, the car body and truck parameters that most significantly affect the response are identified. In this case, the parameters which must be determined are the bounce and pitch natural frequencies and the truck center spacing.

STEP 4(track): The track parameters must be identified which most directly indicate that the track can cause the car responses that lead to significant fatigue loads. In this case, it is the amplitude of the anomaly and the repetitiveness of the geometric variation within the anomaly which are the primary variables. Improvements in the track anomaly analysis capabilities make it possible to determine these parameters (see Section 3.3).

Continuing with step 4(track), Allen (1992) identified anomalies by performing a window analysis at each peak in the track data. Multiple peak anomalies were found by connecting anomalies that occur at sequential peaks. The amplitude of a multiple peak anomaly is the amplitude of the largest single peak anomaly within the group. The greatest possible number of repetitions of track geometry variation within the anomaly corresponds to the number of peaks in an anomaly. For example, an anomaly with one or two peaks can have at most one cycle, i.e. no repetitions of variation. Anomalies with three or four peaks can have at most one repetition of variation, and so on by the relation

$$N = \text{int}[(\text{number of peaks}+1)/2] \qquad \text{eq. 2.1-1}$$

Where N is the maximum possible number of cycles of geometric variation within the anomaly. Although nothing is known about the actual number of repetitions of variation with this analysis, the limits of an anomaly's repetitiveness is known.

The distribution of the number of peaks versus anomaly amplitude is produced by grouping the anomalies together that fall within defined ranges of amplitude and determining the number of peaks in every anomaly within the group. Each group of anomalies has associated with it one anomaly with the maximum potential number of cycles variation. The envelope of the potential number of cycles is the distribution of the maximum potential number of cycles over all the groups. It is not possible for any anomaly on the track to be more repetitive in geometry than the limits defined by this envelope, but this is too conservative an estimate to be used in the threshold analysis.

Track anomaly classification by amplitude and number of peaks was performed on 305 miles of track profile data. Table 2.1.2-1 lists the number of anomalies in each amplitude range, further divided by the number of peaks and potential cycles. The threshold value used to identify *all* the anomalies in this study was 0.5 inch.[1] This tends to maximize the number of peaks in anomalies, thereby making the interpretation of potential cycles conservative.

---

1 A 0.5 inch peak to peak amplitude variation is the smallest amplitude variation associated with spring bottoming or centerplate separation in 70-ton rail cars due to continuous repeated profile anomalies in analytical studies conducted by Schwarz, et al (1988).

Another approach considered to create the distribution of anomaly amplitude versus number of peaks was to perform an anomaly identification analysis at the lower bound of each amplitude group and extract only those anomalies within the group amplitude. As shown in Section 4.3, this approach does not work because the resulting distributions have few multiple peak anomalies.

Peaks	Max Cycles	Amplitude groups (inclusive on lower limit) (inch)						
		.5-.6	.6-.7	.7-.8	.8-.9	.9-1	1-1.1	>1.1
1	1	319	63	14	2	2		
2	1	87	82	43	17	8	1	
3	2	3	14	15	11	4	2	
4	2	2	7	13	8	3	2	
5	3	1	2	5	4	1	1	1
6	3	1	1	3	3	2	2	1
7	4		2			1	1	1
8	4		1			1		
9	5							
10	5				1	1		1
total #		413	172	93	46	23	9	4
% included		98%	97%	97%	98%	96%	100%	100%
# excluded		7	6	3	1	1	0	0

Table 2.1.2-1 Distribution of number of peaks and cycles of anomalies in 305 miles of track data

The line traversing the table marks the limit of the distribution encompassing the vast majority of anomalies. A general goal for this distribution is to include 90% to 95% of all the anomalies, thereby leaving less than 10% of the total anomalies to be considered individually. The outlier anomalies, those outside the limits of the distribution, are extracted and simulations are run over each one individually. The distribution in the Table 2.1.2-1 was developed by applying the following simple criteria to each group of anomalies: The line at each group is the largest number of peaks for which there are four or more anomalies, or 5% or more of the total anomalies. The rows of data at the bottom of the table show the percent of anomalies encompassed and the total number of anomalies exogenous to the distribution in each group. Of the 760 anomalies, 98% are included within the distribution (only 18 anomalies are outliers). The resulting characterization of the track by this distribution of the anomalies is given in Table 2.1.2-2

Anomaly Amplitude Range (inch)	Max. Potential Number of Cycles
$0.5 \leq A \leq 0.6$	1
$0.6 < A \leq 0.7$	2
$0.7 < A \leq 0.8$	3
$0.8 < A \leq 0.9$	3
$0.9 < A \leq 1.0$	4
$1.0 < A \leq 1.1$	4
$A > 1.1$	5

Table 2.1.2-2. Characterization of 98% of anomalies in 305 miles of track data.

The threshold analysis is a tool designed to characterize the *vast majority (90-95%)* of the track anomalies for the ultimate purpose of allowing the analyst to identify all the anomalies that could cause significant fatigue loads and, very importantly, *to ignore the great percentage of anomalies which have no potential of causing significant fatigue loads.* Outlier anomalies are extracted from the track data for individual car-track interaction simulations.[2]

STEP 4(car & track): The two parts are put together: the worst-case input parameters from the vehicle and the worst-case amplitude and potential number of cycles from the track anomaly analyses. A sinusoidal track input produces the worst-case harmonic response (step 3), and the maximum number of cycles of variation versus anomaly amplitude is known (step 4-track).

The correct car speed and sinusoid wavelength are chosen to match the bounce and pitch natural frequencies of the car (step 4-car) to put it in a resonant condition (step 3). Speed (V), wavelength (λ), and natural frequency (f_n) are related by $V = f_n \lambda$ over a

2 Outlier anomalies are rare in amplitude of variation and number of peaks, and very lonely.

sinusoidal track input. The bounce and pitch natural frequencies can be determined from the vehicle model and the wavelength is related to the truck center spacing, thus the car speed for the simulations is determined. All the track segments and car parameters have been defined and analytic simulations can now be run to determine the threshold amplitude (steps 5-7).

Before continuing with the threshold analysis, the rationale supporting steps 5-7 of the methodology for determining the threshold amplitude is shown. The methodology puts the car in the worst case conditions and the track is assumed to provide the worst-case input at each the amplitude considered. Therefore, as soon as the idealized track input can produce a significant fatigue load, the anomaly amplitude associated with that track input is the threshold amplitude. To demonstrate the rationale, the following analysis was performed for a 70-ton articulated flat car (defined in Appendix B) in the worst case scenario on the track defined above.

First, the minimum peak-to-peak amplitude of a sinusoidal track profile variation to cause a significant fatigue load on the bolster is determined. Results are found for traversal of one, two, three, and four cycles of sinusoidal input. A significant load factor was defined as a dynamic-to-static load ratio of 1.5 or greater. The results of this study are given in Table 2.1.2-3

Number of Cycles of sinusoidal track profile variations	Amplitude to cause significant fatigue load (inch)
1	1.14
2	0.69
3	0.57
4	0.52

Table 2.1.2-3.
Peak-to-peak amplitude of a sinusoidal track profile variation to cause significant fatigue loading on the articulated flat car.

Next, the characterization of the track anomalies (Table 2.1.2-2), and results giving the amplitude of sinusoidal variation to cause a significant fatigue load (Table 2.1.2-3), are cross plotted in Figure 2.1.2-1. The curve descending from left to right is the boundary defining the minimum amplitude sinusoid to cause a significant fatigue load versus the number of cycles of the sinusoidal variation. All points below this curve are of track that cannot cause significant fatigue loads.

Next, solid circles are drawn at the upper limit of anomaly amplitude versus number of cycles for each range of amplitude from Table 2.1.2-2. For example, there are solid circles at (0.6,1), and (0.7,2). Then, open circles are drawn at the points corresponding to the lower anomaly amplitude and number of cycles for each range of amplitude, i.e. (0.6,2) and (0.7,3). The lower and upper boundary point of each range is connected by a solid line and dashed lines are drawn down to zero amplitude.

As shown in the figure, 0.5 to 0.6 inch anomalies on the track have, at most, one cycle of variation, but 1.14 inch amplitude is necessary to cause a significant bolster load over one cycle of a sinusoid. Therefore, no anomaly on this track with amplitude less than 0.6 inch can produce a significant bolster load. The threshold amplitude is found at the first intersection of two lines. Two solid lines cross at two cycles of variation, where

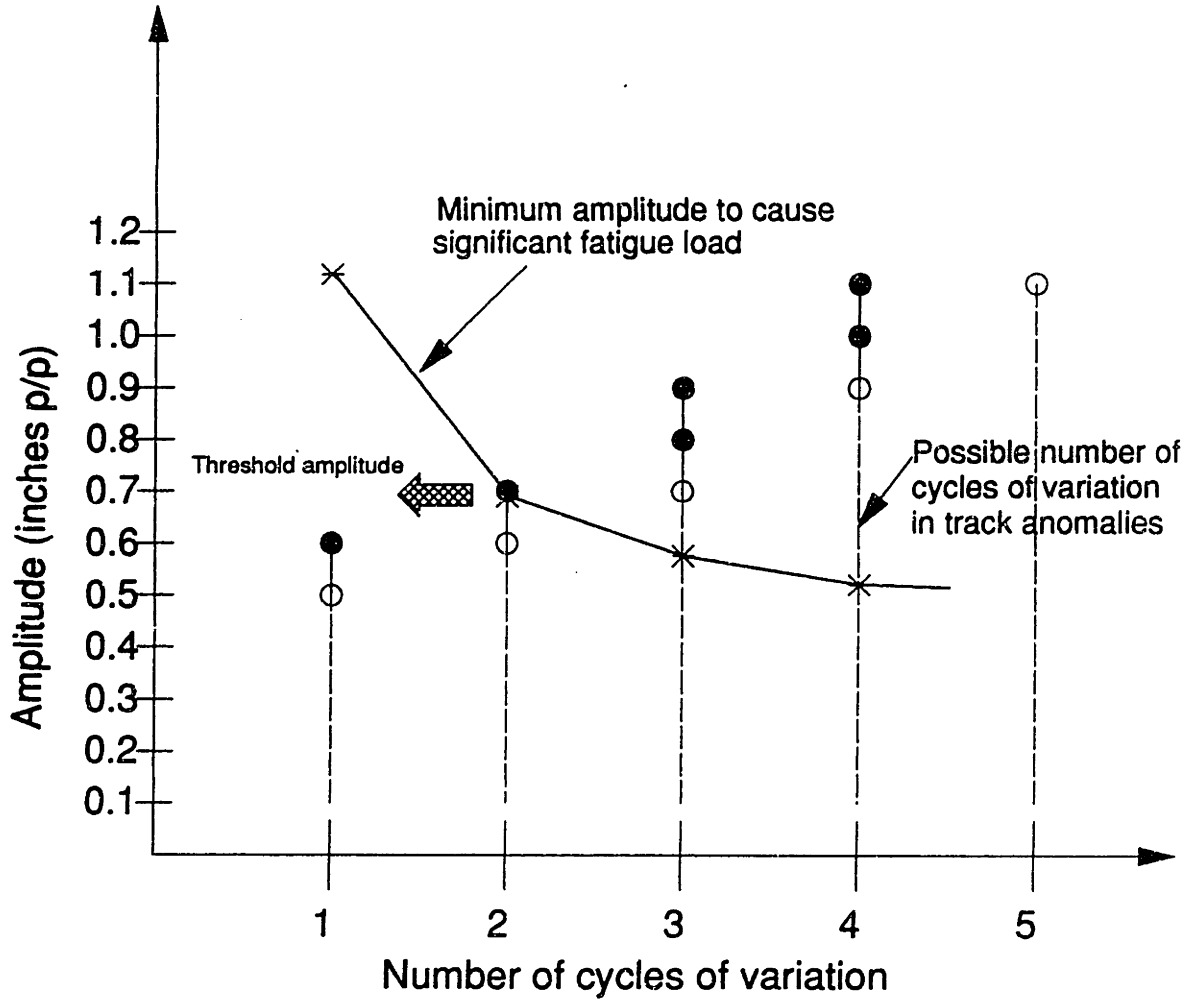

Figure 2.1.2-1. Rationale for the theshold analysis

the minimum amplitude to cause a significant fatigue load is 0.69 inch, and the anomaly amplitude range between 0.6 and 0.7 inch. The threshold amplitude is the point where these two solid lines intersect. (An approximate value of 0.7 was used for the threshold amplitude in the case studies.) If the first intersection is between a solid and a dashed line, the threshold amplitude is found by tracing upwards from the point of intersection to the lower amplitude boundary of the range, i.e. the open circle.

Steps 5-7 of the threshold amplitude analysis for the articulated flat car and the 305 mile long track data set are presented below. The articulated flat car is illustrated and lists of the mass, spring stiffnesses, and the associated linear system natural frequencies at each of the trucks are given in Appendix C.

STEP 5: The possible number of cycles at each anomaly amplitude was given in Table 2.1.1-2. A bounce natural frequency of 2.3 Hz was estimated from the vehicle parameters. It is not possible to put the car into a pure bounce or pitch mode due to the different natural frequencies and truck center spacings. However, a 50 foot wavelength sinusoid is approximately equal to the truck center spacing and, for a natural frequency of 2.3 Hz, the speed corresponding to bounce resonance is 78 mph. These were taken as the critical values of the parameters in the threshold analysis.

Track segments were created of a sinusoidal profile variation with a 50 foot wavelength, one segment for each amplitude range in Table 2.1.2-2. The amplitude of each track segment was equal to the upper bound of amplitude of the range, and number of cycles of variation was equal to the maximum number of cycles in that amplitude range.

STEP 6: Simulations were run using the NUCARS program to determine the bolster load that occurs as the vehicle traverses the track segment. The load ratios were then calculated and the results presented in Table 2.1.2-4. Only one simulation at each anomaly amplitude is required. The fatigue loads occurring in each simulation are found.

STEP 7: The amplitude of the sinusoid for which the fatigue load in the simulation first exceeds the defined significant value is the threshold anomaly amplitude. The load ratio first exceeds 1.5 at an anomaly amplitude of 0.7 inch, therefore 0.7 inch is the threshold amplitude.

Amplitude (inch)	#cycles	Load ratio	Threshold Amp (inch)
0.5	1	1.10	
0.6	1	1.23	
0.7	2	1.51	*(0.7 inch)
0.8	3	1.99	
0.9	4	(not necessary	
1.0	4	to run	
1.1	5	simulations)	

Table 2.1.2-4. Threshold analysis results for articulated flat car and 305 miles of track data.

No anomalies with amplitude less than 0.7 on this track in the 98 percentile distribution can cause significant fatigue loads (>150% of static load) on this vehicle. The outlier anomalies below the threshold amplitude may be able to cause significant fatigue loads and therefore, are extracted from the track data for simulations. The result of this threshold analysis is valid for any vehicle that can be characterized by the same natural frequency and truck center spacing to track variation wavelength ratio, over any track with the same anomaly characterization. The overall methodology to determine the fatigue life of the component can proceed to the next step, extracting all the anomalies with amplitudes greater than 0.7 inch. Using a threshold amplitude of 0.7 inch, only 161 anomalies are found, which is less than one mile of track in 305 miles. If a more conservative value of threshold amplitude, such as 0.5 inch had been chosen by a more conservative approach, a total of 760 anomalies would have to have been considered.

The analysis to determine threshold amplitude is quite efficient especially when compared with previous methods suggested. It captures all the anomalies that could cause significant fatigue loads, while eliminating the vast majority of relatively harmless anomalies, so that the number of anomalies that need be considered is manageable. In the example presented in this section, there were originality 760 anomalies to consider, using a 0.5 inch threshold amplitude. Applying the methodology to determine the threshold amplitude reduces the number of anomalies to consider to 174 (161 anomalies greater than 0.7 inch and 13 outlier anomalies less than 0.7 inch). This is a reduction by a factor of 4.4 in the number of anomalies that need to be considered. On a 486/50-PC a typical NUCARS simulation takes 13.5 minutes. This reduction saves 132 hours in NUCARS simulation time if a simulation is performed for every anomaly just once. And the additional time to set-up and evaluate the simulations has not been considered. The NUCARS simulation time to determine the threshold amplitude was approximately one hour to perform four simulations.

Generally, the methodology is straight-forward and logical which tends to maximize its applicability, however, rail vehicle dynamics are complex and there may be many situations where worst-case responses, inputs, and scenarios are not readily identifiable. The efficiency and accuracy of this methodology may depend upon the component that is being studied.[3]

---

3 Any methodology of determining the threshold amplitude requires that the car body and truck parameters that are primary in determining the dynamic response be identified and calculated, regardless of the ensuing steps. Therefore, the efficiency and accuracy involved in determining these parameters need not be considered in evaluating this particular methodology.

It is the analysis of the track data that complicates the analysis. Track data is random. There are many of analysis techniques, such as Fourier series approximations, shape functions, etc, that could be used to attempt to classify the track appropriately, i.e. finding the potential of the track to produce harmonic inputs to the vehicle. The two variables that most directly effect harmonic response are the amplitude of the variation and the number of cycles of input.

The methodology developed takes advantage of the anomaly identification routine to judge the potential for repeated variation within the anomaly. An anomaly isolated on the track, having only one or two peaks cannot have a repetitive shape. If the anomaly has more than two peaks, i.e. a multiple peak anomaly, then there is the potential for repeated variations. This, of course, does not mean that there are repeated geometry variations in the anomaly, only that there may be. Since multiple peaks anomalies are put together with an existing algorithm it was not difficult to add the ability to count the number of peaks in each anomaly. Thus, all the information necessary to characterize the potential harmonic content of every anomaly can be found. This approach is quite efficient compared to the calculation intensive methods such as Fourier series approximation and labor saving and less ambiguous compared to family shape classification schemes.

2.2 A new technique for augmenting and extracting anomalies

The anomaly segment is the key section of track to identify, but it does not stand alone. If simulations were run by placing the front wheels of the lead truck on the end of the anomaly and progressing, accurate results could not be expected due to initial condition transients and because the potential effects of adjacent track variations are

ignored. The other extreme is to run the simulation over the entire length of track. While this would assure an accurate simulation over the anomaly, it is unnecessary and the time required to do so, on a 486-PC, is prohibitive. Thus, a sufficient but not excessive length of adjacent track data is desired around the anomaly segment. The augmented length of track around an anomaly should be long enough to ensure that initial condition transients settle before the model encounters the anomaly segment, and that the effect on the car response of the neighboring track is considered, but not so long as to result in excessively long simulations.

Two methods of extending the anomaly have been developed: the threshold extension factor (Allen, 1992), and the method of adding track lengths. The threshold extension factor assumes that the track in the neighborhood of an anomaly is significant to the dynamic response only if it has a geometric variation of at least a defined amount proportional to the anomaly amplitude. The method of adding track lengths allows the user to define the precise length of track by which to augment the anomaly.

The threshold extension factor augments anomalies by connecting adjacent sections of track which exceed a defined percentage of the anomaly amplitude. Essentially, this is an anomaly identification analysis for a lower amplitude, performed at the ends of the anomaly. The rationale for this approach is that it allows the inclusion of sections of track that could make a significant load contribution by looking for large amplitude variations in the immediate vicinity of the anomaly. But the threshold extension factor is biased towards a specifically shaped anomaly, namely the sinx/x form presented in Hamid et al (1983). There is no rationale for seeking this shape of anomaly while

potentially neglecting all others. Thus, a limitation of the threshold extension factor is that it does not guarantee inclusion of *all* sections of adjacent track that could have a significant effect on the accuracy of the simulation.

Furthermore, the threshold amplitude is defined as the smallest track geometry variation that can cause a significant fatigue load. And defining the threshold value is quite difficult (a methodology is presented in Section 2.1.2). It is impractical, perhaps impossible, to define a *useful* sub-threshold value that identifies all the neighboring track that, when appearing with any anomaly, can significantly effect the dynamic response of the car.

Concern in augmentation is not the amplitude of variation of adjacent track nor the shape of that track, but to make the state of the simulated vehicle upon entering the anomaly segment as close to the actual state of the car as it traverses the anomalous track. This involves eliminating fictitious transients that occur at the initiation of a simulation and letting the vehicle respond to the actual track data immediately prior and following the anomaly segment. To do these tasks a more general technique to augment anomalies is necessary.

A simple and direct technique was developed. The anomaly is augmented based upon a defined length of track necessary to assure accurate simulations over the anomalies, accounting for the potential cycles of repeated variation, and for the time required to run a simulation. The minimum length to augment an anomaly by in order to ensure that any fictitious transient that occurs in the vehicle due to the initial conditions of the simulation (including the effects of the spline curves) is approximately equal to that length for which the impulse response due to the first data point in the augmented

track has significantly dissipated. For a typical freight car, one cycle of response is enough to sufficiently dissipate the transient response. The minimum length of the augmentation segment is determined once the speed of the simulation is set.

Another factor to consider is that the threshold amplitude of the extracted anomalies is greater than the baseline amplitude used in the threshold amplitude analysis. And, as the threshold amplitude increases, the number of peaks in an anomaly decreases. Therefore, number of peaks distributions at larger threshold amplitudes are skewed towards lower values. In Table 2.2-1 the distributions for the 305 mile set of track data using 0.5 inch and 0.7 inch threshold values are listed. In each group the number of cycles has been reduced by one cycle. To compensate for this potential loss of significant information the anomaly should be augmented by at least a half-window length of data at both ends.[4]

Anomaly Amplitude Range (inch)	Number of Cycles 0.5" threshold	Number of cycles 0.7" threshold
$0.7 \leq A \leq 0.8$	3	2
$0.8 \leq A \leq 0.9$	3	2
$0.9 \leq A \leq 1.0$	4	3
$1.0 \leq A \leq 1.1$	4	3
$A > 1.1$	5	4

Table 2.2-1: Comparison of bulk track characterization at 0.5 inch and 0.7 inch threshold of 305 miles of track profile data

4 The half-window length is the parameter that defines the upper bound of length of track variation of an anomaly in the anomaly identification analysis of Allen (1992). Hamid et al (1983) define an anomaly as a variation in track geometry with a duration of between 20 and 100 feet. Thus, the half-window length is between 10 and 50 feet. The studies conducted here and in Allen (1992) use a half-window length of 39 feet.

Finally, time of simulation must be considered. On a 486/50-PC the NUCARS simulations progress at 26.3 ft/min. Thus a 40 foot track length addition (80 feet total length increase to the anomaly) increases simulation time by approximately three minutes. A typical anomaly with just spline curves attached is about 250 feet in length, and takes about 9:30 to run. Thus a track length addition of 40 feet represents a one-third increase in simulation time. The total time to perform all the simulations using this method is 30 percent of the time to perform simulations over all the anomalies, since the number of simulations is reduced by a factor of at least 4.4, and the time to execute each simulation is increased by a factor of 1.33.

Generally the end points of the augmented segments are non-zero in value. However, a constraint of the NUCARS simulations is that they must start with zero initial conditions. Thus, some method must be used to transition from the zero initial conditions to the end points of the augmented segments.[5] The method of spline fits (Appendix A) provides a good way of making the transition from the zero initial conditions to the end points of the augmented anomaly segment. To further ensure against inaccurate simulations, this method was improved upon by controlling the magnitude of the end points of the augmented segment, thus preventing the occurrence of excessively large end points relative to the anomaly amplitude. Track data is added, one data point at a time, to the augmented segment until the magnitude of the end point is less than the specified maximum or until a specified length of track has been added. The spline fit is then added to complete the segment.

---

5 Ramping down at the end of the segment is not required for single anomaly runs, but there exists the option of connecting two or more segments to condense the number of simulations and, in this case the ramp down is required.

A rationale for defining the end point magnitude is necessary. The end point amplitude should be a magnitude that offers little probability of affecting the response over the anomalous section, i.e. of causing an appreciable dynamic response. The magnitude of response is generally proportional to the amplitude of the anomaly. Since the threshold value is the smallest amplitude of variation that can cause a significant fatigue load, making the end point amplitude a small percentage of the threshold amplitude guarantees the criteria is met.

3 Improvements to the PFILT computer programs

The PFILT programs were updated to perform the tasks required by the updated methodology and for application to larger sets of track data. A computer program was created for preprocessing data incompatible with the format required by the PFILT programs. This program is described in Section 3.1. Section 3.2 describes the changes made to the PFILT programs to disable the threshold extension factor and to incorporate the new technique for augmenting and extracting anomalies. In Section 3.3, the changes made to the programs are described which allow for processing large volumes of data and to calculate and report anomaly statistics which can be used to derive the distributions of number of peaks versus amplitude and also to locate the anomalies on the track.

Computer program usage is described in the PFILT users guide in Allen (1992) and the PFILT user's guide supplement in Appendix A.

3.1 Preprocessing data with track location information

Three sets of data were acquired. The first two sets were three and twenty miles long, respectively. And, although the format of the raw data was not compatible with the PFILT programs, only very simple preprocessor programs were created because of the short lengths and the goals of the analysis using these data sets required only the profile data. The preprocessor programs created for theses two data sets merely stripped all the data except the left and right track profile data from each field leaving two column ASCII data files.

The third set of data acquired was also in a format incompatible with the PFILT programs. The programs require each variable to be in its own column separated by blank spaces. The raw data violated this format in the milepost and feet fields. Figure 3.1-1a shows a sample of a raw data file. From left to right the columns of data are location (milepost+feet), left rail profile, right rail profile, track curvature, and superelevation. It is clear from the figure that the "+" between the milepost and feet data violates the format conditions required by the PFILT programs.

A computer program was written whose primary function was to convert the raw data into a compatible format. The program, PREPROS, is a preprocessor which reads each record, separates the milepost and feet fields, ignoring the "+", and rewrites the data to a new file with milepost and feet each in their own columns separated by blank spaces, as shown in Figure 3.1-1b.

Taking advantage of the preprocessor reading every record in the file, other capabilities were built into the program. Data files can be of any length and can start and end at any point on the track. It is sometimes useful before beginning the PFILT analyses to know such information as the beginning and end locations of the data, the length of the track segment contained within the file, and the number of records in the data file. The preprocessor automatically performs the necessary calculations and reports this data to the screen. The start and end locations and number of records are correctly reported. The length of track in the file is reported but it is not necessarily correct. The program has been written assuming there is one record for each foot of data. This was done because all the track analyzed in the following studies were sampled at one foot per sample. To

add the option to the preprocessor where the user would input the data sample rate manually, would have slowed the processing of the data unnecessarily. Adding this option to the preprocessor program is a simple task should the user find it desirable.

Input Filename: **DIAMON.RAW**

```
LOCATION LPROF RPROF CURVE SUPER

13+5486 .0513  1250 .1700 0.000
13+5485 .0738 .1287 .1700 0.000
13+5484 .0863 .1450 .1800 0.000
13+5483 .0987 .1612 .1800 0.000
13+5482 .1112 .1700 .2000 0.000
13+5481 .1213 .1712 .1800 0.000
13+5480 .1238 .1587 .2000 0.000
13+5479 .1188 .1387 .2000 0.000
13+5478 .1188 .1162 .2000 0.000
13+5477 .1200 .1200 .2000 0.000
13+5476 .1262 .1325 .2000 0.000
13+5475 .1400 .1350 .1800 0.000
  .    .    .    .    .
  .    .    .    .    .
  .    .    .    .    .
```

INPUT
(RAW DATA)
ASCII file

Output Filename: **DIAMON.TXT**

```
13 5486  0.0513  0.1250  0.1700  0.0000
13 5485  0.0738  0.1287  0.1700  0.0000
13 5484  0.0863  0.1450  0.1800  0.0000
13 5483  0.0987  0.1612  0.1800  0.0000
13 5482  0.1112  0.1700  0.2000  0.0000
13 5481  0.1213  0.1712  0.1800  0.0000
13 5480  0.1238  0.1587  0.2000  0.0000
13 5479  0.1188  0.1387  0.2000  0.0000
13 5478  0.1188  0.1162  0.2000  0.0000
13 5477  0.1200  0.1200  0.2000  0.0000
13 5476  0.1262  0.1325  0.2000  0.0000
13 5475  0.1400  0.1350  0.1800  0.0000
 .  .     .     .     .     .
 .  .     .     .     .     .
 .  .     .     .     .     .
 .  .     .     .     .     .
 .  .     .     .     .     .
```

OUTPUT from preprocessor
Same filename as input file with .TXT extension (ASCII text file)

FIGURE 3.1-1: Sample of input and output files for PREPROS.

3.2 Implementing the improved technique for augmenting and extracting anomalies

Anomaly augmentation and extraction is the process by which track anomaly segments are properly removed from the track data for use as input to NUCARS simulations. There are two parts to the process: including adjacent track data and adding spline fits. Both of these have been changed in the PFILT programs.

In the previous version of the PFILT programs, the first task was given to the threshold extension factor routine in the PFILT program, and the second task was automatically performed by the VUTRACK program when the anomaly was extracted. The threshold extension factor technique, however, is not an anomaly augmentor. The rationale for its use in PFILT was that it was an anomaly completer, i.e. it looked at the edges of an anomaly for variations in geometry that competed a particular shape, namely sinx/x. The practical problems which make using the threshold extension factor difficult were described in Section 2.2. One of the major limitations of this approach for use as an anomaly augmentor was that there was no precise control over the ability to add track data around the anomaly. Because the threshold extension factor led to unpredictable results it was disabled and the new technique, described in Section 2.2 was added to the VUTRACK program.

In the new version of VUTRACK, the user is given complete control over the length of track to add around both sides of an anomaly. When the anomaly is extracted, track data of the length specified is added to the end points of the anomaly. Then the spline curves are added from the end points of the augmented anomaly segment.

The spline fit method of transitioning from zero initial conditions to the end points of the anomaly is satisfactory, but the magnitude of the end points on some anomalies can be large (greater than 50%) with respect to the anomaly amplitude. For these reasons, control was placed on the magnitude of the end points of the augmented segments in the VUTRACK program. The control scheme is as follows; if the end point of the segment exceeds the defined allowable magnitude, then the segment is extended by one data point and the test is performed again until either the data point magnitude meets the criteria or a specified length of data has been added. Once the test is completed, the spline curve is added and the anomaly is extracted. The user defines the maximum amplitude of the end point of the anomaly as a percentage of the anomaly amplitude and also the length of track to search and add to the anomaly if the end point does not fall below the specified minimum.

The updated VUTRACK program performs the complete anomaly augmentation and extraction: track length addition, end point control, and adding spline fits, before extracting the anomaly. The user controls the key parameters. Default values are a 39 foot rail length, 1 rail length augmented to each end of the anomaly, end point maximum magnitude is 33% of the threshold value, and up to 1 rail length of data added in the end point magnitude test.

3.3 Miscellaneous changes to the PFILT family of programs

A number of other changes were made to the programs in response to different requirements. All the programs were modified to accept command line inputs. This was done to facilitate batch file executions for processing large amounts of track data efficiently, such as the 305 mile data set in Section 4.3. The previous versions, using

interactive input, made this task impractical. The ability was added to determine the milepost and feet location at the start and end of each anomaly. This has very important implications in verifying the methodology, its implementation, and in maintenance practice and procedures. An anomaly summary file is created by PFILT which gives a list of information about each anomaly found. The graphics in VUTRACK were improved and control over the anomaly extraction was added. The threshold extension factor was disabled in PFILT. These changes are described in greater detail in the following paragraphs.

The primary function of DSTREAM is to find the peaks in the data, its secondary function is to create a separate binary file for each column of data in the input data file to facilitate I/O operations in PFILT and VUTRACK. The program was updated to include the option of creating binary data files for the milepost and feet columns in the data so that it is possible to determine the location of an anomaly. DSTREAM requires entering seven variables to execute. The previous version of the program allowed only interactive input to the program which severely inhibited batch file processing of large data sets. Great benefit was gained by adding the capability of command line inputs to this program.

PFILT is the heart of the anomaly detection routine. Its primary function is to find and record the start and end points of all the anomalies. For each anomaly, the program now calculates its peak-to-peak amplitude, the number of peaks in the anomaly, the length (in feet assuming 1 ft/sample), and locates the beginning and end points milepost and feet locations. Note the threshold extension factor variable in the data structure utilized by both PFILT and VUTRACK was removed, thus making previous versions of

PFILT incompatible with the current version of VUTRACK.

The new version of VUTRACK was given the new anomaly augmentation duties as described in Section 3.2. The graphic display of anomalies was updated. Updated graphics consist of a display of each component of the extracted anomaly segment. The spline fits are shown in white, the augmented track segments in yellow, and the anomaly segment in magenta.

4 Analysis of track surface profile data

The goal of the data analysis was to determine the character of the track. Specifically, this meant determining the distribution of anomalies by amplitude and determining the repetitive nature of anomalies as a function of amplitude. Data was acquired over the course of the year in three sets, and the analysis capabilities improved as the year progressed. Thus, the scope of analyses and results differ from the first data set to the third.

Data set 1 is three miles of data separated into three-one mile sections of very anomalous track. Data set 2 is a 20 mile section of continuous track data used to help develop the ability to process large data sets. Data set 3 is 305 miles of track data in seven continuous sections. The most detailed study is performed on data set 3.

The distribution of anomalies by amplitude gives an indication of the quality of the track. The first two data sets are relatively short and the anomalies were classified by range of amplitude. For the third data set, this approach was found impractical and would become more so with ever larger sets of data. Instead the distribution was formed by counting the total number of anomalies exceeding a given amplitude. Both methods produced similar distributions.

The total number of anomalies exceeding each anomaly amplitude was found in all three data sets. This is important in estimating the time required to perform a fatigue analysis at a particular threshold value. As will be shown, it also provides a great incentive to carefully select the threshold value.

The repetitiveness of anomalies, i.e. number of peaks as a function of amplitude is found in data set 3. The original motivation for this study was the concern that there might be small amplitude, multiple-peak anomalies that can cause large dynamic responses, thus driving down the threshold amplitude. The ability to perform this analysis was instrumental in the development of the rational threshold amplitude methodology presented in Section 2.1.

4.1 Data set 1: three-one mile segments of track data

The first data set consists of three miles of track geometry. The set is divided into three approximately one mile long segments, referred to as the Margo, Montjoli, and Rivers segments, from disparate locations. As will be shown in the analysis that follows, it appears that each segment was chosen because it is particularly anomalous track in three ranges of traffic (light, medium, and heavy). Annual traffic on the Montjoli, Margo, and Rivers segments are 3MGT, 10MGT, and 35MGT, respectively.

Data included in each file consists of left rail profile, right rail profile, milepost and feet. The data is from track sampled at one foot per sample.

The data came in a form different from the format compatible with the PFILT programs so a simple preprocessor program was created and used to adjust the data format. Then the three data files (one for each segment) were analyzed for anomalies using DSTREAM and a number of PFILT executions. DSTREAM need only be run once for each file as it finds all the peaks in the data with no criteria for amplitude. PFILT must be run once for each anomaly amplitude, thus it was run seven times for each file to obtain the following results.

Figure 4.1-1 shows the distribution of anomalies from 0.5 inch peak-to-peak through values greater than 1.1 inches peak-to-peak.

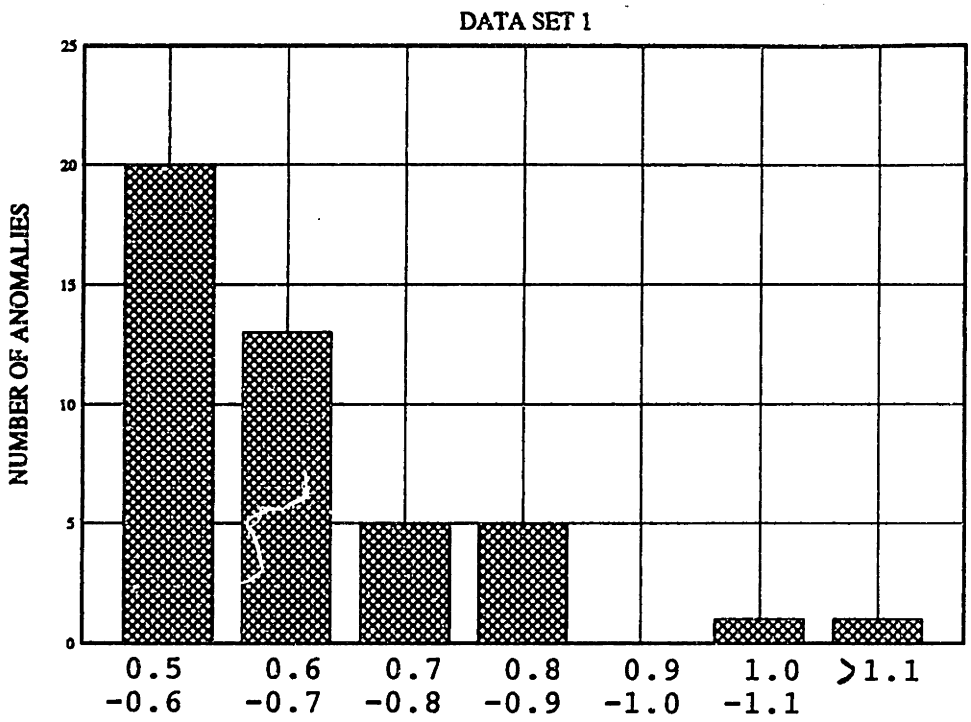

FIGURE 4.1-1. Anomalies identified on three mile long data set.

The figure shows the number of anomalies within each 0.1 inch range of amplitude. A total of 45 anomalies were found. Table 4.1-1 lists the cumulative number of anomalies exceeding each amplitude.

	Maximum amplitude of anomalies (inch)						
	0.6	0.7	0.8	0.9	1.0	1.1	>1.1
Cumulative number of anomalies	45	25	12	7	2	2	1

Table 4.1-1. Cumulative distribution of anomalies in data set 1.

Notice that for each 0.1 inch increase in amplitude the total number of anomalies decreases by approximately one-half. Using the first two data points (45, 25) one finds the exponential $n = 15\exp[-5.9(a - 0.5)]$ to reasonably approximate the distribution of anomalies. The coefficient of 15 is the total number of anomalies (45) divided by the length of the track data (3 miles), i.e. the average number of anomalies per mile of track.

Comparing the segments to each other one finds that 24 of the 45 anomalies occur on the Montjoli segment, 19 on the Margo segment, and 2 on the Rivers segment. Complete tables of anomaly amplitude are given in Appendix C.

The largest amplitude anomaly occurs on the Margo section (1.115 inches). The next five largest anomalies all occur on either the Rivers or Montjoli segment, see Table 4.1-2. This table lists the largest 12 anomalies, i.e. all anomalies with amplitudes greater than 0.7 inch. Of this anomaly subset, the Montjoli segment has only 4 anomalies (1/6 of the total greater than 0.5 inch), whereas the Margo segment has 6 anomalies (1/3 of the total), and both Rivers segment anomalies are greater than 0.7 inch. Thus, Rivers retains the highest proportion of anomalies as anomaly amplitude increases and Montjoli retains the lowest proportion of anomalies. Simply put - the low MGT track is dominated by low amplitude anomalies and the high MGT track is dominated by large amplitude anomalies. Why should the proportions (distributions) of anomalies be so different? What sort of natural process or maintenance practice causes or creates such distributions?

The number of peaks for each anomaly and the resulting distribution of number of peaks versus amplitude was not determined for this set of data.

Anomaly name	Anomaly Amplitude (inches p/p)
Montj4	0.712
Margo1	0.722
Margo6	0.725
Margo4	0.755
Margo5	0.770
Margo2	0.817
River1	0.848
Montj1	0.850
Montj2	0.850
Montj3	0.897
River2	1.020
Margo3	1.115

Table 4.1-2: Anomaly Amplitudes on data set 1 with a 0.7 inch threshold

4.2 Data set 2: 20 continuous miles of track data

Data set 2 consists of approximately 20 continuous miles of data contained in 20 data files. Each record within the files contains the left rail profile, right rail profile, milepost, feet and superelevation. The data sample rate is one foot per sample. Previous to this data set, data was analyzed on a piece-meal basis, with short track segments being selected based upon some knowledge of the existing track conditions. This set of data was chosen to test the methodology and tools on a larger set of data than had been attempted before.

The data was in a form incompatible with that necessary to run DSTREAM and also different than the format of data set 1, so the original preprocessor was modified to

allow reformatting of the data set. The analysis then proceeded exactly like the analysis of the previous set; namely one run of DSTREAM for each data file and then 7 runs of PFILT for each file at increasing anomaly amplitudes, a total of 140 PFILT runs.

Figure 4.2-1 shows the distribution of anomalies for amplitudes greater than 0.5 inch peak-to-peak. The figure shows the number of anomalies within each 0.1 inch range of amplitude.

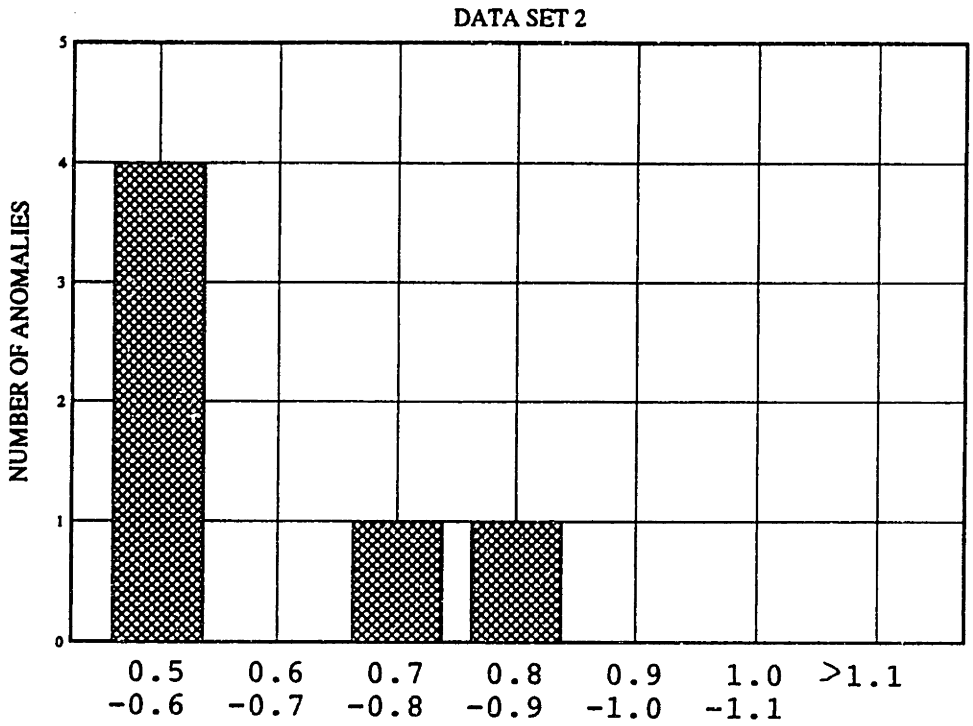

FIGURE 4.2-1. Anomalies identified on 20 mile long data set.

A total of six anomalies were found. Table 4.2-1 lists the number cumulative number of anomalies exceeding each amplitude.

Even though the number of data points is very low, the exponentially decaying occurrence of anomalies is again suggested by this data set.

The number of peaks for each anomaly and the resulting distribution of number of peaks versus amplitude was not determined for this set of data.

	Maximum amplitude of anomalies (inch)						
	0.6	0.7	0.8	0.9	1.0	1.1	>1.1
Cumulative number of anomalies	6	2	2	2	0	0	0

Table 4.2-1. Cumulative distribution of anomalies in data set 2.

4.3 Data set 3: 305 miles of data

The purpose of analyzing a set of data as large as this was to put the methodology and tools to a full scale test of its effectiveness and efficiency. And this it did; many improvements to the methodology (Chapter 2) and changes to the programs (Chapter 3) and were made, in response to the needs generated by attempting to analyze this set of data.

The data came in ASCII format in 65 data files. A typical data file contained approximately 5 continuous miles of track data, totalling 305 miles. The set was divided into 5 segments of continuous track data. The five segments KTNGRL, STHCIN, DRMVRL, DIAMON, and MTMGM were 130 miles, 31 miles, 95 miles, 14 miles, 33 miles long, respectively. The segments were not analyzed separately from each other; they were treated as a single continuous stream of data. Each data record consisted of milepost and feet location, left and right profile, curvature and superelevation. Data formats in all the files were identical and incompatible with DSTREAM data format

requirements. A preprocessor program was created to convert the data (Section 3.1). The DSTREAM analysis required 65 runs and the PFILT analysis required 9 runs for each file, a total of 585 executions, to complete the data analysis.

Before proceeding with the results of the analysis, a discussion of the data is necessary. A check of the data was performed after noticing that there were several instances of impossibly large amplitude anomalies (300+ inches) and also that sequences of anomaly amplitudes repeated themselves in some files. A careful study was undertaken to find all the "bad" and repeated data in the entire set of data. The search found invalid data in five files; KTNGRL13, KTNGRL14, KTNGRL15, DIAMON02 and DIAMON03. Table 4.3-1 lists the sections of the files that were found to be erroneous.

File	from record #	to record #
KTNGRL13	20157	23494
KTNGRL14	16230	28251
KTNGRL15	2559	8765
DIAMON02	23292	26335
DIAMON03	1622	8606

Table 4.3-1. Files with erroneous data

Proceeding with the results of the data analysis, Figure 4.3-1 shows the distribution of anomalies as a function of anomaly amplitude for amplitudes greater than 0.3 inch peak-to-peak. Each bar in the graph gives the number of anomalies that exceed that amplitude.

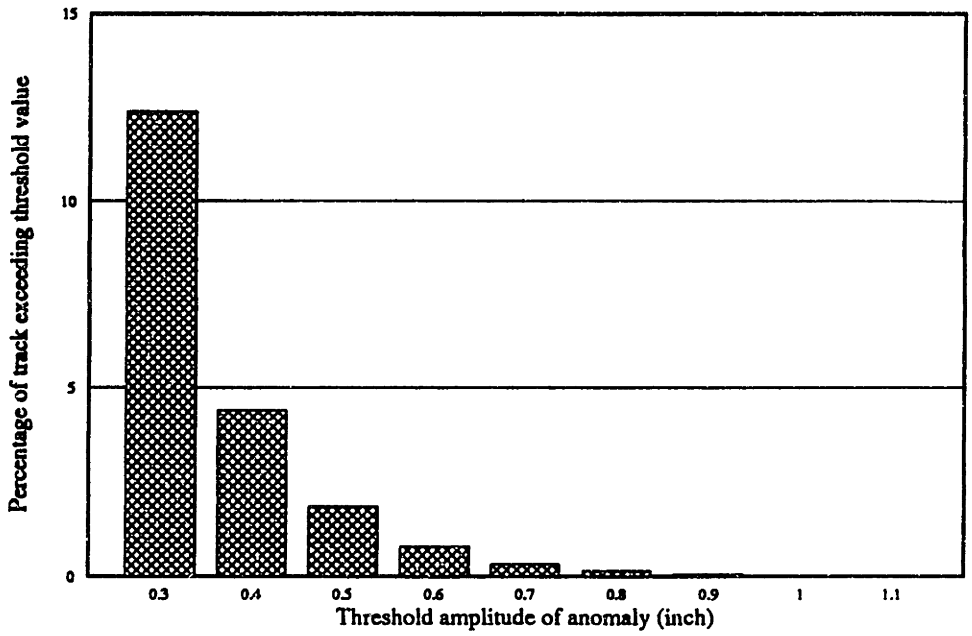

FIGURE 4.3-1. Anomalies identified on 305 miles of track data. Percentage of track length anomalous.

Table 4.3-2 gives the numbers corresponding to the graph, the cumulative length of the anomalies exceeding the referent amplitude, and the percentage of the total length of track which is part of an anomalous geometry variation. A total of 3,540 anomalies were found. The number of anomalies drops by approximately one-half for each 0.1 inch increase in anomaly amplitude. These findings provide a great incentive to find and use the largest possible threshold amplitude in the fatigue load analysis, since for every 0.1 inch the value is less than the maximum, the number of anomalies that must be considered doubles.

	Anomaly Threshold Amplitude (inches)								
	0.3	0.4	0.5	0.6	0.7	0.8	0.9	1.0	1.1
num. anomalies	3540	1521	760	366	161	77	28	13	4
Cumulative length (mi)	37.8	13.5	5.7	2.5	0.9	0.4	0.2	0.0	0.0
% of track anomalous	12.4	4.4	1.9	0.8	0.3	0.1	0.1	0.0	0.0

Table 4.3-2. Summary of 305 miles of mainline track profile data

Using the data at 0.5 and 0.7 inch, the exponential function $n = 2.52\exp[-7.8(a - 0.5)]$ closely approximates the behavior of the distribution. The coefficient of 2.52 in front of the exponential is the total number of anomalies exceeding 0.5 inch (760) divided by the length of the track data (305 miles). This track data has one-sixth the anomalies per mile than the three mile track segment in data set 1 (Section 4.1).

Finally, an analysis of the relationship between anomaly amplitude and number of peaks per anomaly was performed. The number of peaks is a measure of the potential repetitiveness of variation of the anomaly. Figure 4.3.-2 shows the distribution of peaks that occurred in all anomalies with amplitudes between 0.5 and 0.6 inch. The vast majority of anomalies within this range contain only one peak, and only 7 in 413 (1.7%) had between three and six peaks. An anomaly with six peaks can, at most, have three cycles of repeated geometry variation. *This study shows that small amplitude, multiple-peak anomalies that could cause large dynamic responses do not regularly occur on this track.*

The distributions have been found for the entire range of anomaly amplitudes and are shown in Figure 4.3-3a-c for amplitude ranges 0.6 to 0.7 inch, 0.7 to 0.8 inch, 0.8 to 0.9 inch, and in Figure 4.3-4a-c for the ranges 0.9 to 1.0 inch, 1.0 to 1.1 inches, and

greater than 1.1 inches. The data used to develop these figures is given in the Table 4.3-3. As seen in the graphs, the maximum number of peaks within an anomaly amplitude range tends to increase with anomaly amplitude.

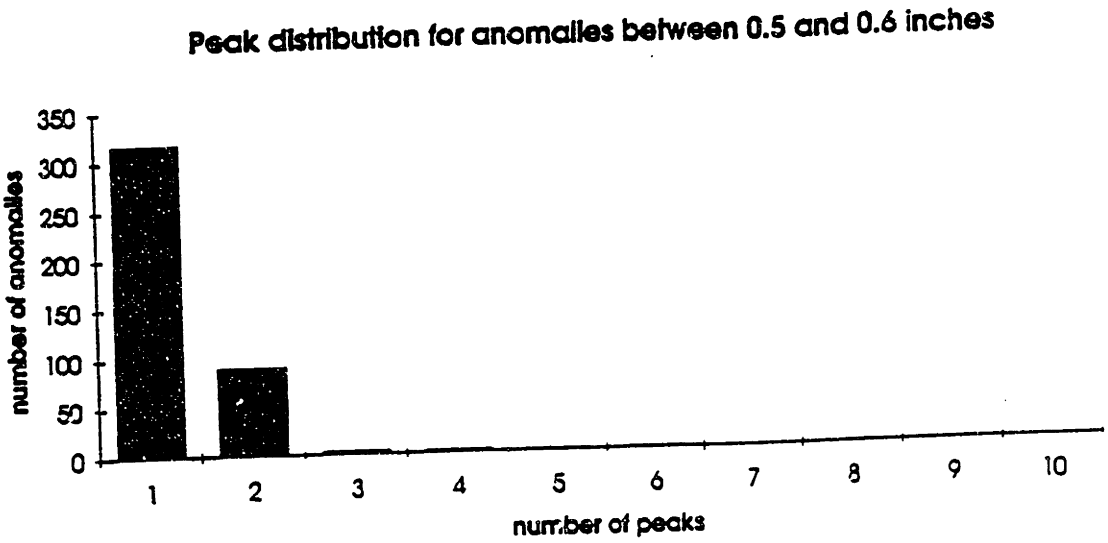

FIGURE 4.3-2: Distribution of the number of anomalies vs. the number of peaks in the anomaly for anomaly amplitudes between 0.5 and 0.6 inch, inclusive.

By 0.7 inch there is an anomaly with the potential of three cycles of repetition, by 0.8 inch an anomaly with the potential for five cycles of variation has appeared. However, the most frequent number of peaks per anomaly for anomalies between 0.6 and 1.0 inch is two peaks, indicating that the most common anomalies do not have a repetitive shape.

Peaks	Cycles	Amplitude groups (inclusive on lower limit)						
		.5-.6	.6-.7	.7-.8	.8-.9	.9-1	1-1.1	>1.1
1	1	319	63	14	2	2		
2	1	87	82	43	17	8	1	
3	2	3	14	15	11	4	2	
4	2	2	7	13	8	3	2	
5	3	1	2	5	4	1	1	1
6	3	1	1	3	3	2	2	1
7	4		2			1	1	1
8	4		1			1		
9	5							
10	5				1	1		1
total #		413	172	93	46	23	9	4

Table 4.3-3 Distribution of number of peaks and cycles of anomalies in 305 miles of track data

The distribution has become quite spread out by 0.9 inch showing that multiple peak anomalies are quite common at this amplitude range. By 1.0 inch the distribution is essentially uniform. The anomalies range between two and seven peaks with no clear shape to the distribution evident. Four anomalies with amplitude greater than 1.1 inches were found, all are multiple peak anomalies. The anomalies have the potential for repetitions of between three and five cycles. Also notice that there are no anomalies which are not multiple peak.

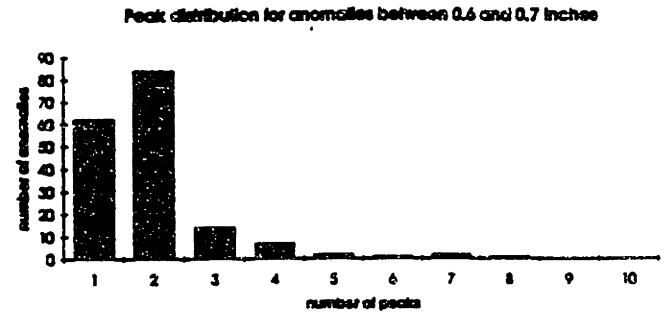

(a)

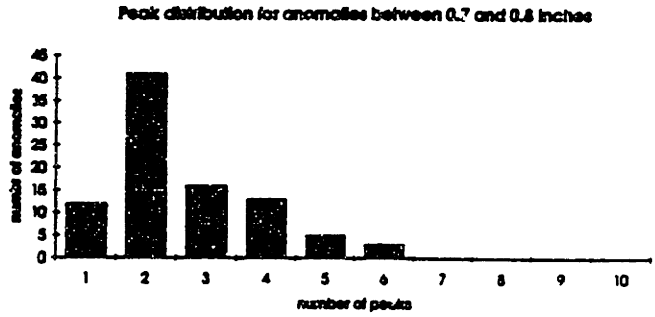

(b)

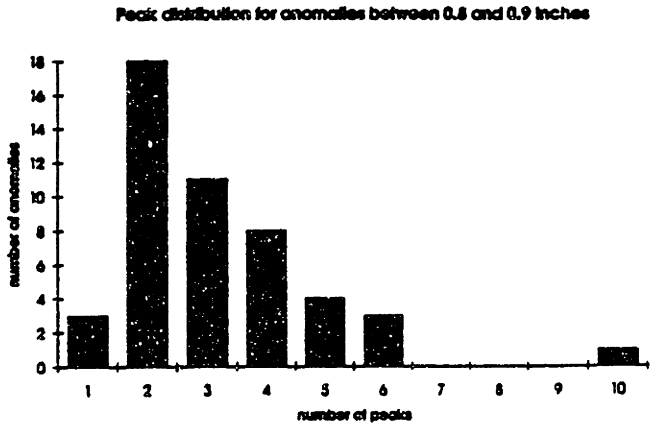

(c)

FIGURE 4.3-3: Number of anomalies vs. peaks 0.6 to 0.9 inch anomalies

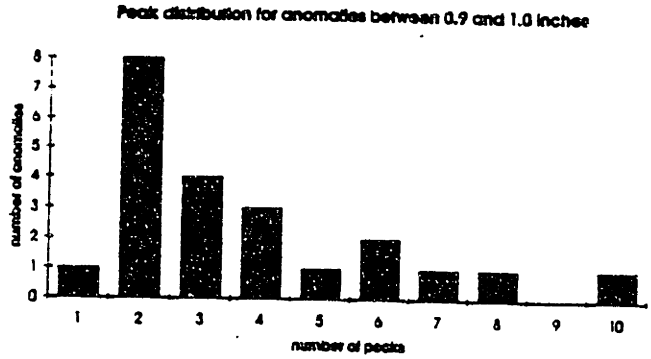

(a)

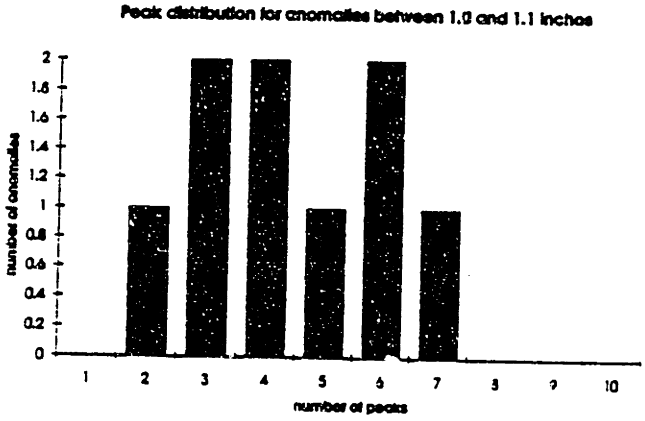

(b)

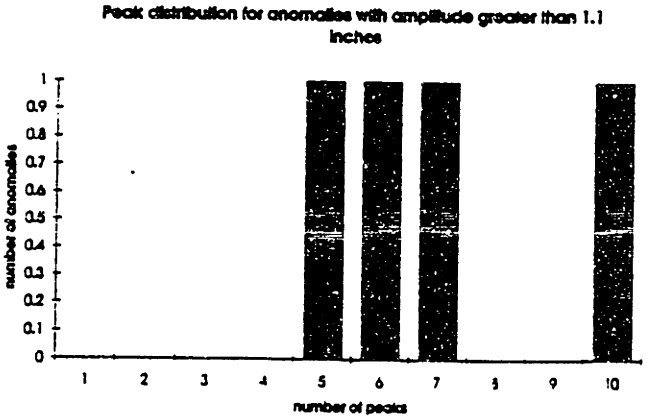

(c)

FIGURE 4.3-4: Number of anomalies vs. peaks anomalies g.t. 0.9 inch

Another approach considered to create the distribution of anomaly amplitude versus number of peaks was to perform an anomaly identification analysis using the lower bound of each group as the threshold value. Then the anomalies whose amplitudes were within the 0.1 inch range from the threshold values were considered as the anomalies that fell into that range. All the other anomalies identified at that threshold were ignored. This procedure produced the distribution given in Table 4.3-4. This representation of the distribution would indicate that there is a decrease in the potential for repeated variations of geometry as anomaly amplitude increases. This is known not to be the case. Therefore, this technique for characterizing the track is not correct.

Peaks	Cycles	Amplitude groups (inclusive on lower limit)						
		.5-.6	.6-.7	.7-.8	.8-.9	.9-1	1-1.1	>1.1
1	1	319	157	72	41	18	4	1
2	1	87	40	11	16	4		
3	2	3	3	2	4	1		
4	2	2						
5	3	1						
6	3	1						
total #		413	200	84	61	23	4	1

Table 4.3-4 Distribution of number of peaks and cycles of anomalies in 305 miles of track data using a moving threshold amplitude.

5 Three case studies: two vehicles, three sets of track data

Three case studies were performed. In each case study, one of the three track data sets from the previous chapter was used in conjunction with either the paintspotter car model or the three platform articulated flat car model. The case studies were of dynamic simulations of the cars negotiating anomalies extracted from the track data. Fatigue loads on the car bolsters were predicted. Dynamic simulations are the fourth step of the methodology: following anomaly identification, vehicle modelling, and threshold analysis.

The purpose of these studies was to determine the relationship between anomaly amplitude and fatigue loads. Another goal was to determine if the overall methodology captures all the anomalies that cause *significant* fatigue loads. A 1.8 dynamic load factor is used in car body structural design (Kalaycioglu and Tajaddini, 1988). If the peak bolster load exceeds 1.5 times the static bolster load, it is deemed a significant fatigue load level (Singh, 1992).

The first case study, in Section 5.1, used the paint spotter 70-ton car with three miles of track data. The goal of this study was to evaluate the ability of the methodology to find and extract anomalies for use in NUCARS simulations. From this study the changes to the methodology were made that replaced the threshold extension factor and added the anomaly extraction controls described in Section 2.2. The second case study, described in Section 5.2, used the paintspotter car with 20 miles of continuous track data. This study tested the ability to apply the methodology and tools to a larger set of track data. The third case study, in Section 5.3, used a three platform articulated flat car with 305 miles of data. The goal of this study was to develop the programs for application to

very large sets of track data, and demonstrate the overall methodology. An approach for evaluating a sub-set of the set of anomalies to estimate fatigue loads is presented. Peak load predictions from the case studies are given in Appendix D. All the dynamic simulations and bolster load predictions were done with the NUCARS program.

5.1 Case Study 1: Paint spotter car with three miles of track data

The motivation for this study was to evaluate the efficacy of the anomaly extraction routine. This case study analyzed the movement of the paintspotter vehicle over the three miles of track data described in Section 4.1. The data came in three, one-mile long sections, named the Margo, Montjoli, and Rivers sections. Because the methodology for determining the threshold amplitude described in Section 2.1 was not yet created, the threshold was determined iteratively. Also not yet developed, was the ability to add lengths of rail to the end of the anomaly segments, nor to control the magnitude of the anomaly end points.

Two criteria were used to identify and extract anomalies. In the first, Criteria A, the threshold amplitude was 0.7 inch peak-to-peak. The threshold extension factor was 71% (corresponding to 0.5 inch peak-to-peak) and a 39 foot half-window length was used. The threshold amplitude of 0.7 inch was chosen because this corresponds to the smallest amplitude variation associated with significant bolster loads in Allen (1992).

Using Criteria A (0.7, 71%, 39) on the data set yielded 12 anomalies. The Montjoli segment had 4 anomalies covering approximately 4.6% of total track length. The Margo segment had 6 anomalies covering 7.1% of the total track length. And the Rivers

segment had 2 anomalies covering 2.6% of the track length. Later studies of track data, specifically data sets 2 and 3, showed that set 1.had the highest proportion of anomalous data.

Another set of analyses was performed using a second criteria, Criteria B. A 0.5 inch threshold amplitude, a 100% threshold extension factor and a 39 foot half-window length were chosen. This threshold was chosen because 0.5 inch is the smallest amplitude associated with significant response in the vehicle due to continuous repetitive profile variations in analytical studies conducted by Schwarz, et al (1988). A threshold extension factor of 100% means that no augmentation of lower amplitude variations takes place.

Finally, a 39 foot half-window was chosen in both criteria because the truck center spacing is 40 feet, and profile anomalies are dominated by the 39 foot bolted rail length (Hamid, et al, 1983). A 78 foot window ensures capture of long wavelength perturbations without making the window so long as to increase computing time excessively.

Using Criteria B (0.5, 100%, 39) a total of 45 anomalies were found, approximately four times as many as Criteria A. There were 24 anomalies on the Montjoli segment, 23% of total length, 19 on the Margo segment, 14% of total length, and still only 2 on the Rivers segment, 4% of total length.

Because the threshold extension factor in both criteria was set to capture any variation greater than 0.5 inch peak-to-peak around the ends of an anomaly, one would expect that any anomaly identified by Criteria A would be the same length as that

identified by Criteria B. This, however, was not the case. Evidence of this is found immediately upon looking at the total track length that is anomalous on the Rivers section, where 2.6% of the track is anomalous by Criteria A and 4.0% is anomalous by Criteria B. Only two anomalies were found in both cases, but the anomalies are shorter using Criteria A. This should not be. Investigation of all 12 anomalies identified by both criteria showed that anomalies identified by Criteria A tended to be shorter than the anomalies identified by Criteria B. This brought to question the applicability of the shape function characterization of anomalies and raised questions about the original extraction technique's ability to capture all the track information surrounding an anomaly which could significantly effect the dynamic response of the car. Since anomaly length tends to get shorter as anomaly amplitude increases, this could force the use of lower threshold amplitudes to ensure capturing all the significant adjacent track data.

A comparison of the peak loads predicted on the same track anomaly extracted by the two criteria was performed. The findings of this study are illustrated in Figures 5.1-1a-b, 5.1-2a-b, and 5.1-3a-b. In each of these figures the top plot is of a track anomaly extracted from the track segment using Criteria A (0.7, 71%, 39), and the bottom plot is of the same anomalous track extracted using Criteria B (0.5, 100%, 39). In each case the anomaly extracted using Criteria B includes significantly more track data around the anomaly peaks.

Note: The anomalies identified by Criteria A are given five letter prefixes corresponding to the first five letters of the section name from which they came, the anomalies identified by Criteria B are given two letter prefixes corresponding to the first two letters of the section name from which they came.

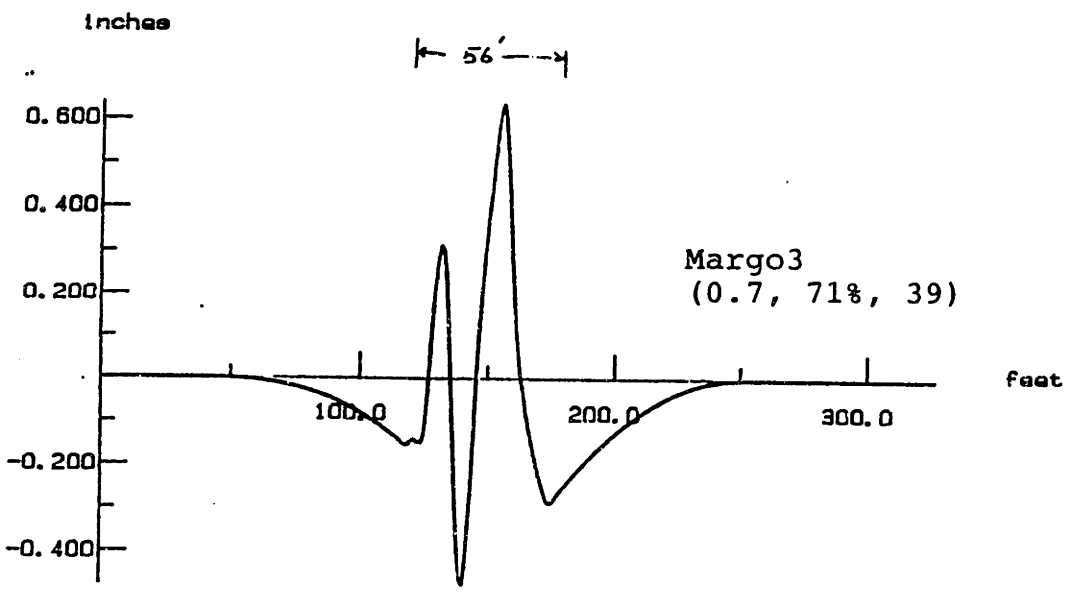

(a)

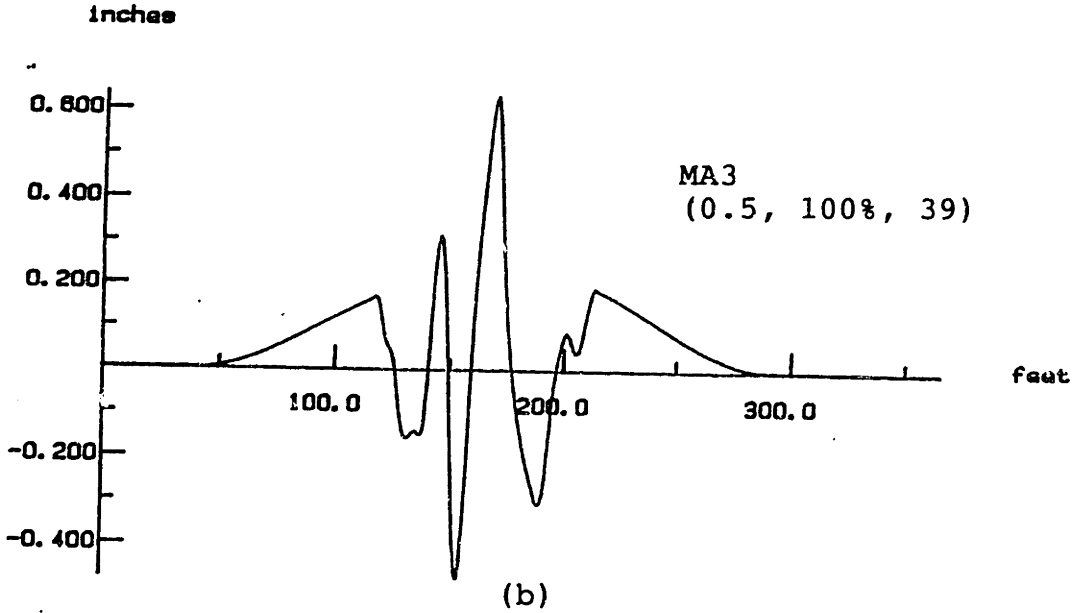

(b)

FIGURE 5.1-1: Comparison of anomaly identified by different criteria

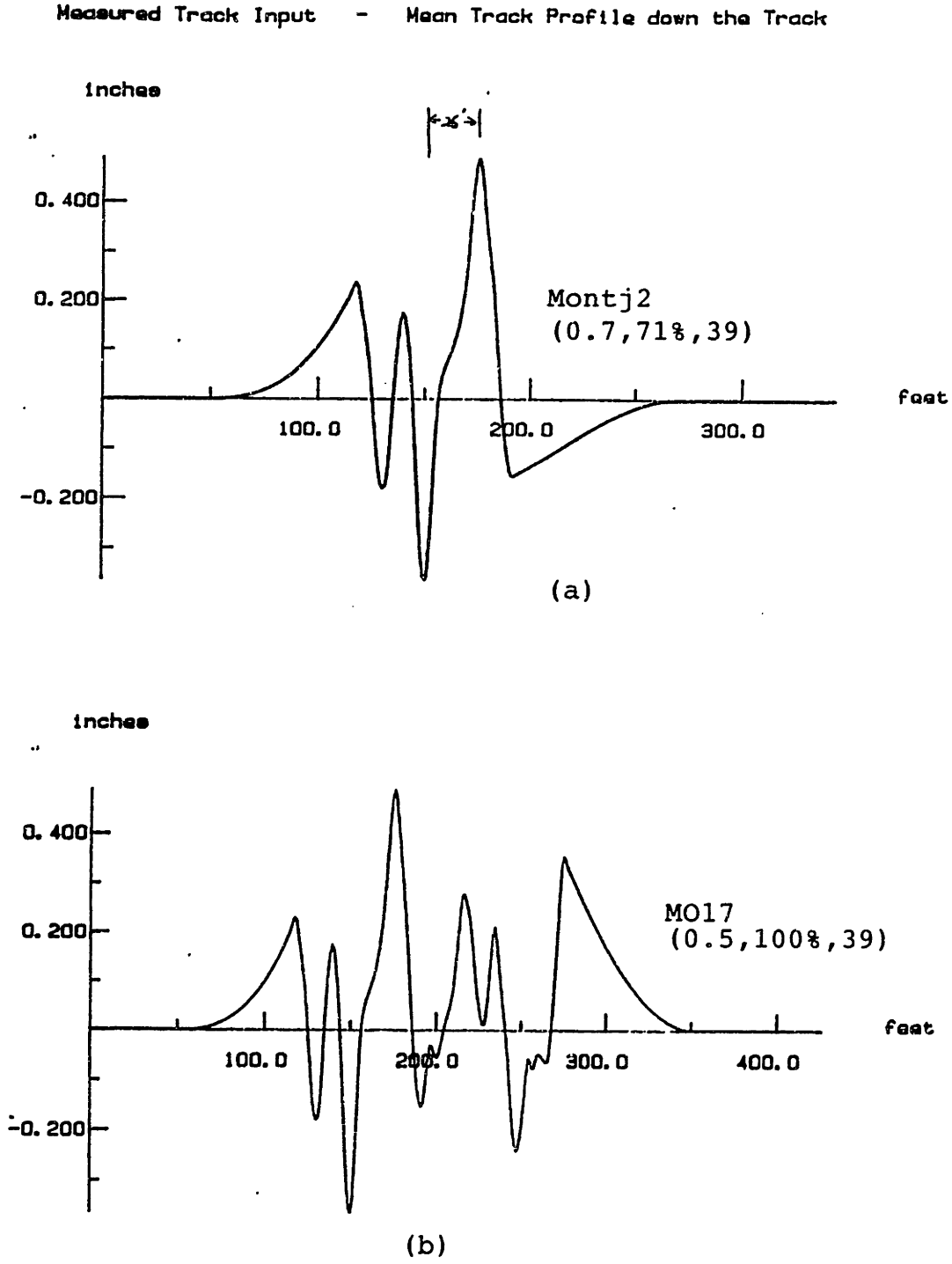

FIGURE 5.1-2: Comparison of an anomaly identified by different criteria

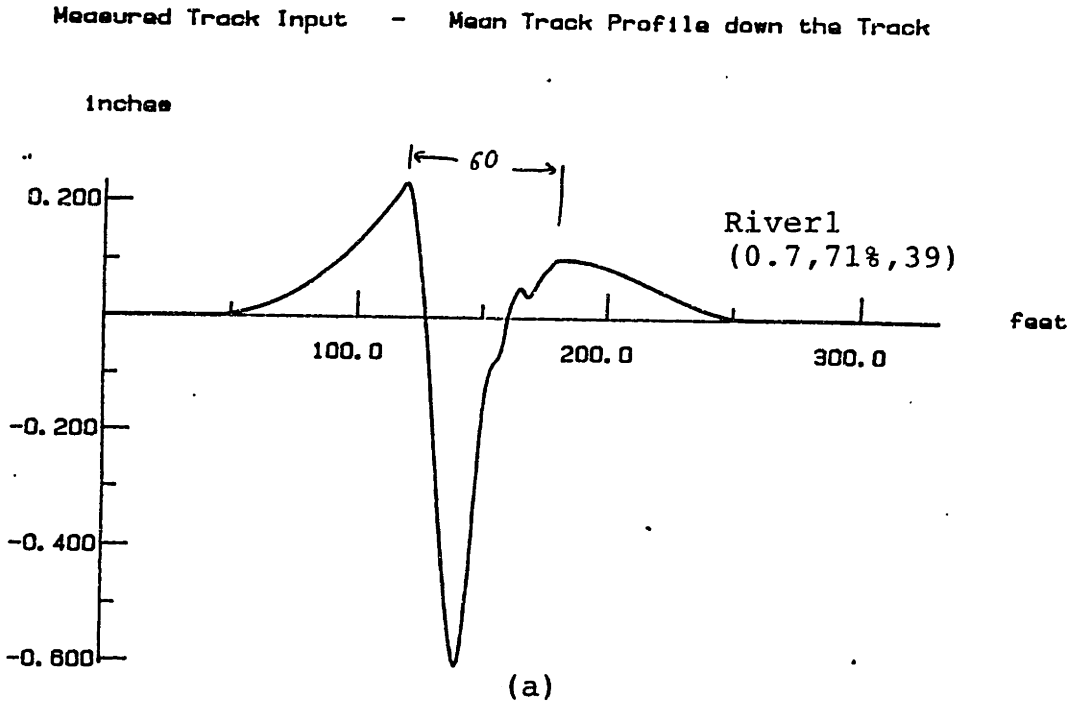

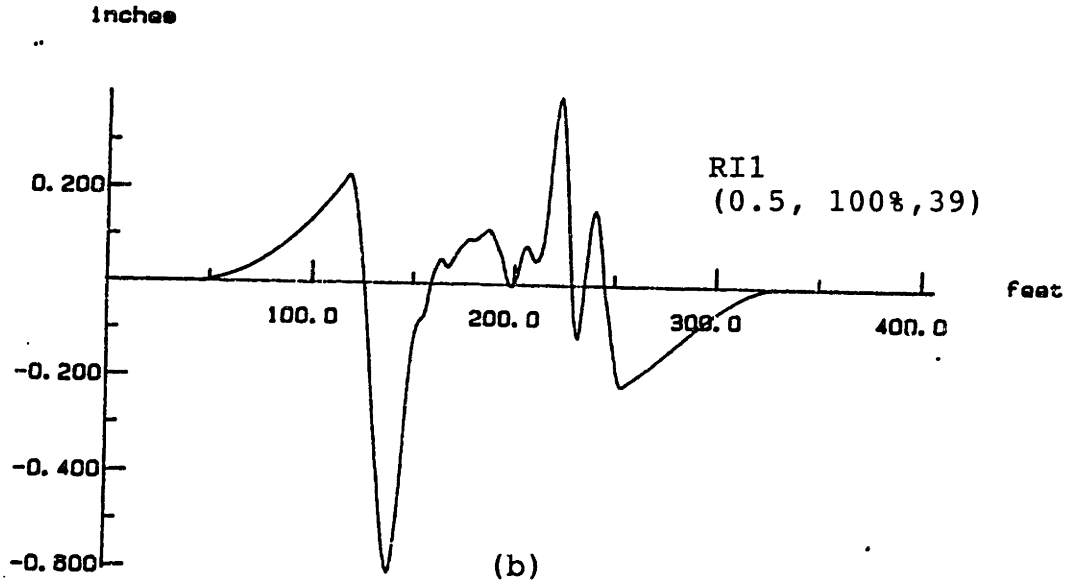

FIGURE 5.1-3: Comparison of an anomaly identified by two criteria

The Margo3, MA16 anomaly, which caused the most severe fatigue load predictions in this set of anomalies, is shown in Figure 5.1-1. The anomaly identified by Criteria A is a three peak anomaly with an amplitude of 1.115 inches. Using Criteria B, the same anomaly is extended at both ends to include an extra 20 feet of track data. This effected the peak bolster load predictions. On the Margo3 anomaly a peak bolster load of 181.1 kips is predicted, but on the MA16 anomaly the peak bolster load predicted is 173.2 kips, a difference of approximately 5%. Figure 5.1-2 shows the Montj3, MO17 anomaly. The track geometry in MO17 from 50 feet to 190 feet encompasses the entire Montj3 anomaly segment. The remaining 100 feet of MO17 is identified by Criteria B only. It appeared that Criteria B may have identified a multiple-peak anomaly of a substantial length that Criteria A did not, and if so, the peak load predicted over MO17 will potentially be much greater than over Montj2. At 80 mph the peak load prediction were 125.5 kips and 145.9 kips, a 15% difference.

Figure 5.1-3 shows the River1, RI1 anomaly. This is a dip anomaly with a 0.848 inch amplitude. Criteria A identifies just the dip portion of the track variation. Criteria B finds a series of track variations on the tail end of the dip, which extends the anomaly approximately 100 feet from the end of the dip. The peak load prediction on these two anomalies were 135.4 kips and 136.6 kips on River1 and RI1, respectively. Thus Criteria B extended the anomaly a significant length, but it was not track that significantly effected the response of the car.

In the first example, the peak load predicted using Criteria A was greater than that predicted by Criteria B. In the second example, the peak load predicted using Criteria B was greater than that predicted by Criteria A. In the third example the two Criteria produced significantly different anomalies that produced the same peak bolster load predictions.

It must be assumed that the longer anomalies lead to more accurate simulations. This is problematic for the extraction technique since the shorter anomalies at larger amplitudes do not necessarily lead to conservative results. These examples raised concerns about whether anomalies extracted with larger thresholds have long enough lead and tail sections to allow initial condition transients to die or of including all the track adjacent to the anomaly which can significantly effect the dynamic response of the car. To compensate for this concern, an extraction amplitude less than the threshold amplitude could be used, and those anomalies below the threshold amplitude discarded. A better anomaly extraction technique would avoid this problem. A technique has been developed and is presented in Section 2.2.

Another potential problem identified was that the end points of the anomalies were large with respect to anomaly amplitude. Two examples of this are shown in Figure 5.1-4a-b where the MO5 and MO4 anomalies are plotted. The spline fits on the MO5 anomaly are greater than 0.3 inch in amplitude on an anomaly of 0.6 inch. On the MO4 anomaly, Figure 5.1-4b, the end point of the leading spline fit has a magnitude greater than 0.4 inch on an anomaly of just over 0.6 inch, and it ends right at the start of the anomaly. This brought forward questions about artificial transients and inaccurate

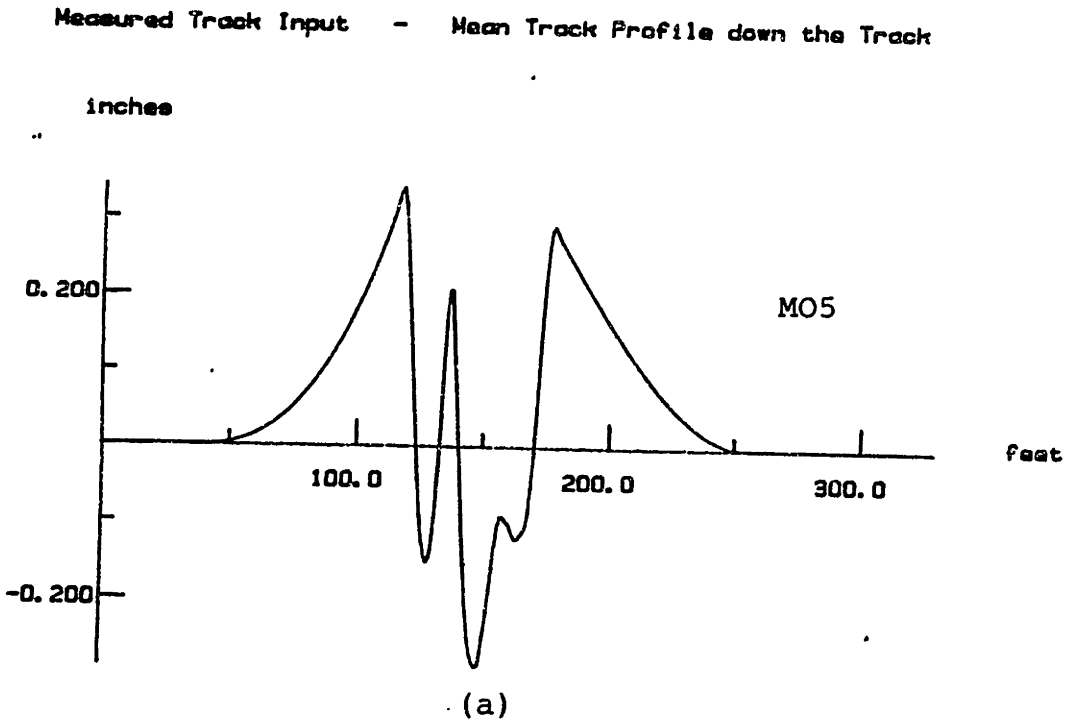

(a)

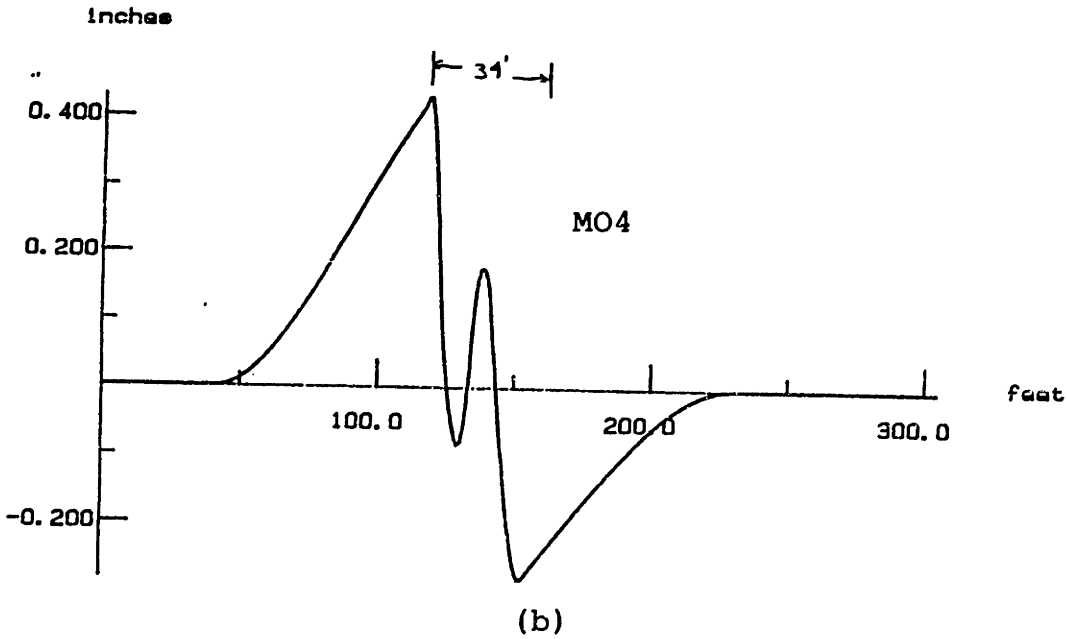

(b)

FIGURE 5.1-4: Examples of anomalies with large magnitude end points.

simulation caused by the car encountering the anomaly too soon after reaching the real track data at a large magnitude relative to the anomaly amplitude. This problem has been solved using a new technique for extracting anomalies, described in Section 2.2.

NUCARS simulation runs at 60 mph and 80 mph, were made over all the anomalies identified by both criteria. A speed of 60 mph was used because it is close to the vehicle bounce natural frequency on 39 foot wavelength anomalies (62 mph) and it corresponds to the maximum speed on Class 4 track (Track Safety Standards, 1992). All three miles of track met the FRA Class 5 track specifications for track profile variations, so a speed of 80 mph was used because it corresponds to the maximum speed on Class 5 track.

Figures 5.1-5a-c show typical lead and trailing bolster loads predicted by NUCARS for the paintspotter car, over three anomalies identified by Criteria A: Margo3, Margo5, and Margo6. The car response to the Margo3 anomaly was a combined bounce and pitch motion. A peak bolster load of 181.1 kips occurred at 60 mph on the trailing bolster of the car at 180 feet into the anomaly. Over the Margo5 anomaly at 60 mph the motion was almost pure bounce. Margo5 had an amplitude of 0.770 inch and the resulting peak bolster load was 129 kips. On the Margo6 anomaly, the car response is close to pure pitch at 60 mph. The peak bolster load due to the 0.725 inch anomaly is 127 kips.

Figure 5.1-6 shows the dynamic-to-static load ratio versus anomaly amplitude that resulted from the simulations at 60 mph, for anomalies identified using Criteria B. The trend generally can be described as linear growth in load ratio with anomaly amplitude. The peak load ratio in response to anomaly amplitudes less than 0.7 inch is 1.35, the average load ratio is 1.17.

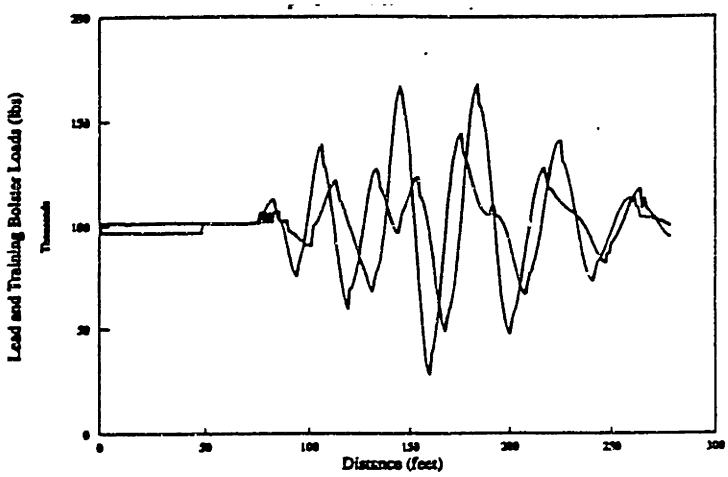

(a) Margo3

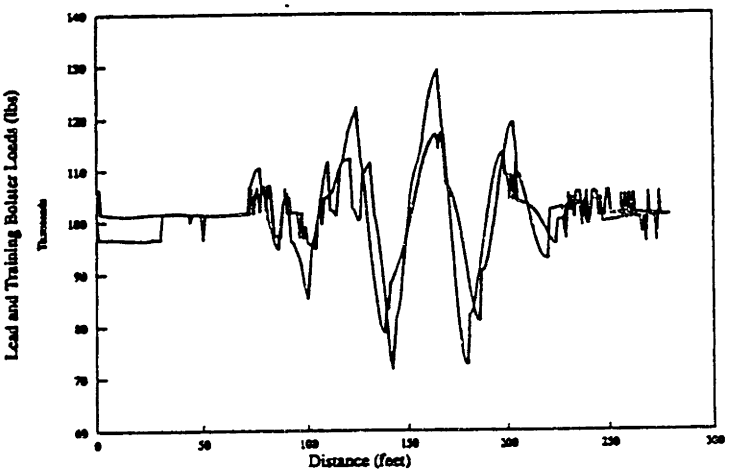

(b) Margo5

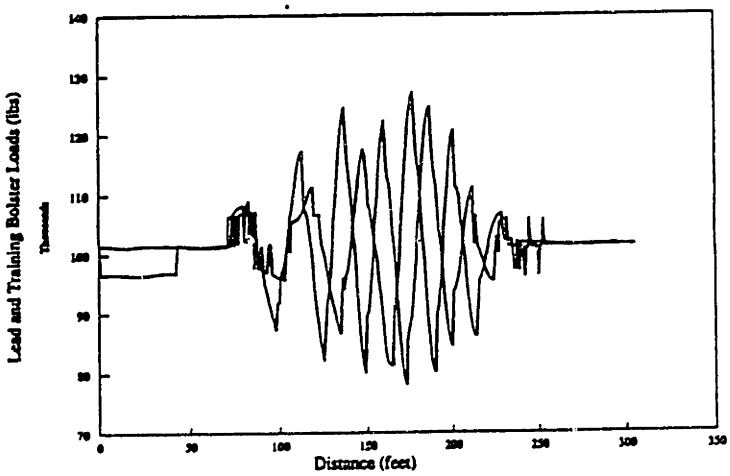

(c) Margo6

FIGURE 5.1-5: Typical lead and trailing bolster loads predicted by NUCARS for the paintspotter car at 60mph.

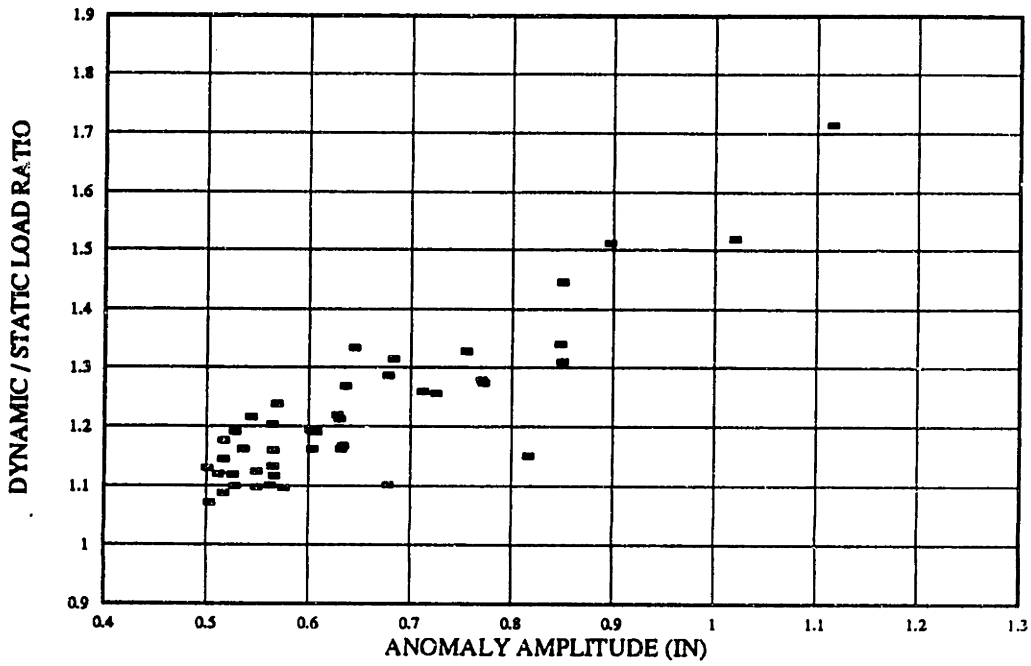

Figure 5.1-6: Analysis of 3 miles of track profile data. Simulations over all anomalies at 60 mph.

A comparison of the responses at 60 mph and 80 mph was done. In Figure 5.1-7 the load ratio versus anomaly amplitude for simulations at 60 mph and 80 mph over the Margo segment are plotted. The peak bolster loads at 80 mph are generally greater than those at 60 mph for all anomalies except the largest. The MA16 anomaly, which is the largest amplitude and produces the largest bolster load, is repetitive in shape. Figure 5.1-8 shows the load ratio versus amplitude at 60 mph and 80 mph over the Montjoli anomalies. Here there is no tendency for either speed to produce a larger peak load.

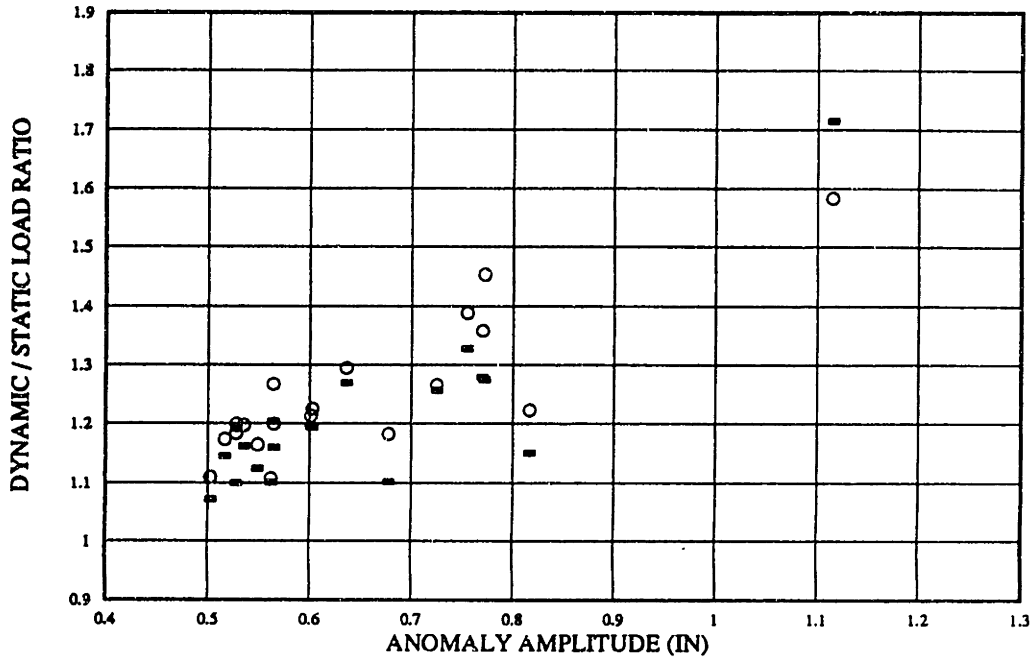

Figure 5.1-7: Analysis of 3 miles of track profile data. Simulations over Margo anomalies at 60 and 80 mph.

The results from simulations at both speeds over all the anomalies (including Rivers segment anomalies) are plotted in Figure 5.1-9. There is no single amplitude where it is evident that the loads at 60 mph or 80 mph produce the larger response. Instead it appears that, as amplitude grows there is more of a tendency for the peak loads at 60 mph to be greater than the loads at 80 mph. This could indicate a growing tendency towards multiple peak repetitive variation anomalies near 39 feet long with larger amplitude anomalies.

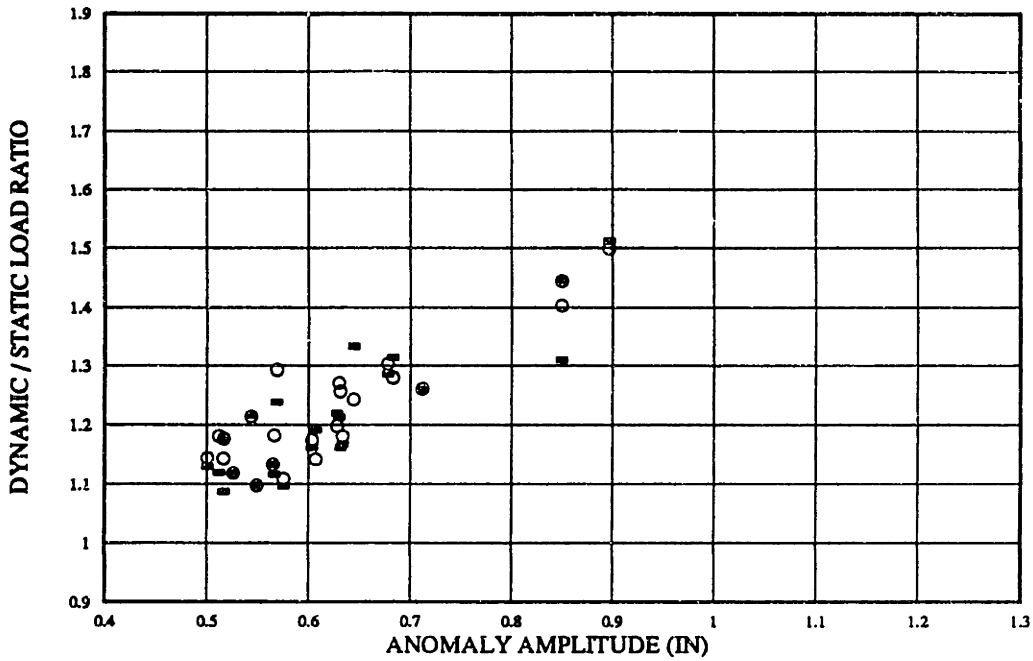

Figure 5.1-8: Analysis of 3 miles of track profile data.
Simulations over Montjoli all anomalies at 60 and 80 mph.

These results show that a threshold amplitude of 0.7 inch is satisfactory, i.e. there are no significant fatigue loads due to anomalies with amplitudes below 0.7 inch. The problem is that there is no justification to use 0.7 inch a priori: no independent criteria for finding the threshold amplitude. While using 0.5 inch was justified by independent analysis, it is too conservative a value since it identifies four times as many anomalies as the 0.7 inch threshold. These results motivated the development of a rational methodology to determine threshold amplitude. The methodology developed is described in Section 2.1.

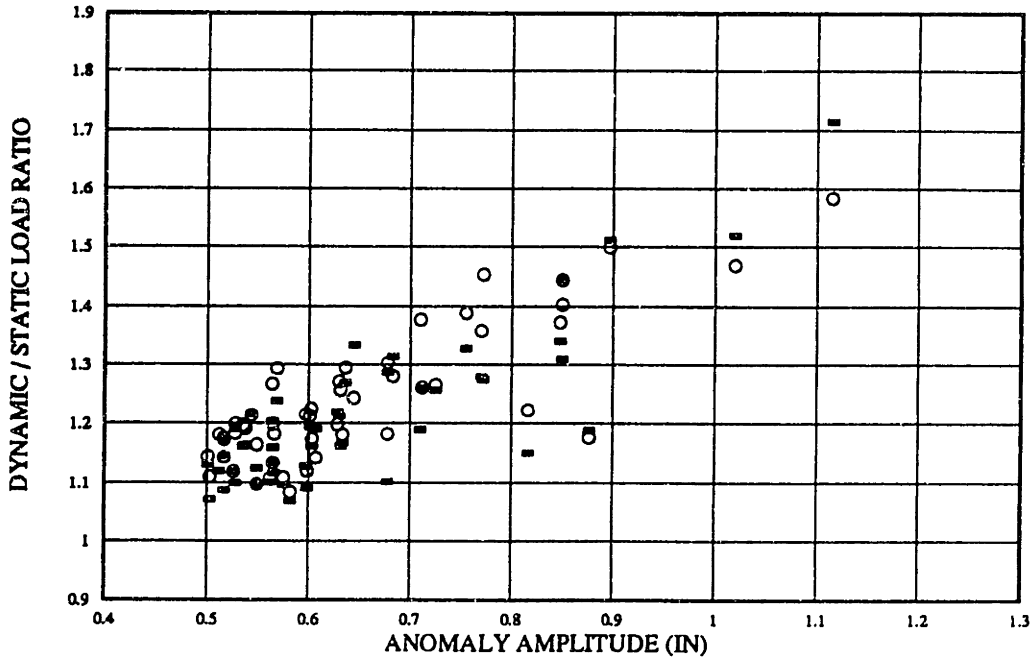

Figure 5.1-9: Analysis of 3 miles of track profile data. Simulations over all anomalies at 60 and 80 mph.

5.2 Case Study 2: Paint spotter car with 20 continuous miles of track data

Having shown the ability of the methodology to find and extract anomalies on short segments of track that contain numerous anomalies, the next step was to test the methodology on a longer set of data. A set of data was obtained, consisting of 20 miles of continuous track geometry. Again, the methodology to determine the threshold amplitude described in Section 2.1 was not yet developed. Nor was the track length

addition and end point control capabilities so that one again sees the threshold extension factor. The purpose of this study was to evaluate the ability of the methodology and programs to perform anomaly detection, extraction, and dynamic simulations on a larger set of data.

Only Criteria B, was used to identify anomalies because there were so few anomalies on this track segment. Using this criteria on the data set yielded only six anomalies, four between 0.5 and 0.6 inch, one anomaly with an amplitude of 0.710 inch and one anomaly with an amplitude of 0.877 inch.

The anomalies were extracted and used as input in NUCARS simulations. The paint spotter vehicle model was used and simulations were run at 60 mph and 80 mph. The resulting peak bolster loads are given in Table 5.2-1. A slightly larger load is predicted at 60 mph than at 80 mph on the largest anomaly. On all the anomalies except the largest, the predicted fatigue loads are larger at 80 mph than at 60 mph.

The results showed that the methodology was applicable on a longer data set with few anomalies, i.e. the anomalies were identified and extracted efficiently and the simulations could progress without requiring modification to the programs.

Table 5.2-1: Results of case study two: The paintspotter car and 20 miles of continuous data.

Anomaly number	Amplitude (inches p/p)	Peak bolster load (kips) at 60mph	Peak bolster load (kips) at 80mph
1	0.538	117.7	120.4
2	0.582	108.0	109.4
3	0.597	113.9	122.7
4	0.598	110.2	113.1
5	0.710	120.2	129.1
6	0.877	120.1	118.8

5.3 Case Study 3: Articulated flat car with 305 miles of track data

The third case study models the movement of an articulated flat car over the anomalies extracted from the third data set. This study combined the complexity of a three-platform articulated flat car with the a track data set 15 times longer than data set 2.

One of the major goals of this case study was to determine the validity of the threshold amplitude analysis of Section 2.1, which suggested a 0.7 inch threshold anomaly amplitude. If 0.7 inches is a valid threshold, then no anomaly on this track with amplitude less than 0.7 should be able to cause a significant fatigue load. Verifying this by running simulations over every anomaly below 0.7 inch would be prohibitively time consuming. Another way to judge was necessary. In Section 2.1, the outlier anomalies were identified and separated from the other 98% of anomalies. Thirteen of the outlier anomalies had amplitudes between 0.5 and 0.7 inch. These anomalies must be treated individually, i.e. simulations must be run over these anomalies to determine if they can cause significant fatigue loads. Hypothesizing that the outliers are the most probable of the anomalies below 0.7 inch amplitude of causing significant fatigue loads, it was concluded that, if there were no outliers that could cause significant fatigue loads, then none of the anomalies below the threshold amplitude could. If it was found that one or more of the outliers could cause significant fatigue loads, then anomalies from the 98% distribution would have to be sampled and simulations run to determine if 0.7 inch is a valid threshold amplitude.

The 13 outlier anomalies were identified, extracted, and put into a format compatible with NUCARS. Runs were made at 78, 60, and 40 mph over each of the anomalies. Table 5.3-1 lists the maximum, minimum, and average peak load factors occurring over the outliers at each speed.

Load factor	78 mph	60mph	40mph
maximum	1.37	1.34	1.24
average	1.30	1.27	1.19
minimum	1.24	1.19	1.17

Table 5.3-1: Peak load factors on the outlier anomalies.

The largest values of maximum, average, and minimum occurred at 78 mph. The largest peak load factor was 1.37. The lowest values occurred at 40 mph. Figure 5.3-1 is a plot of the peak load factors predicted over all the outliers versus anomaly amplitude. The significant result of this study is that no simulation produced a peak load factor above 1.50.

Figure 5.3-2 is a plot of the peak load factor versus number of peaks in the anomaly predicted at 78 mph over the 13 outliers. There is a minor trend towards increasing peak load factor with increasing number of peaks. Note that there is also a positive correlation between anomaly amplitude and number of peaks. Thus, it is expected that a similar trend will occur for peak load factor versus amplitude. The data is plotted versus amplitude if in Figure 5.3-3, but there the correlation between amplitude and peak load factor is not as clear in this figure.

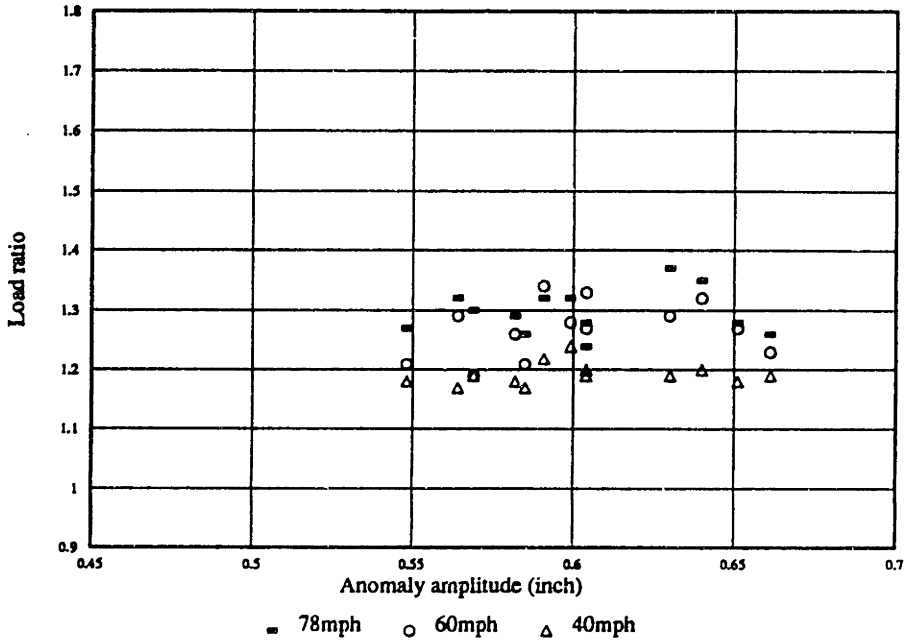

Figure 5.3-1. Peak load factor over outlier anomalies versus anomaly amplitude

This analysis showed that there were no outliers that could cause significant fatigue loads on this track. Since the outliers were most likely to cause significant fatigue loads, it follows that there was no chance that there were any other anomalies of less than 0.7 inch amplitude that could cause significant fatigue loads. Therefore, the methodology to determine the threshold amplitude finds a valid conservative value of the threshold.

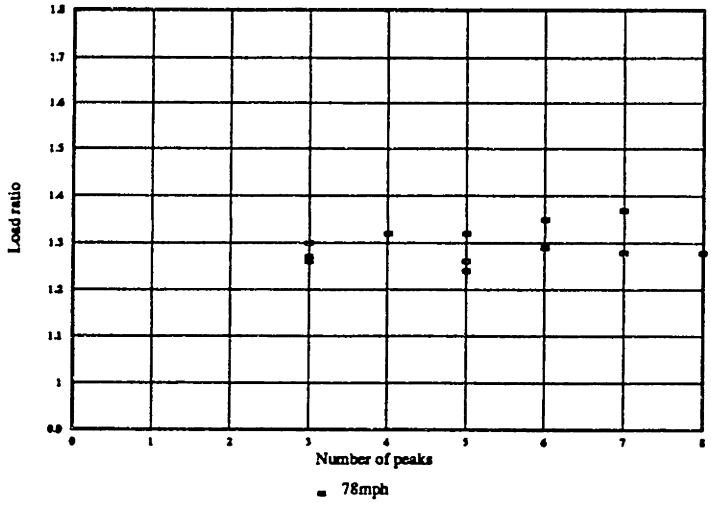

Figure 5.3-2. Peak load factor at 78mph over outlier anomalies versus anomaly amplitude

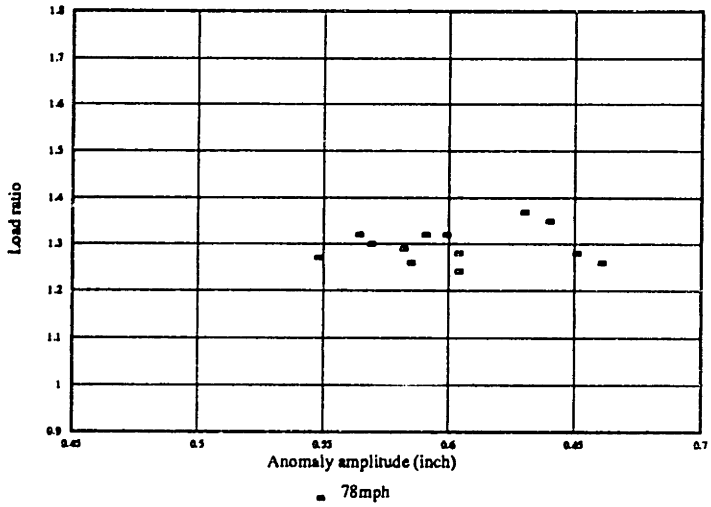

Figure 5.3-3. Peak load factor at 78 mph over outlier anomalies versus anomaly amplitude

Once the threshold amplitude was verified, analysis of the anomalies with amplitudes greater than 0.7 inch could proceed. An anomaly identification analysis was performed using a 0.7 inch threshold amplitude and the resulting distribution of anomalies by number of peaks and amplitude range is presented in Table 5.3-2. A total of 161 anomalies were identified, 45% of them are one peak anomalies with amplitudes between 0.7 and 0.8 inch.

number of peaks	0.7-0.8	0.8-0.9	0.9-1.0	1.0-1.1	>1.1
1	72	32	11	2	
2	11	13	5	3	
3	2		1	1	2
4		1	2	1	
5				1	
6					1
Total	85	46	19	8	3
# reduced	8	0	4	1	1
% reduction	9%	0%	17%	11%	25%

Table 5.3-2: Distribution of anomalies by amplitude and number of peaks for 305 miles of track with a 0.7 inch threshold.

Note that using a 0.5 inch threshold a total of 175 anomalies were identified with amplitudes greater than 0.7 inch (Table 2.1.2-1). The discrepancy is caused by the routine in VUTRACK that calculates anomaly amplitude. The program calculates anomaly amplitude by taking the difference between the maximum and minimum values of the data over the entire anomaly. Thus, if the anomaly has multiple peaks, the amplitude over this anomaly can be the maximum from one single peak anomaly and the minimum from another single peak anomaly, giving a larger amplitude than any single peak variation within the anomaly. An anomaly with many peaks has a high likelihood of having its reported amplitude be incorrect. As threshold amplitude increases the number of peaks in multiple peak anomalies decreases. This reduces the number of

anomalies whose amplitudes are erroneously determined using the current method. This is the reason there is a 9% reduction in total number of anomalies identified with amplitude greater than 0.7 inch, but none of the anomalies eliminated really have amplitudes greater than 0.7 inch. It is likely that there were multiple peak anomalies in the distribution of anomalies using a 0.7 inch threshold that had reported amplitudes greater than the maximum single peak anomaly amplitude.

A goal of this case study was to develop an approach for selecting the anomalies that exceed the threshold value. With the current set of tools, a 486-PC and NUCARS, 161 simulations, one per anomaly, takes about 36 hours of computer time. The initial setup for this number of runs, identifying and extracting anomalies and creating the input files for NUCARS, would take about 24 hours of labor. The time to perform a simple peak load determination study would be about 19 hours of labor. Thus, the first set of runs would take at least a calender week. Subsequent setup times would be about 2 hours to change the value of simulation speed in every input file. Assuming that 10-161 run simulations are necessary for a fatigue load study, there would be a total of 360 hours of simulation time. If all the simulations could be done in one large batch file, it would take 15 days of continuous computer time to perform. Total time for setup and peak load determination would be 232 labor hours, about one and one-half months of labor. Thus, the total time from start to finish would be about two months. This is a long period of time. An approach to reduce the number of simulations necessary has been developed.

The line traversing Table 5.3-2 divides the groups of anomalies with more than 5% of the total number of anomalies from those groups with less. It was assumed that the groups of greater than 5% can be represented by a random sampling of one-third of the

members within the group. Of the 139 anomalies within the these groups only 47 of the anomalies are used for simulations. All of the 22 anomalies in groups of less than 5% are used in simulations. The number of anomalies used in simulations is reduced to 69, or 43% of the original set of 161.

The 47 anomalies were chosen randomly and these plus the 22 others were extracted. Simulations were made with the articulated flat car at 78 mph over the anomalies and the peak load factor was calculated for each simulation. Figure 5.3-4 is a plot of the peak load factor predicted over each anomaly versus anomaly amplitude. There were 10 exceedences of the 1.5 load limit ratio. Seven of the exceedences occurred on anomalies that were in the groups of *less than 5% of the anomalies*. The other three all occurred in the 0.8-0.9 inch, 2 peak anomaly group. Table 5.3-3 lists the anomalies that caused exceedences.

Amplitude range	Number of Peaks	Amplitude	Load Factor
0.8-0.9	2 2 2	0.874 0.832 0.833	1.54 1.50 1.58
0.7-0.8	3	0.798	1.51
0.9-1.0	2	0.924	1.63
1.0-1.1	1 2 4	1.046 1.024 1.086	1.57 1.60 1.55
>1.1	3 3	1.238 1.248	1.74 1.61

Table 5.3-3: Anomalies that caused significant fatigue loads.

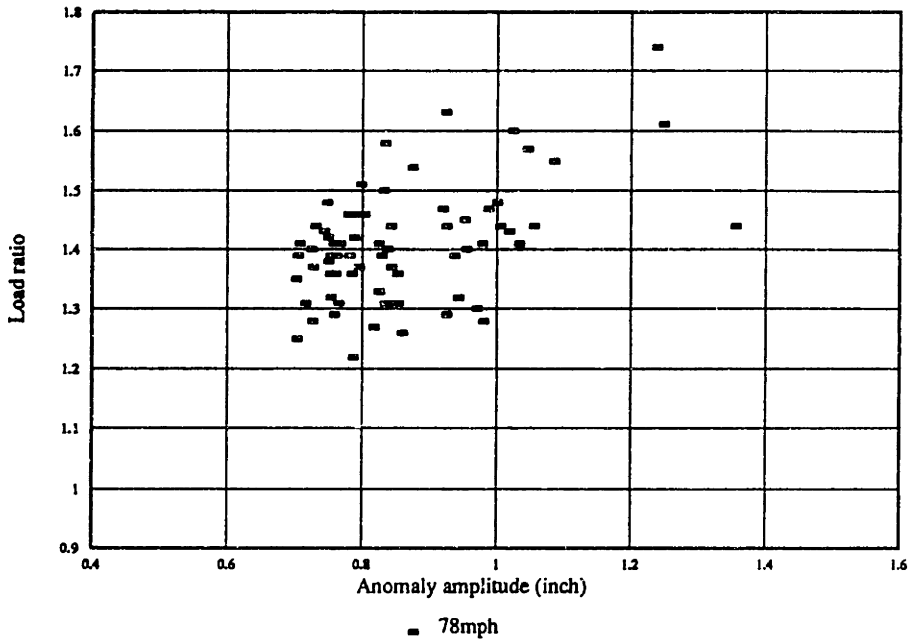

Figure 5.3-4. Peak load factor over 69 anomalies with amplitude greater than 0.7 inch versus amplitude

Not shown in Table 5.3-3 are the results of one simulation over a 1 peak, 0.758 inch anomaly where load ratio of 1.54 was predicted. This anomaly is in the group of 72 single peak, 0.7-0.8 inch anomalies. Observation of the anomaly revealed that an anomaly with amplitude of about 0.6 inches directly preceded this anomaly. This variation was picked up by the anomaly augmentation routine. Preceding the smaller anomaly was another variation with about 0.5 inch amplitude which was not included in the original anomaly. This geometry variation was unlike any of the other 23 anomalies in this group. It was decided to re-extract and simulate the anomaly using two track lengths of augmentation to include all the variations around the anomaly. The resulting

peak load ratio was 1.48, 4% lower than the original prediction. It must be assumed that extracting more track data around the anomaly results in a more accurate load prediction. Therefore, it was concluded that the original value was erroneous and was caused by fictitious transients occurring because the lead-in track was not long enough.

Another anomaly in this group of 72 (also not shown in the table) came close to exceeding the 1.5 limit. The predicted peak load ratio over this anomaly was 1.49. Observation of this anomaly revealed no large amplitude variations in the vicinity like the previous anomaly. The anomaly was re-extracted using two track lengths of augmentation and a simulation was performed. The new predicted peak load ratio over this anomaly was 1.46, a reduction of 2% from the original prediction. This and the results from the previous anomaly in this group suggest that the parameters used for the anomaly augmentation and extraction produce slightly conservative peak load predictions.

These results prompted the investigation of the 0.798 inch, 3 peak anomaly that caused a 1.51 load ratio, shown in Table 5.3-3. This was the only anomaly remaining with an amplitude less than 0.800 inch for which the first simulation predicted an exceedence. The anomaly was extracted with two rail lengths of augmented track data and the simulation was rerun. The resulting peak load factor was 1.51, exactly the same as the original prediction. Thus, this anomaly does cause an exceedence.

The maximum predicted peak load ratio within each group of anomalies is shown in Table 5.3-4. Those groups where significant fatigue loads are predicted are indicated in boldface. Notice that only in one group with 10 or more anomalies were significant bolster loads predicted. This is the 2 peak, 0.8-0.9 inch group, which contains 13

anomalies. Because three of five anomalies in this group were predicted to cause significant fatigue loads, the remaining anomalies were also extracted and simulations run to determine the peak bolster loads they caused. Three more anomalies in this group were found to cause significant fatigue loads. Six of the thirteen anomalies in this group cause significant bolster loads! The anomaly parameters and the peak load ratios for these anomalies are listed in Table 5.3-5.

number of peaks	0.7-0.8	0.8-0.9	0.9-1.0	1.0-1.1	>1.1
1	1.48	1.46	1.47	**1.57**	
2	1.44	**1.58**	**1.63**	**1.60**	
3	**1.51**		1.40	1.43	**1.74**
4		1.33	1.47	**1.55**	
5				1.44	
6					1.44

Table 5.3-4: Peak load ratio predicted in each group for 305 miles of track with a 0.7 inch threshold.

Note that no anomaly in either the 1 peak, 0.8-0.9 inch, or the 1 peak, 0.9-1.0 inch amplitude group caused significant bolster loads even though the amplitudes are equal or larger. And no anomaly in the 0.7-0.8 inch, 2 peak group cause significant bolster loads either. This demonstrates how the number of peaks and the amplitude of an anomaly are both significant measures of its potential of causing significant bolster loads. Of the 10 significant anomalies, one anomaly had only one peak, five had two peaks, three had three peaks, and one had four peaks. One of the anomalies had an amplitude less than 0.8 inches, three had amplitudes between 0.8 and 0.9 inch, one had an amplitude of 0.924 inch and five of the had amplitudes greater than one inch.

Anomaly Amplitude (inch)	Peak load ratio
0.832	1.50
0.833	1.58
0.868	1.57
0.874	1.54
0.876	1.63
0.896	1.53

Table 5.3-5: Anomalies in the 2 peak, 0.8-0.9 inch group that caused significant fatigue loads.

A study was done to determine the effect of increasing number of peaks in anomalies. The peak load ratio versus the number of peaks in the anomaly is plotted in Figure 5.3-5 for the original 69 anomalies. The figure shows that there is a correlation between increasing peak load factors and number of peaks in an anomaly *up to three peaks*. For four peak anomalies the range and maximum peak load ratios decrease. And for the five and six peak anomalies there is no peak load ratio above 1.5. Nine of the 10 anomalies which caused significant fatigue loads had one, two, or three peaks. Only one had four peaks. Investigation of the largest amplitude anomaly which had six peaks revealed that the reported amplitude of the anomaly is erroneous. The anomaly shape is a large dip of about a 0.7 inch followed by a relatively flat portion of track then a large spike of about 0.7 inch. The anomaly amplitude calculation routine reported the difference between these two disconnected extremes in track geometry (1.355 inches). The reason this multiple peak anomaly had six peaks was because there were a number of small peaks between the two large variations that were counted. These findings suggest that maintenance practices prevent anomalies from developing more than three peaks if the anomaly could cause significant fatigue loading. Perhaps this is because anomalies become quite visible when the number of peaks and amplitude becomes large.

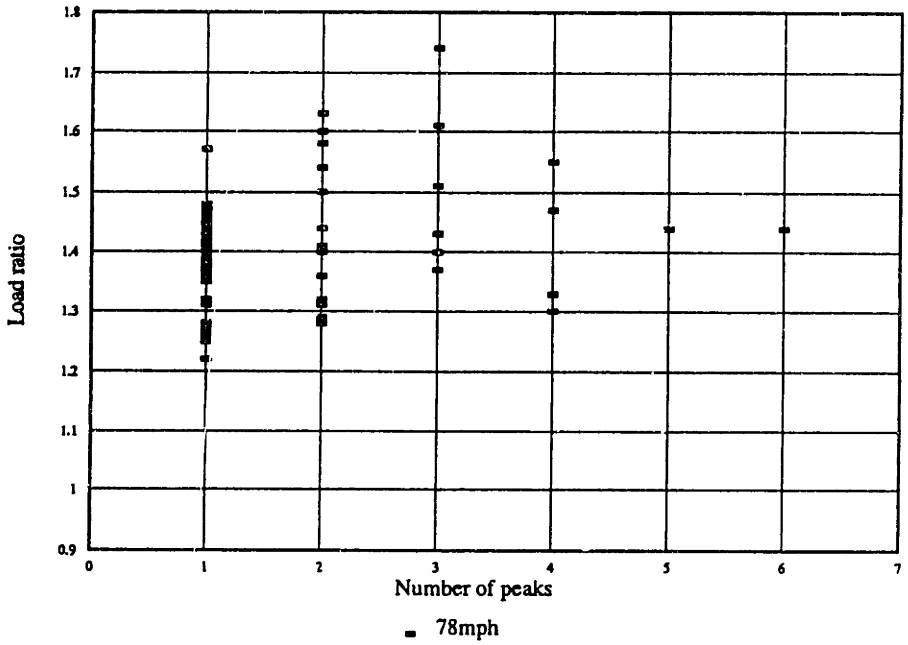

Figure 5.3-5. Peak load factor over 69 anomalies versus number of peaks in the anomaly

With the result of this preliminary study of the anomalies greater than 0.7 inch, the threshold can now be defined as a function of the number of peaks in the anomaly and the amplitude of the anomaly. The threshold for this data set is 3 peaks, 0.7-0.8 inch; 2 peaks 0.8-0.9 inch; 2 peaks 0.9-1.0 inch; 1 peak 1.0 inch or larger. The line traversing Table 5.3-4 shows the boundary of the threshold. In general, only those anomalies outside the threshold boundary need to be considered in the fatigue load analysis. But, in this case study all of the anomalies outside the threshold boundary have been individually used in simulations, therefore, all the anomalies that can cause significant fatigue loads have been

identified. Instead of 35 anomalies, only 13 anomalies need to be used in simulations.

Combining the advantages of the threshold amplitude determination and the grouping of anomalies, there is a reduction by a factor of 15 in the number of anomalies that need to be considered! Validation of the threshold amplitude allowed a reduction in the number of anomalies that must be considered, from 760 to 161, since it was known with confidence that anomalies with amplitudes between 0.5 and 0.7 inch cannot cause significant fatigue loads. And, of the 161 anomalies greater than 0.7 inch amplitude, only 13 anomalies need to be considered in order to find the anomalies that could cause the largest fatigue loads.

Finally, the time to perform a simple fatigue load study is determined. For 13 anomalies, one simulation per anomaly would take about 3 hours of computer time. The initial setup for this number of runs, identifying and extracting anomalies and creating the input files for NUCARS, would take about 2 hours of labor. The time to perform a simple peak load determination study is about 1 hours of labor. The time to perform 130 fatigue load determinations would be about 3 days. The amount of time to find the thirteen anomalies that are used in the fatigue load study would be about 2 days. Thus, the whole study could be performed in about one week.

6 Conclusions and discussion

The primary goals of this two year MIT research effort were to develop a methodology to compute freight car fatigue loads from track-vehicle models, to demonstrate the methodology on an extensive set of track data, and to evaluate the ability of the methodology to accurately predict fatigue loads in rail cars due to track anomalies.

The methodology that was developed finds all the track geometry variations that could cause significant fatigue loads, uses these actual geometric variations as the track input in computer simulations of the vehicle-track interaction, and then determines the resulting fatigue loads. The methodology was implemented in a six step process: vehicle modelling, track data analysis, threshold analysis, anomaly extraction, simulation, and fatigue load analysis.

Computer programs were developed to perform specific steps of the methodology. These programs are able to process large volumes of track data, identify and extract all significant anomalies, find the precise location on the track of each anomaly, and produce important information about each anomaly such as its amplitude, length, and the number of peaks. The extracted anomalies are then used as the track geometry input to the NUCARS program to determine vehicle response and the resulting fatigue loads.

The methodology currently is fully developed and provides the tools necessary to predict the fatigue life of a new car at the design stage. To reach this capability, a large volume of track data was acquired, processed, and analyzed. Long lengths of track were characterized by a relatively small number of anomalies of different amplitudes and number of peaks. The anomalies were classified under two headings: amplitude and number of peaks. This produced a data base from which anomalies were pulled for the

determination of fatigue loads. Anomaly amplitude was shown to be the primary factor influencing car fatigue loads. The number of peaks (a measure of the potential number of cycles of repeated variations) is the second most important factor influencing vehicle response.

The ultimate use of the methodology is to predict the fatigue life of a rail car at the design stage. This is accomplished by modelling the car in NUCARS and selecting a set of anomalies representative of the track the car will traverse over its life. Then a threshold analysis is performed, and the anomalies with amplitudes greater than the threshold amplitude are extracted. NUCARS simulations for each anomaly over a range of car operating speeds are performed, and the fatigue load histories are extracted. Finally, a rainflow analysis is performed, and the fatigue life of the car or component is predicted. To perform this analysis a very large data base of anomalies, representing the track the car will see in revenue service, must be created.

The efforts reported in this, the second report, are aimed at evaluating and furthering the methodology and giving it the capability of processing large volumes of track data. Thus, the work performed in this study focused on the second through fourth steps: track data analysis, threshold analysis, and anomaly extraction. To this end, an improved technique was developed for extracting anomalies, which replaces the threshold extension factor technique. This new technique allows the addition of any desired length of data to the end of an anomaly, and will lengthen an anomaly segment, if necessary, to ensure that the amplitude at the end points of the segment are not greater than a specified maximum. This technique guarantees that a sufficient buffer of track can be added to allow the transients caused by the initial conditions of the simulation to settle.

A significant advance to the overall methodology is the development of a rational methodology for determining the threshold amplitude. This method of finding the minimum anomaly amplitude that can cause significant fatigue loading ties together the interactions between the vehicle and track which produce fatigue loads.

Severe dynamic response is theoretically possible for certain cars at resonance on track geometry variations as small as 0.5 inches. However, a large number of repeated variations are necessary. A study of 305 miles of track data was performed to determine if this condition occurred. This study showed that there is very little probability for repetitive geometric variations (so called multiple-hit anomalies) in anomalies with amplitudes less than 0.6 inch peak-to-peak. A threshold amplitude analysis for a car of this type showed that anomalies of at least 0.7 inch are necessary on this track to have the potential of causing bolster loads in excess of 150% of static. These results provided the reason for using a anomaly threshold of 0.7 inch, which reduced by a factor of four the number of anomalies that had to be considered in the fatigue load analysis.

The PFILT computer programs, which embody the anomaly identification and extraction parts of the methodology, have been improved in a variety of ways. Improvements in data reporting include: reporting of the amplitude, length, number of peaks, and track location of every anomaly.

All the programs were updated to allow for the processing of large volumes of track data. The most significant improvement in this regard is the ability to enter all the input to the programs on the command line, thus allowing simple and extensive batch file processing necessary for large data sets.

To achieve the above results and conclusions, 328 miles of track data were analyzed, and three case studies of the methodology were performed. The track data consisted of three sets of data from distinct locations, and the case studies utilized two sets of vehicle characteristics: the paintspotter car and a three platform articulated flat car.

And finally, the documentation was enhanced, including an update to the PFILT user's guide and documentation of the discrete-time differentiating filter originally presented in Allen (1992).

The research described herein focused on finding the track geometry anomalies that cause large fatigue loads so that cars could be better designed to withstand the fatigue environment that exists on the track. There are also potential benefits to be derived from this research in track maintenance practices.

Currently, railroads use statistical track surface roughness indexes to determine the condition of the track. These indexes typically measure the variance of track surface from the mean over a short segment of track. The value of the variance is called the track quality index (TQI) (Roney and McIveen, 1991). When the TQI of a segment of track exceeds some limit determined by experience, the track surface has degraded. But, only when the TQI of a number of contiguous segments exceed the limit is the track resurfaced. The track segments are typically 500 ft long. Special track features such as switches, bridges and grade crossings are taken out of the data.

There are limitations inherent in the current practice and costly surface maintenance practice is required to compensate for it. The variance is a statistical measure of the difference from the mean value of the geometry of the whole track segment, but anomalies have geometries which are by definition outside the norm. A large TQI

indicates a track segment with the potential of causing severe dynamic response of cars, but not necessary a track segment with an anomaly on it. Since anomalies occur only rarely and the peaks are isolated. it is not guaranteed that a large TQI will occur on a segment with an anomaly on it, i.e. whether the variance is sensitive enough to pick up a track segment that contains an anomaly. Thus, large sections of track with no anomalies may be resurfaced at considerable cost. At the same time, anomalies that may be missed by the TQI remain on the track causing severe car and track loads.

Another limitation of the TQI is the removal of special track features. Anomalies are likely to occur at these points since the subgrade and rail stiffnesses can change significantly over these points. These tend to cause vehicle responses that put dynamic loads on the track which leads to geometry degradation. Neglecting these locations in track surface maintenance scheduling may leave anomalies on the track with cause severe car and track loads.

Track surface maintenance planning based on anomaly identification offers the possibility of improved track conditions at lower cost. Using the methodology presented in this report, all the anomalies in the track data can be identified and classified. The potential loads that each anomaly can cause can be estimated and the anomalies listed in order of the severity. *The anomalies can be located on the track and repair of the track surface at just the anomaly can be performed.* The resurfacing of several segments of track which may or may not have an anomaly is eliminated. This approach also guarantees that there are no locations on the track where the load exceed a prescribed limit.

Using anomaly detection, time and money is saved in track surfacing costs since anomalies typically are about 100 feet in length while the TQI requires resurfacing of a number of contiguous 500 foot track segments. The approach should also lead to longer car life and longer track maintenance cycles since the large loads which lead to rapid component fatigue and track deterioration are eliminated.

These are the potential benefits of an anomaly detection approach to track surface maintenance. Research should be conducted to determine the viability of this approach, the benefits and limitations of its use. A technical and economic comparison of the two methods should also be conducted.

Bibliography

Allen, J.J., "Track-Based Fatigue Load Determination in Rail Vehicles," Master's Thesis in Mechanical Engineering, Massachusetts Institute of Technology, Cambridge, 1992

Blader, F., and Klauser, P., "User's Manual for NUCARS Version 1.0," Report R-734, Association of American Railroads, Chicago, September 1989.

Den Hartog, J.P, Mechanical Vibrations, Fourth Ed. McGraw-Hill, New York, 1984

Hamid, A., Owings, R., and M. Kenworthy, "Characterization of Relatively Large Track Geometry Variations," DOT-TSC-FRA-81-18, U.S. Department of Transportation, Washington D.C., March 1982.

Hamid, A., Rasmussen, K., Baluja, M., and T-L Yang, "Analytical Descriptions of Track Geometry Variations, Volume 1-Main Text" Report number DOT/FRA/ORD-83/03.1., U.S. Department of Transportation, Washington, D.C., December 1983

Kalaycioglu, S., and Ali Tajaddini, "Locating Vertical Track Irregularities Which Cause Excessive Vehicle Loads," Report R-694, Association of American Railroads, Chicago, March 1988.

Roney, M.D., and E.R. McIlveen, "Predicting the future needs for programmed track maintenance on CP rail," Presented at the International Heavy Haul Railway Conference, Vancouver, B.C. Canada, June 1991.

Schwarz, B., Weinstock, H., Greif, R., and R. Briere, "An analytical study of the bounce motion of a freight car model in response to profile variations," Presented at the Winter Annual Meeting of the American Society of Mechanical Engineers, Applied Mechanics/Rail Transportation Symposium-1988, AMD-Vol.96, RTD-Vol.2, American Society of Mechanical Engineers, New York, December 1988.

Singh, S.P., 1992, Discussion at a meeting of the AAR Affiliated Lab at the Massachusetts Institute of Technology., Cambridge, July 1992.

"Track Safety Standards," U.S. Department of Transportation, Federal Railroad Administration, Office of Safety, Washington, D.C., January 1992.

Appendix A:

Threshold-based anomaly detection:

Documentation of the methodology including detailed presentation of discrete-time differentiating filter

A1 Threshold-Based Anomaly Identification

A systematic method for identifying and extracting anomalies from a set of track profile data is proposed in Allen (1992). The method developed is actually a modified application of a feature-based extraction method used in Fu (1977) which was also based on data peaks. The procedure searches through the data seeking the peak characteristics which are associated with anomalies, and extracts them accordingly.

In Hamid et al (1983), an anomaly was described as a displacement in the track geometry, lasting between 20 and 100 feet. Of the various features characterizing a discrete anomaly, the *magnitude* most influences the dynamic response of the vehicle. Thus, an anomaly should have some minimum magnitude (define as a peak-to-peak rail displacement over some maximum interval) for consideration as a *significant* anomaly. The precise magnitude of an anomaly which makes it a significant anomaly is vehicle dependent and must be determined through experimental characterization of the dynamic load response.

Anomalies are always associated with some form of peaking in the data. Give this fact, it is reasonable to assume that windows about all peaks will capture all displacements which exceed a defined magnitude threshold. It follows, then, that it should only be necessary to do window analysis at each data peak rather than each data sample. The detection and extraction procedure involves moving a window of fixed length to each peak within the data, and calculating the maximum profile displacement within the window. The computational cost saved by peak-to-peak analysis are significant, especially when one considers that a few miles of track can have many thousands of samples, depending on the sampling rate.

A2 Preprocessing

The anomaly detection and extraction strategy presented is best illustrated using the example depicted in Figure A1. Figure A1(a) shows the preprocessing stage in which the profile data are passed through a digital differentiating filter (Oppenheim, 1989) to identify locations of the data peaks.

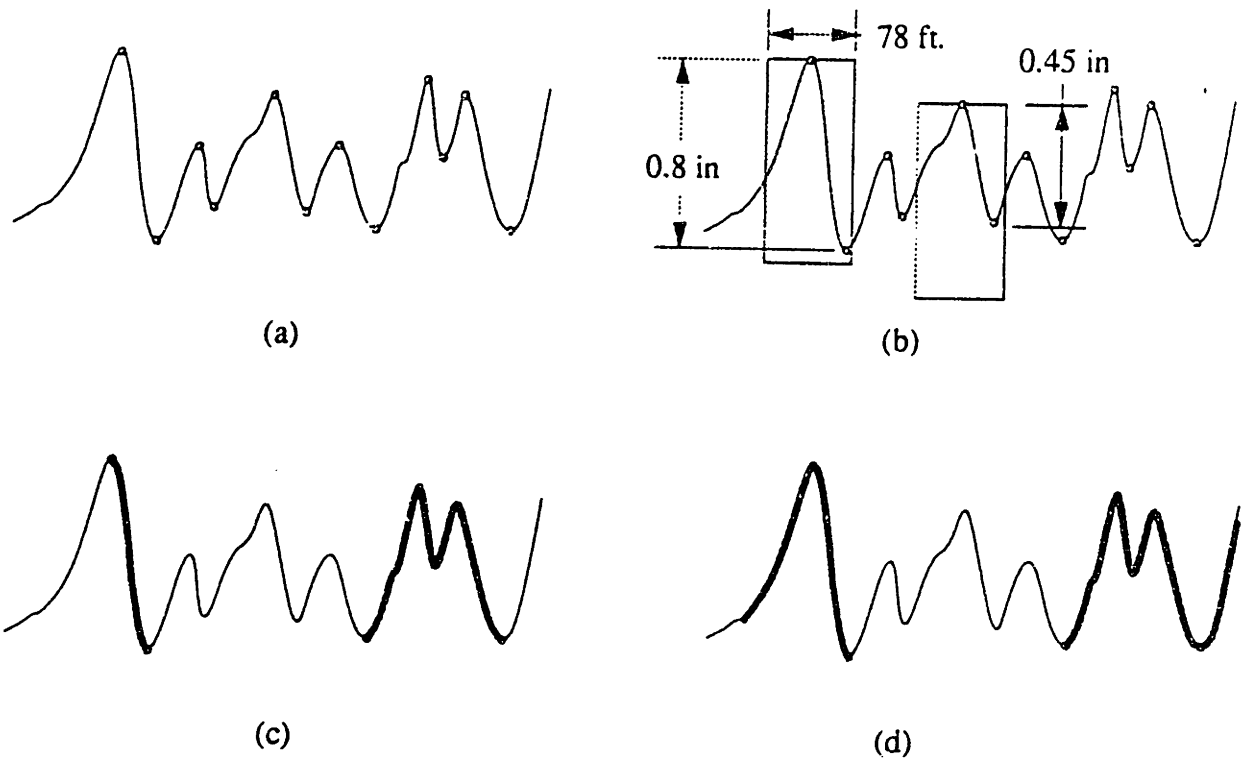

FIGURE A1: Threshold-based anomaly detection

This is the first step in the anomaly detection method. The input data is a sequence of numbers, i.e. a discrete representation of the track surface profile. The output desired is the derivative of the data. The method employed to determine the derivative is to use a discrete-time differentiating filter. This linear time-invarient system determines the derivative of the data by convolving the input sequence with the impulse response of the differentiating filter system, as explained below[1]. Note, in the following discussion the independent variable is referred to as time, not distance or location along the track. This is for brevity and in keeping with the nomenclature used by practitioners of discrete-time filtering.

A2.1 Input Sequence Representation

Any sequence of numbers can be represented as a sum of scaled, delayed impulses. Consider the 40 point data stream presented in Figure A4. Given the first three points samples of this sequence x[0] = 0.1620, x[1] = 0.1540, and x[2] = 0.1450, the sequence can be expressed

$$x[n] = 0.1620\,\delta(n) + 0.1540\,\delta(n-1) + 0.1450\,\delta(n-2) + \ldots$$

where

$$\delta[n-k] = \begin{cases} 0 & n \neq k \\ 1 & n = k \end{cases}$$

is the discrete-time impulse.

The significant property of the unit impulse is that it has a value of zero for all time **except** where its argument is zero, when its value is equal to one. The sequence is not zero between integer values, but simply undefined.

More generally, the data sequence, x[n], can be represented as a sum of scaled, delayed impulses in the form:

$$x[n] = \sum_{k=-\infty}^{\infty} x[k]\,\delta[n-k] \qquad eq.\ A1$$

---

1 The explanation of the discrete-time differentiating filter is included for the sake of completeness. Utilizing the filter to determine the derivative does not necessitate understanding how the filter works, just as driving a car does not require the driver to know how an internal combustion engine works.

This representation of the input sequence is very important as will become clear in the following section.

A2.2 Linear time-invarient systems

The desired output from the filter is the derivative of the input sequence. The filter can be thought of as a system that transforms the input sequence, x[n], into the derivative, y[n], symbolically shown in Equation A2.

$$y[n] = T\{x[n]\} \qquad eq.\ \ A2$$

where T{•} is the symbolic representation of the system which operates on the input sequence to produce the output.

By inserting the series representation of the input sequence into Equation A2 the output the system can be expressed

$$y[n] = T\left\{\sum_{k=-\infty}^{\infty} x[k]\delta[n-k]\right\} \qquad eq.\ \ A3a$$

The operation of differentiation is linear and time-invarient, and it follows that a discrete-time differentiating filter is also a linear time-invarient system. The property of linearity allows important simplifications to take place. The first property of linearity is superposition, i.e. the response of the system to the series, is the sum of individual responses of the system to each member of the series. This is shown in Equation A3b.

$$y[n] = \sum_{k=-\infty}^{\infty} T\{x[k]\delta[n-k]\} \qquad eq.\ \ A3b$$

The second property of linearity is the scalar property. This property says that any multiple of a unit input causes the unit response scaled by the same multiple. Since the amplitudes of the input series are merely constants, it follows that Equation A3b can be further simplified

$$y[n] = \sum_{k=-\infty}^{\infty} x[k]T\{\delta[n-k]\} \qquad eq.\ \ A3c$$

The last term in the above equation, $T\{\delta[n-k]\}$, is the response of the system to a unit impulse at n=k. Like a hammer striking a bell, the impulse is nonzero at only one time, namely at n=k, whereas response of the system to that impulse can be of infinite length. A causal system, like a bell, will have no response at any time before n=k. If the impulse is shifted by a certain amount of time, say τ, then the response of a time-invarient system is also shifted by the same τ. With this, Equation A3c is written in final form as

$$y[n] = \sum_{k=-\infty}^{\infty} x[k]h[n-k] \qquad eq.\ A4$$

Where $h[n-k]$ is the response of the linear-time invarient system to a unit impulse at n=k.

Thus, the output of the system at any time n is the sum of all the impulse responses due to all the impulses occurring before n, properly weighted by the input sequence amplitudes and superposed in time. The above equation has a special form called a convolution sum and the equation says: the derivative at n is the convolution of the input sequence with the impulse response.

A2.3 Impulse response of a linear-time invarient system

The purpose of this section is to present the impulse response of the discrete-time differentiator. However, before entering the realm of the discrete, the impulse response of a continuous-time filter is presented. The procedure and results for the discrete-time system are analogous.

First, we desire the impulse response of the continuous-time differentiator. This system is schematically illustrated in the Figure A2. A sequence of impulses come into the system and the system operates upon them to produce the impulse response.

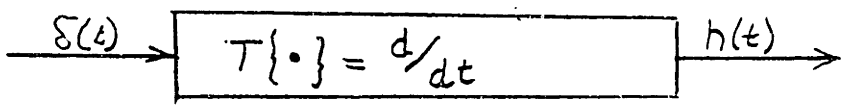

FIGURE A2. Continuous-time differentiator system.

The time domain equation associated with this system for a single impulse is

$$h[t] = T\{\delta[t]\} = \frac{d}{dt}\delta[t] \qquad eq.\ A5$$

First, to determine the impulse response, the Fourier transformation of the system is determined. This transforms the system from the time domain to the complex frequency domain. Let $\hat{\delta}(j\omega)$ be the Fourier transformation of the function $\delta(t)$. Recall the following property of Fourier transformations, which relates the Fourier transform of the derivative of the unit impulse to the Fourier transform of the unit impulse function.

$$\delta(j\omega) = j\omega \quad \delta(j\omega) \qquad eq.\ A6$$

where j is $\sqrt{-1}$ and ω is circular frequency.

Generally, the impulse response equation in the frequency domain has the following form

$$H(j\omega) = S(j\omega)\Delta(j\omega) \qquad eq.\ A7$$

which equates the impulse response, $H(j\omega)$, to the system frequency response, $S(j\omega)$, multiplied by the input frequency response, $\Delta(j\omega)$.

The frequency response of the derivative is the system in Figure A2. Mapping Equation A6 into Equation A7, the system frequency response is $j\omega$.

Next, the Fourier transformation in the frequency domain of a unit impulse is determined[2]. The Fourier transformation of a unit impulse is identically one (1), i.e. an impulse has equal proportions of all frequencies within it. Thus, the impulse response in

---

2 The Fourier transformation of a continuous function is

$$\hat{X}(j\omega) = \int_{-\infty}^{\infty} x(t)e^{-j\omega t}dt$$

And the inverse Fourier transformation equation is

$$x(t) = \int_{-\infty}^{\infty} \hat{X}(j\omega)e^{j\omega t}d\omega$$

The following is the definition of the unit impulse $\int_{-\infty}^{\infty} \delta(t)f(t)dt = f(0)$

the frequency domain, Equation A7, is identically the system frequency response.

$$H(j\omega) = j\omega \qquad -\infty < \omega < \infty \qquad eq.\ A8$$

To find the impulse response of the system in the time domain, the inverse Fourier transformation formula is applied. However, the frequency response of this system is infinitely long, making the inverse Fourier transformation computationally impossible.

The system we desire the impulse response to is the discrete-time differentiator. This system is

$$h[m] = T\{\delta[m]\} = \frac{d}{dm}\delta[m] \qquad eq.\ A9$$

Analogous relationships exist for the system frequency response of discrete and continuous time systems. Since we are considering discretized input, the input sequence is limited to a frequency band bounded by the sampling rate. Thus, we need only to define the system response over the same range of frequencies as the input sequence. This is accomplished by normalizing the frequency response by the sampling rate, T. The resulting discrete time system has frequency response

$$H(e^{j\omega}) = \frac{j\omega}{T} \qquad -\pi < \omega < \pi \qquad eq.\ A10$$

Here the argument of the frequency response is $e^{j\omega}$ to indicate that it is periodic with period 2π. Unlike the continuous-time system, the inverse Fourier transformation of this system can be realized because the limits on the frequency range. Applying the inverse *discrete* Fourier transform equation

$$h[m] = \frac{1}{2\pi}\int_{-\pi}^{\pi} H(e^{j\omega})e^{j\omega m}d\omega \qquad eq.\ A11$$

the impulse response of the differentiator is

$$h[m] = \frac{\pi m \cos m - \sin \pi m}{\pi m^2 T} \qquad -\infty < m < \infty \qquad eq.\ A12$$

Thus, if a discrete-time system with this impulse response were used, the output for any band-limited input would be the derive of the input. However, the impulse response of this filter is infinitely long making the calculation computational unrealizable. The simplest way to obtain a finite length impulse response is to truncate it. If we define $h_w[m]$ as a new system with impulse response given by

$$h_w[m] = \begin{cases} h[m] & 0 \le m \le M \\ 0 & otherwise \end{cases} \qquad eq.\ A13$$

The new system is a "windowed" impulse response with a window length of M+1 samples.

This introduces a linear phase shift in the system response equal to M/2 samples, i.e. half the window length. The Fourier transformation of an input time delay of M/2 samples is $e^{-j\omega M/2}$. Thus, the impulse frequency response of this system is

$$H(e^{j\omega}) = \frac{j\omega}{T} e^{-j\omega\frac{M}{2}} \qquad -\pi < \omega < \pi \qquad eq.\ A14$$

And the corresponding impulse response is:

$$h[m] = \left(\frac{1}{T}\right)\left(\frac{\cos\pi(m - M/2)}{m - M/2} - \frac{\sin\pi(m - M/2)}{\pi(m - M/2)}\right) \qquad -\infty < m < \infty \qquad eq.\ A15$$

A2.4 Derivative of the Input Sequence

We now have all the results necessary to determine the derivative of the input sequence. We need only to define the window length of the filter to proceed. The window is a low pass filter where the cutoff frequency is determined by the window length. If the window length is one, then every data point is a peak. If the window length is infinite, then there are no peaks because the impulse response is zero. Generally, the longer the window the more prominent a peak must be in order to be identified by the filter. A window length of ten was chosen. Thus, all peaks surrounded by variations of less than ten samples are filtered out. For a filter with M equal to 10, the impulse response of the system is given by:

$$h_w[m] = \left\{ \begin{array}{ll} 0 & m = M/2 \\ \dfrac{\cos \pi(m - M/2)}{m - M/2} & 0 \le m \le M \\ 0 & otherwise \end{array} \right\} \qquad eq. \quad A16$$

This produces the antisymmetric impulse response sequence listed below and plotted in Figure A3.

$h[m] = \{0.2, \ -0.25, \ 0.33, \ -0.5, \ 1.0, \ 0, \ -1.0, \ 0.5, \ -0.33, \ 0.25, \ -0.2\}$

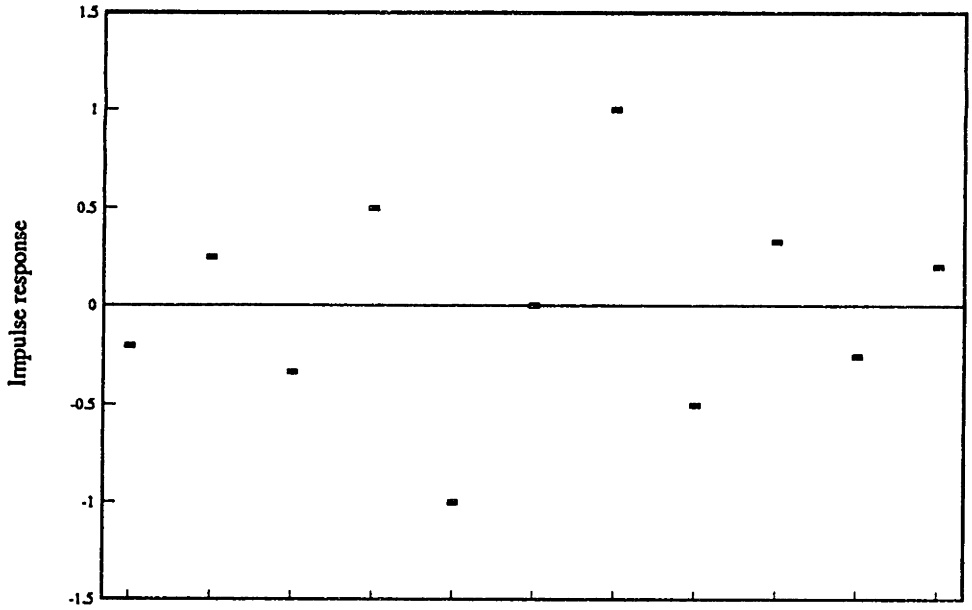

FIGURE A3. Impulse response of an 11 point discrete-time differentiator.

With this we can now realize the derivative of the input sequence. Because the derivative lags the input sequence by 5 samples, Equation A4 is rewritten

$$y[n-5] = \sum_{k=n-10}^{n} x[k] h_w[10-(k-n)] \qquad eq. \quad A17$$

Equation A17 tells us that the derivative at sample n is the convolution of the 11 data points centered on sample n with the impulse response of the discrete-time filter.

Consider the 40 sample sequence shown in Figure A4. The amplitude of the sequence and the derivative computed by the above formula are shown at each integer. The line connecting the points is merely for illustrative purposes and does not imply either sequence takes on values between samples.

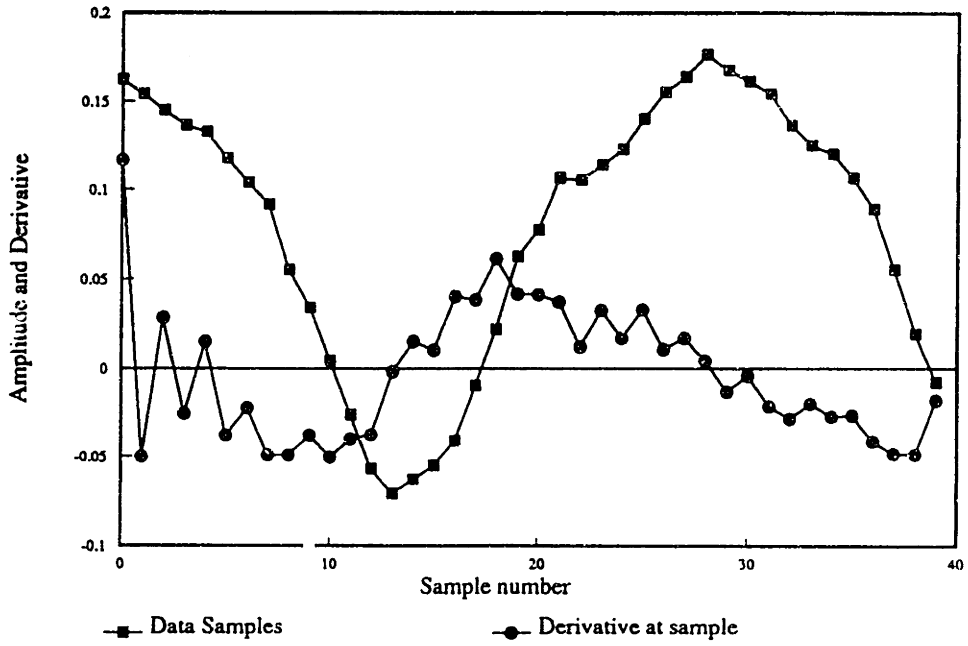

FIGURE A4. Data stream and its derivative.

The calculation of derivative of the first and last five points of the sequence require data outside the range of the sequence. To enable calculation of the derivative, zeros are padded to the ends of the sequence. Since non-real, zero inputs are used at the ends of the sequence the first and last five points are only approximate. This is not a problem since actual input sequences tend to be many thousands of samples thus the lost accuracy due to approximating with zero padding is negligible.

A3 Processing

Peaks are detected by noting the indices where the sign of the derivative changes. When peaks are located in the data, they are represented by the discrete-time series index.

This index is then signed according to the orientation of the peak. For example, a concave downward peak located at sample 613 in the data would be marked at n = -613. (This notation assumes that the series stars at n>0.) The preprocessing stage creates a list of these indices which locate each sequential peak and its orientation

A window of track data about each peak is then analyzed as seen in Figure 1(b). If the location of a data peak is:

$$|I_l| \equiv peak\,location$$

and $$S = sgn(I_l) \equiv sign\,of\,peak$$

then the window, W, centered about that peak with length 2M+1 is:

$$W = \{Zn\} \qquad (|I_l| - M) \le n \le (|I_l| + M) \qquad eq.\ A18$$

where Z[n] is the value at sample n.

The profile transition from the peak to any point inside the window is defined as:

$$\Delta Z = S(\ \ Z[n] - Z[|I_l|]\ \ ) \qquad eq.\ A19$$

Thus, the maximum transition distance is:

$$\Delta Z_{max} = \max\{S(\ \ W - Z[|I_l|]\ \ )\} \qquad eq.\ A20$$

If $\Delta Z_{max} > T$, the threshold, then peak I_l is categorized as a significant peak. This analysis is conducted for all of the peaks, which will reduce the original peak list to a shorter list consisting of only significant peaks.

In Figure 1(b), a 78 foot window is used. If the threshold were 0.5 inches, the peak of the window to the left would be considered a significant anomaly peak while the other windowed peak to the right would not.

One the analysis at each peak is completed, any neighboring significant peaks (those which lie within a half-window length, M, form each other) are connected, as depicted in Figure 1(c). this stage capture the actual profile transitions which characterize all anomalies. Beginning with the first, significant peak, peaks are grouped as follows:

Let $I_L = I_1$, the location of the first peak

if $|I_{L+1}| - |I_L| < M$

then if $|I_{L+2}| - |I_{L+1}| < M$

then if $|I_{L+3}| - |I_{L+2}| < M$

and so on until $|I_{L+m+1}| - |I_{L+m}| < M$

The first anomaly would thus consist of the set of samples from I_L to I_{L+m}:

$$A_1 = \{Z[n]\}, \qquad |I_L| \le n \le |I_{L+m}| \qquad eq.\ A21$$

The start of the next anomaly would then begin with $I_L = I_{L+m+1}$, and the above iterations repeated. This completes anomaly identification.

A4 Anomaly Extraction

Anomaly extraction is use dependent on the use of the anomaly information. If one desires only to know where on the track the anomaly is and the shape of the anomaly then the extraction process is simply to copy the exact start and end points of the anomaly and the track data to a file. If, however, the anomaly is to be used for input to a dynamic simulation then the data needs to be augmented to assure that the simulation is accurate. The following section describes two techniques to augment and extract anomalies with the goal of assuring accurate prediction of vehicle dynamic response. These techniques allow some of the anomalies to be more fully formed and allows inclusion of sections of track that would make a significant dynamic load contribution. It also changes initial conditions for simulations by more accurately representing the track in the neighborhood of the anomaly.

A4.1 Threshold extension factor

The anomalies are augmented by connecting sections which do not exceed the threshold but are above some defined percentage of it. For example, the highlighted anomaly on the left in Figure 1(d) develops another section of track on the end with this segment augmentation. Using anomaly A_1 from Equation A21, the maximum transition from the significant peak I_1 to a point in the section of track to the left of it would be:

$$\Delta Z_{max} = \max\{S_1(W[n] - Z[|I_1|])\} \qquad |I_L| - M \le n \le |I_L| \qquad A22$$

and if

$$\Delta Z_{max} > \alpha T \qquad 0 < \alpha \leq 1 \qquad eq.\ A23$$

then the section of track up to the location of ΔZ_{max} is augmented to the anomaly. The above steps are then repeated for the section to the right of the anomaly by analyzing over the interval $|I_{L+m}| \leq n \leq |I_{L+m}| + M$.

A4.2 Track length addition

Here anomalies are augmented by extending additional lengths of track data of the adjacent track. This techniques allows all the anomalies to be more fully formed.

A4.3 Hermite cubic fits

When the anomalies are reconstructed from the data, the resulting end-points often leave a sharp discontinuity from the nominal track level to the actual ends of the anomaly definition. In Figure A5, the sharp discontinuity can be readily seen. Some smoothing is necessary, so that the dynamic simulation is not adversely affected by these sharp jumps. The following method uses a cubic polynomial to the end point to smooth these drop offs over the length of one window.

End point max discontinuity needs also to be controlled. The values of the end point are made a percentage of the threshold magnitude to assure that the smooth transition to the real data is not controlling the response of the vehicle by the time it hits the actual anomaly.

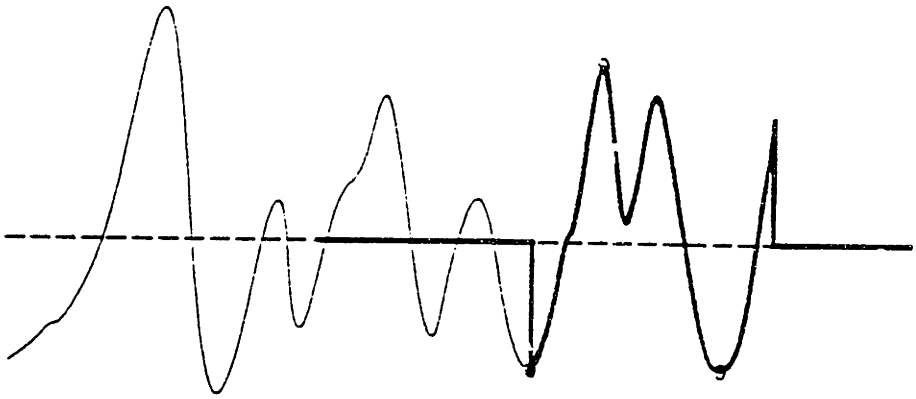

(a) Without smoothing

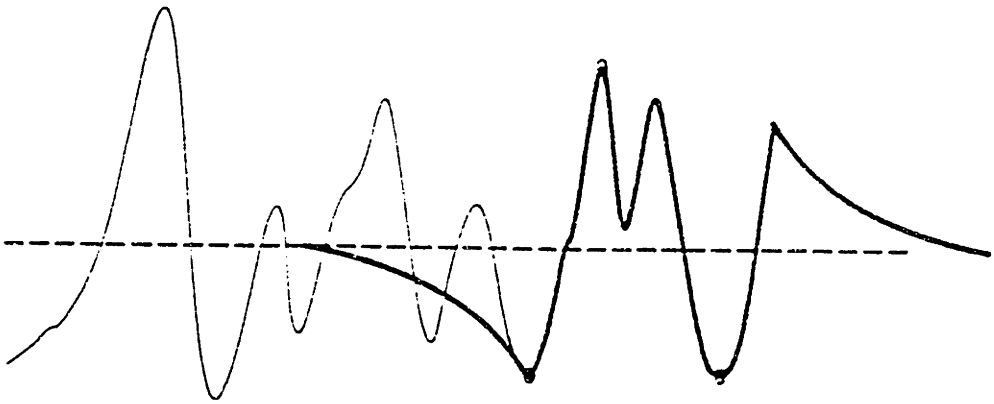

(b) With cubic spline smoothing

FIGURE A5: Polynomial smoothing at anomaly ends.

The polynomial is the Hermite cubic (Strang, 1986) whose general form is:

$$y = a(x-1)^2(2x+1) + b(x-1)^2x + cx^2(3-2x) + dx^2(x-1) \qquad eq.\ A24$$

The linear coefficients are determined simply by the displacement and slopes at the ends of the smoothing curves. Thus for the smoothing polynomial on the left of the anomaly, a is the displacement at the beginning of the polynomial, and b is the slope at the beginning. Similarly, c is the displacement at the end of the polynomial, where it connects with the anomaly, and d is the slope at that point. The coefficients a, b, and c are determined directly: a and b are both zero, since we want the smoothing curve to approach y=0 with a slope of 0; c is simply the edge displacement of the anomaly. The final slope coefficient, d, is calculated by finding the slope of the least-squares linear fit of the ten data samples leading up to the anomaly edge.

Bibliography

Allen, John J., "Track Based Fatigue Load Determination in Rail Vehicles," Masters Thesis, Massachusetts Institute of Technology, Massachusetts, January, 1992.

Fu, K.S., "Syntactic Pattern Recognition," Springer-Verlag, 1977.

Hamid, A., Rasmussen, K., Baluja, M., and T-L. Yang, "Analytical Descriptions of Track Geometry Variations," DOT Report DOT-FR-82-02, December 1983.

Oppenheim, Alan V., and Schafer, Ronald W., Discrete-Time Signal Processing, Pretence-Hall, New Jersey, 1989.

Strang, Gilbert., Introduction to Applied Mathematics, Wellesley-Cambridge Press, Massachusetts, 1986.

Appendix B:

PFILT user's guide supplement

PFILT Users Guide Supplement

Brandon Schwarz

Carl Martland

May 5, 1993

A Users Guide to the PFILT family of programs was included as Appendix A of John Allen's thesis, which was completed in January of 1992. Since that time, a number of improvements have been made to the programs, which require some changes in running the model. This document identifies the changes necessary to run the PFILT family of programs. It is intended to supplement, not replace, the original Users Guide.

The major changes are as follows:

1. A preprocessor (PREPROS) was added to convert raw data to the format required for DSTREAM.
2. The mile-post and feet were added to each of the input data records, which changes the format of many of the intermediate files. DSTREAM now creates six binary files: the left, right, average, and cross level profiles, and the mile-post and feet.

Running the Programs

This section explains how to use the PFILT programs. The sample input file, which is called DIAMON.RAW, was provided. The format of this file is shown at the top of Figure 1.

Each program can be run in two modes:

1. Interactive mode: the user enters the name of the program, hits return, and answers the questions
2. Command mode: the user enters the name of the program followed by the appropriate parameters, then hits return

PREPROS

Notice that the location of each record in DIAMON.RAW is shown as the mile-post plus feet, e.g. "13+5486." PREPROS removes the "+" from each record and creates a new file with the proper input for DSTREAM. This file will have the same name as the original file plus an extension .TXT (in this case DIAMON.TXT). This is a standard ASCII text file, as shown in the bottom of Figure 1.

In the interactive mode, PREPROS asks 2 questions:

1. What is the input data file (the name can be up to 6 characters)? **DIAMON.RAW**

2. How many leading rows are there in the input data set before the first line of geometry data? **2**

For the command mode, simply enter

PREPROS DIAMON.RAW 2

When the program is done, it displays the screen shown in Figure 2. Note that the length of the segment is calculated assuming that there is one record for every foot of track, which is the sampling interval for the data shown. The distance is *not* calculated by subtracting the beginning mile post plus feet from the ending mile post plus feet. If the sampling rate is not one record per foot, then the distance will not be calculated correctly in this version of the program. Also note that the distance between two successive mile posts does not always equal 5280 feet (for example, in figure 1, the first record begins at mile post 13 plus 5486 feet.)

DSTREAM

DSTREAM.EXE has two functions. Since binary data can be processed much faster than ASCII data, DSTREAM converts DIAMON.TXT into six separate binary files, one for each variable. The program also identifies the location of all of the peaks in the data base and produces separate binary files with an index of peaks for each of the geometry measurements. A peak is record where the measurement is higher (lower) than the measurement for both the preceding and following records. The following files are created:

DIAMON_L.DAT	Left rail measurement
DIAMON_R.DAT	Right rail measurement
DIAMON_A.DAT	Surface profile measurement
DIAMON_X.DAT	Cross level profile measurement
DIAMON_S.DAT	Curvature at this point in the track
DIAMON_M.DAT	Milepost
DIAMON_F.DAT	Feet

DIAMON_L.PKS	Left rail index of peak locations
DIAMON_R.PKS	Right rail index of peak locations
DIAMON_A.PKS	Surface profile index of peak locations
DIAMON_X.PKS	Cross level index of peak locations
DIAMON_S.PKS	Curvature index of peak locations

To run the program in interactive mode, enter DSTREAM and then hit return. The following information must be provided (sample responses are shown in bold type):

File name: **DIAMON.TXT**

Output header (this will be the first six letters of the name of each of the output files):

DIAMON

The type of profile measurement in the input file (xxxxxxxx.TXT), which can be either "L/R measurement" or "TGM format" is entered next. Some data sets, like the sample data, give the profile for the left and for the right rails. If this is the case, enter **1**. Other data sets, such as those used in the xxxxxxxx.TGM files used by NUCARS, give the

average profile and the cross level. If this is the case, enter **2**, and DSTREAM will estimate the left and right profiles as the average profile plus (or minus) half of the cross level.

The geometry measure being studied, either vertical (enter **1**) or lateral (enter **2**). *(Note that the program is designed to detect either vertical or lateral anomalies, but it has only been tested for vertical anomalies.)*

The number of columns in the input data: **6**

The number of the column containing the left profile: **3**

The number of the column containing the right profile: **4**

The number of the column containing the curvature: **5**

The number of the column containing the mile post: **1**

The number of the column containing the feet: **2**

Scale factor: if the measurements of profile and cross level are given in inches, enter **1.** If the measurements are not given in inches (sometimes they are given in volts), enter the scale factor that must be used to convert the measurements to inches.

To run the model in the command mode for the sample data set, enter the following command:

DSTREAM DIAMON.TXT DIAMON 1 1 6 3 4 5 1 2 1

When the program has been run, a screen shows the program parameters and lists the files that were created (Figure 3).

PFILT

PFILT.EXE will look at any of the xxxxxx_y.PKS files that are produced by DSTREAM.EXE. However, the program has only been tested for the mean profile, i.e. for xxxxxx_A.PKS. PFILT identifies the location of anomalies and creates an index file (xxxxxx_y.ANO) that contains the number of the record for the peak value of each anomaly.

To run PFILT in the interactive mode, enter PFILT and hit return. The program asks for the following information:

Name of the data file: **DIAMON_A**

The threshold for an anomaly, in inches: **0.7**

The sampling rate, in feet, in the original data: **1**

Half of the length of the window (in feet) that will be used to select data for the anomaly (i.e. this length of data will be searched on each side of the peak location): **39**

In command mode, enter the following for the sample data:

PFILT DIAMON_A .7 1 39

The output from PFILT includes a list of the anomalies along with the threshold parameters and the total length of the anomalous data (as shown in Figure 4).

NOTE: On some computers there is a bug so that PFILT will run only in the command mode, but not in the interactive mode.

VUTRACK

Using VUTRACK is the same as described in the original User's Guide with one addition. Options have been added to control the anomaly augmentation parameters; to set the length of leading and trailing track data added to the anomaly, and to control the maximum magnitude of the end data points of the spline fits.

On the first occurrence of either pressing <F5> or <F6> (save current anomaly or save all anomalies), the program will display the default augmentation parameters and prompt for keeping or changing the values (as shown in Figure 5). Pressing "D" for default will return the program to the save procedure. Press "C" for change and the program will prompt the user with three questions (as shown in Figure 6). When all three responses have been entered the program will echo the results. Pressing "C" to continue will return the program to the save procedure with the new parameters saved.

Input Filename: **DIAMON.RAW**

```
LOCATION LPROF RPROF CURVE SUPER

13+5486 .0513 .1250 .1700 0.000
13+5485 .0738 .1287 .1700 0.000
13+5484 .0863 .1450 .1800 0.000
13+5483 .0987 .1612 .1800 0.000
13+5482 .1112 .1700 .2000 0.000
13+5481 .1213 .1712 .1800 0.000
13+5480 .1238 .1587 .2000 0.000
13+5479 .1188 .1387 .2000 0.000
13+5478 .1188 .1162 .2000 0.000
13+5477 .1200 .1200 .2000 0.000
13+5476 .1262 .1325 .2000 0.000
13+5475 .1400 .1350 .1800 0.000
  .    .    .    .    .
  .    .    .    .    .
  .    .    .    .    .
```

INPUT
(RAW DATA)
ASCII file

Output Filename: **DIAMON.TXT**

```
13  5486  0.0513  0.1250  0.1700  0.0000
13  5485  0.0738  0.1287  0.1700  0.0000
13  5484  0.0863  0.1450  0.1800  0.0000
13  5483  0.0987  0.1612  0.1800  0.0000
13  5482  0.1112  0.1700  0.2000  0.0000
13  5481  0.1213  0.1712  0.1800  0.0000
13  5480  0.1238  0.1587  0.2000  0.0000
13  5479  0.1188  0.1387  0.2000  0.0000
13  5478  0.1188  0.1162  0.2000  0.0000
13  5477  0.1200  0.1200  0.2000  0.0000
13  5476  0.1262  0.1325  0.2000  0.0000
13  5475  0.1400  0.1350  0.1800  0.0000
.   .     .       .       .       .
.   .     .       .       .       .
.   .     .       .       .       .
.   .     .       .       .       .
.   .     .       .       .       .
```

OUTPUT from preprocessor
Same filename as input file with .TXT extension (ASCII text file)

FIGURE 1: Sample of input and output file for PREPROS.

Input data file name:== diamon.raw
Ouput data file name:== diamon.txt

Number text rows at beginning of input file :== 2
Rows of data in file :== 26526

Starting Milepost and Feet :== 13 5486
Ending Milepost and Feet :== 9 1
Length of data (miles) :== 5.02*

* Length is rows/5280, i.e. assuming one foot data sampling interval. This does account for the differences in length of "miles"(between mileposts), if the sample rate is 1/foot. The program could be modified to input the sampling interval. (Note this message is not part of the PREPROS screen display)

FIGURE 2: Screen display at completion of PREPROS

filename == diamon.txt
output header == diamon *(a)*
L/R measured (1), TGM format (2) == 1 *(b)*
Vertical (1) or Lateral (2) == 1 *(c)*
Num cols == 6 *(d)*
Left == 3 *(e)*
Right == 4
Milepost == 1
Feet == 2
Super col == 5
Scale factor 1.000000 *(f)*

(a) Six characters maximum
(b) The input data has left and right profiles, but some data might have mean profile and crosslevel (which is the .TGM format used for NUCARS). If .TGM, you add half the crosslevel to one profile and subtrack half from the other.
(c) This has only been used for vertical data, so enter 1.
(d) Number of columns of data
(e) Column number of left profile
(f) Scale factor to convert from volts to inches

The following data files are being produced:
diamon_L.DAT, diamon_L.PKS: Left Rail measured data
diamon_R.DAT, diamon_R.PKS: Right Rail measured data
diamon_A.DAT, diamon_A.PKS: Surface Profile data
diamon_X.DAT, diamon_X.PKS: Cross Level data
diamon_S.DAT, diamon_S.PKS: Curvature data
diamon_M.DAT: Milepost data
diamon_F.DAT: Feet data

FIGURE 3: DSTREAM user supplied input: This screen appears after you answer the last input questions and run the DSTREAM program.

Created: Thu Apr 29 23:09:09 1993

Anomaly Filename :== diamon_a.dat

Threshold value: 0.70 inches
Half-window length: 39.00 feet
Original data sampling period: 1.000 feet

Anomalies detected: 7
Cumulative length of anomalies: 248.0 (0.93%)

Total data length 26526.0 ft (5.02 miles)
Starting Milepost and Feet :== 13 5486
Ending Milepost and Feet :== 9 1

Anomaly Number	Amplitude (inches)	Num of Peaks	Length (feet)	Start		End	
				MP +	feet	MP +	feet
1	0.833		30.00	12	277	12	247
2	0.785	2	20.00	11	3138	11	3118
3	1.238	1	81.00	11	1170	11	1089
4	0.725	3	14.00	10	5024	10	5009
5	0.706	1	13.00	9	5210	9	5197
6	0.876	1	33.00	9	4890	9	4857
7	0.924	2	57.00	9	999	9	941
		2					

PFILT produces a summary file, DIAMON_A.STA, shown here. PFILT also create a binary file, DIAMON_A.ANO which tells VUTRACK the start and end of the anomalies.

FIGURE 4: Output from PFILT.

```
Anomaly Extraction Parameters
Default values:

The ends of each anomaly will be extended  1 rail length(s).
The default rail length is 39.0 feet.

Maximum amplitude of anomaly endpoints is 0.231 inches.
        Based upon the threshold of 0.700 inches.
        And extension percentage of 33.0%.


Press D for default values, C to change them:
```

FIGURE 5: Prompt in VUTRACK for option to change anomaly augmentation and extraction parameters.

```
Press D for default values, C to change them:c

Enter new value of number of track lenghts to extend :==2

Enter new value-rail length :==40

Enter new value of extension percentage (as a decimal) :==.25


The ends of each anomaly will be extended  2 rail length(s).
The rail length is 40.0 feet.

Maximum amplitude of anomaly endpoints is 0.175 inches.
        Based upon the threshold of 0.700 inches.
        And extension percentage of 25.0%.

Press C to continue:
```

FIGURE 6: VUTRACK screen display after anomaly augmentation and extraction parameters were changed.

Appendix C:

NUCARS definitions of the paintspotter car and the three platform articulated flat car

```
-SYSTEM FILE (.SYS) for the program NUCARS Version 1.0
 N.B. Parameters are in lb., in. & sec. unless otherwise stated.
-Enter a title up to 80 characters long between the lines,
--------------------------------------------------------------------------
 70 TON LOADED PAINT SPOTTER USING 89 ft TTX Car TRUCKS (FOR PS3)
--------------------------------------------------------------------------
-FOR THE BODIES
-Provide the number of heavy bodies including axles (IMM), and the number
 of input or light bodies (IBIN, used for input degrees of freedom )
   IMM   IBIN
    11    8
-List the number, name, in single quotes up to 15 characters long, and position
 of each body, (and axle body), relative to a datum on the system center,
 in inches, followed by the number of degrees of freedom required,
 followed by a list of the degrees of freedom for each, in turn,
 from  1=x, 2=y, 3=z, 4=phi, 5=theta, 6=psi, 7=epsx, 8=epsy, 9=epsz.
 The 4 degrees of freedom required for each axle are  2 3 4 6
 Body #  ' 15 CHAR NAME  '  Posn in X, Y & Z  No. & list of DoF's
   1   ' 89-ft TTX Car '  -280.0   0.0  98.0    5   2 3 4 5 6
   2   'Leading Bolster'   -34.0   0.0  16.5    4   2 3 4 6
   3   'Trailng Bolster'  -526.0   0.0  16.5    4   2 3 4 6
   4   'Lead Lft Sframe'   -34.0  39.0  16.5    5   1 2 3 5 6
   5   'Lead Rgt Sframe'   -34.0 -39.0  16.5    5   1 2 3 5 6
   6   'Trail Lt Sframe'  -526.0  39.0  16.5    5   1 2 3 5 6
   7   'Trail Rt Sframe'  -526.0 -39.0  16.5    5   1 2 3 5 6
   8   ' Axle number 1 '     0.0   0.0  16.5    4   2 3 4 6
   9   ' Axle number 2 '   -68.0   0.0  16.5    4   2 3 4 6
  10   ' Axle number 3 '  -492.0   0.0  16.5    4   2 3 4 6
  11   ' Axle number 4 '  -560.0   0.0  16.5    4   2 3 4 6
 continue the body list with the number and position of each input body,
 relative to the same datum, in inches, followed by the number of input
 degrees of freedom required, followed by a list of the degrees of freedom,
 from  1=x, 2=y, 3=z, 4=phi, 5=theta, 6=psi, the number of the input history
 for each degree of freedom, in turn, followed by a choice of input phase lag
 for the input to this body, 0 = no, 1 = yes.
 Body #  ' 15 CHAR NAME  '  Posn in X, Y & Z  No. & DoF list  Input list  Lag
   12   'Lft Rail Axle 1'     0.0  29.75  0.0    2   2 3     1 3       1
   13   'Rgt Rail Axle 1'     0.0 -29.75  0.0    2   2 3     2 4       1
   14   'Lft Rail Axle 2'   -68.0  29.75  0.0    2   2 3     1 3       1
   15   'Rgt Rail Axle 2'   -68.0 -29.75  0.0    2   2 3     2 4       1
   16   'Lft Rail Axle 3'  -492.0  29.75  0.0    2   2 3     1 3       1
   17   'Rgt Rail Axle 3'  -492.0 -29.75  0.0    2   2 3     2 4       1
   18   'Lft Rail Axle 4'  -560.0  29.75  0.0    2   2 3     1 3       1
   19   'Rgt Rail Axle 4'  -560.0 -29.75  0.0    2   2 3     2 4       1
-For all heavy bodies with flexible modes, give the position of each body
 geometric center, in the X direction from the datum, backward is -ve, its
 length in inches, the natural frequencies, in Hz., and the damping ratios
 in twist, vertical & lateral bending, as required.
 Body #   X-Posn    X-Length    Nat Frequencies(Hz.)       Damping Ratios
```

-List the mass, roll, pitch and yaw inertias, in order,
for each heavy body, including axles,

518.23	1.50E06	1.38E07	1.37E07
3.78	2.76E03	0.0	2.76E03
3.78	2.76E03	0.0	2.76E03
2.85	0.0	1.31E03	1.31E03
2.85	0.0	1.31E03	1.31E03
2.85	0.0	1.31E03	1.31E03
2.85	0.0	1.31E03	1.31E03
6.47	4.93E03	1.26E03	4.93E03
6.47	4.93E03	1.26E03	4.93E03
6.47	4.93E03	1.26E03	4.93E03
6.47	4.93E03	1.26E03	4.93E03

-FOR THE CONNECTIONS (including suspensions)
Identify the following parameters,
-Number of connections:

IALLC
68

-Complete the following tables for each connection, identifying:
a name, in single quotes up to 20 characters long;
its position relative to the chosen datum in x, y, z inches;
the number of the body at each end, 0 for an earth in local track coords.;
a number indicating the degree(s) of freedom, translational 1,2,3 or
rotational 4,5,6; in x,y,z resp., including 2 for lateral wheel motion;
the type 1 - parallel pair of spring and damper characteristics
2 - series pair of spring and damper characteristics
3 - device with hysteresis between 2 PWL characteristics,
e.g. carriage spring or load sensitive suspension
4 - lateral/longitudinal suspension of the wheel on rail
in the track plane
5 - connection force as a history of the distance moved
and the identification number for each of type 1, 2 and 3;
axle number for type 4; input function number for type 5.
Note - single characteristics are treated as parallel pairs with the
missing characteristic set to zero in the subsequent table.
-Complete for all connections in turn,

Conn #	' 20 CHARACTER NAME '	Posn in X, Y & Z			Body1	Body2	DoF.	Type Number	
1	' Ax 1 Lft Long Conn.'	0.0	39.0	16.5	4	8	1	1	2
2	' Ax 1 Rgt Long Conn.'	0.0	-39.0	16.5	5	8	1	1	2
3	' Ax 2 Lft Long Conn.'	-68.0	39.0	16.5	4	9	1	1	2
4	' Ax 2 Rgt Long Conn.'	-68.0	-39.0	16.5	5	9	1	1	2
5	' Ax 3 Lft Long Conn.'	-492.0	39.0	16.5	6	10	1	1	2
6	' Ax 3 Rgt Long Conn.'	-492.0	-39.0	16.5	7	10	1	1	2
7	' Ax 4 Lft Long Conn.'	-560.0	39.0	16.5	6	11	1	1	2
8	' Ax 4 Rgt Long Conn.'	-560.0	-39.0	16.5	7	11	1	1	2
9	'Car-Bolster Y- sprg'	-34.0	0.0	25.5	1	2	2	1	2
10	'Car-Bolster Y- sprg'	-526.0	0.0	25.5	1	3	2	1	2
11	' L. Bolst-s.f Y-Susp'	-34.0	39.0	16.5	2	4	2	1	4
12	' L. Bolst-s.f Y-Susp'	-34.0	-39.0	16.5	2	5	2	1	4

```
13  ' T. Bolst-s.f Y-Susp' -526.0  39.0  16.5   3   6   2   1   4
14  ' T. Bolst-s.f Y-Susp' -526.0 -39.0  16.5   3   7   2   1   4
15  ' Ax 1 Lft Lat. Conn.'   0.0  39.0  16.5   4   8   2   1   2
16  ' Ax 1 Rgt Lat. Conn.'   0.0 -39.0  16.5   5   8   2   1   2
17  ' Ax 2 Lft Lat. Conn.' -68.0  39.0  16.5   4   9   2   1   2
18  ' Ax 2 Rgt Lat. Conn.' -68.0 -39.0  16.5   5   9   2   1   2
19  ' Ax 3 Lft Lat. Conn.' -492.0  39.0  16.5   6  10   2   1   2
20  ' Ax 3 Rgt Lat. Conn.' -492.0 -39.0  16.5   7  10   2   1   2
21  ' Ax 4 Lft Lat. Conn.' -560.0  39.0  16.5   6  11   2   1   2
22  ' Ax 4 Rgt Lat. Conn.' -560.0 -39.0  16.5   7  11   2   1   2
23  ' Lead c.p. Vert. Sup' -34.0   7.0  25.5   1   2   3   1   1
24  ' Lead c.p. Vert. Sup' -34.0  -7.0  25.5   1   2   3   1   1
25  'Trail c.p. Vert. Sup' -526.0  7.0  25.5   1   3   3   1   1
26  'Trail c.p. Vert. Sup' -526.0 -7.0  25.5   1   3   3   1   1
27  ' Lead c.p. Yaw  Sup' -34.0   0.0  25.5   1   2   6   1   7
28  'Trail c.p. Yaw  Sup' -526.0   0.0  25.5   1   3   6   1   7
29  'Lead Lf s.b Z-suspen' -34.0  29.8  25.5   1   2   3   1   3
30  'Lead Rt s.b Z-suspen' -34.0 -29.8  25.5   1   2   3   1   3
31  'Trail Lf s.b Z-suspn' -526.0  29.8  25.5   1   3   3   1   3
32  'Trail Rt s.b Z-suspn' -526.0 -29.8  25.5   1   3   3   1   3
33  'Lead Lf s.f Z-suspen' -34.0  39.0  16.5   2   4   3   1   8
34  'Lead Rt s.f Z-suspen' -34.0 -39.0  16.5   2   5   3   1   8
35  'Trail Lf s.f Z-suspn' -526.0  39.0  16.5   3   6   3   1   8
36  'Trail Rt s.f Z-suspn' -526.0 -39.0  16.5   3   7   3   1   8
37  'Ld bol. sf YAW LFT  ' -34.0  39.0  16.5   2   4   6   1  10
38  'Ld bol. sf YAW RGT  ' -34.0 -39.0  16.5   2   5   6   1  10
39  'Trail s.b Yaw Suspen' -526.0  39.0  16.5   3   6   6   1  10
40  'Trail s.b Yaw Suspen' -526.0 -39.0  16.5   3   7   6   1  10
41  ' Ax 1 Lft Vert Conn.'   0.0  39.0  16.5   4   8   3   1   5
42  ' Ax 1 Rgt Vert Conn.'   0.0 -39.0  16.5   5   8   3   1   5
43  ' Ax 2 Lft Vert Conn.' -68.0  39.0  16.5   4   9   3   1   5
44  ' Ax 2 Rgt Vert Conn.' -68.0 -39.0  16.5   5   9   3   1   5
45  ' Ax 3 Lft Vert Conn.' -492.0  39.0  16.5   6  10   3   1   5
46  ' Ax 3 Rgt Vert Conn.' -492.0 -39.0  16.5   7  10   3   1   5
47  ' Ax 4 Lft Vert Conn.' -560.0  39.0  16.5   6  11   3   1   5
48  ' Ax 4 Rgt Vert Conn.' -560.0 -39.0  16.5   7  11   3   1   5
49  ' Ax 1 Lft Lat Wh/Rl.'   0.0  29.75  0.0   8  12   2   4   1
50  ' Ax 1 Rgt Lat Wh/Rl.'   0.0 -29.75  0.0   8  13   2   4   1
51  ' Ax 2 Lft Lat Wh/Rl.' -68.0  29.75  0.0   9  14   2   4   2
52  ' Ax 2 Rgt Lat Wh/Rl.' -68.0 -29.75  0.0   9  15   2   4   2
53  ' Ax 3 Lft Lat Wh/Rl.' -492.0  29.75  0.0  10  16   2   4   3
54  ' Ax 3 Rgt Lat Wh/Rl.' -492.0 -29.75  0.0  10  17   2   4   3
55  ' Ax 4 Lft Lat Wh/Rl.' -560.0  29.75  0.0  11  18   2   4   4
56  ' Ax 4 Rgt Lat Wh/Rl.' -560.0 -29.75  0.0  11  19   2   4   4
57  ' Ax 1 Lft Ver Wh/Rl.'   0.0  29.75  0.0   8  12   3   1   6
58  ' Ax 1 Rgt Ver Wh/Rl.'   0.0 -29.75  0.0   8  13   3   1   6
59  ' Ax 2 Lft Ver Wh/Rl.' -68.0  29.75  0.0   9  14   3   1   6
60  ' Ax 2 Rgt Ver Wh/Rl.' -68.0 -29.75  0.0   9  15   3   1   6
61  ' Ax 3 Lft Ver Wh/Rl.' -492.0  29.75  0.0  10  16   3   1   6
62  ' Ax 3 Rgt Ver Wh/Rl.' -492.0 -29.75  0.0  10  17   3   1   6
```

```
 63   ' Ax 4 Lft Ver Wh/Rl.' -560.0  29.75  0.0   11   18   3   1    6
 64   ' Ax 4 Rgt Ver Wh/Rl.' -560.0 -29.75  0.0   11   19   3   1    6
 65   ' Ld lft bol sf Long '  -34.0  39.0  16.5   2    4    1   1    11
 66   ' Ld Rgt Bol Sf Long '  -34.0 -39.0  16.5   2    5    1   1    11
 67   ' Trl Lft Bol Sf Long' -526.0  39.0  16.5   3    6    1   1    11
 68   ' Trl Rgt Bol Sf Long' -526.0 -39.0  16.5   3    7    1   1    11
```

-List for each pair of type 1 - parallel connections, its number, followed by the identification numbers of the piecewise linear characteristics for the stiffness and damping respectively, zero if absent, and the combined force or moment limit in extn & compn, lb or lb-in., 0.0 in extension at the vertical rail/wheel conn. allows valid wheel lift. (If no limit exists, set the F-values outside the expected range.)

Pair #	Stiff PWL	Damp PWL	F-extn.	F-compn.
1	1	2	1.0E08	-1.0E08
2	3	4	1.0E08	-1.0E08
3	7	8	0.0E08	-1.0E08
4	9	14	1.0E08	-1.0E08
5	11	12	1.0E08	-1.0E08
6	15	16	0.0E08	-1.0E08
7	8	6	1.0E08	-1.0E08
8	5	13	1.0E08	-1.0E08
9	8	14	1.0E08	-1.0E08
10	17	18	1.0E08	-1.0E08
11	19	20	1.0E08	-1.0E08

-List for each pair of type 2 - series connections, its number, followed by the identification numbers of the piecewise linear characteristics for the stiffness and damping respectively, and the stroke limit in extension & compression for the pair, in or rad, and the stiffness of the stop at the limit in lb/in or lb-in/rad. (If no limit exists, set the S-values outside the expected range.)

Pair #	Stiff PWL	Damp PWL	S-extn.	S-compn.	Stop K

-List the type 3 - hysteresis loop characteristics, giving to each a number, the identification numbers of the piecewise linear characteristics and a linear viscous bandwidth and force limits during extn and compn.

Loop #	Extn PWL	Comp PWL	LVB width	F-extn	F-compn

-List the type 4 - axle to track characteristics, the general lateral rail stiffness and damping coefficient, and, for each axle, IAX, an identification number, IBDAX, its general body number, WRAD, the nominal wheel radius and INDWH, a wheel rotation index, 1 for solid, 2 for independent wheels, and ITRQ, traction torque input nos. for left and right wheels, 0 for none.

Lateral Rail Stiffness lb/in 0.5E05 — Lateral Rail Damping lb-sec/in 1.0E03

IAX	IBDAX	WRAD	INDWH	ITRQ-L	ITRQ-R
1	8	16.5	1	0	0 0
2	9	16.5	1	0	0 0
3	10	16.5	1	0	0 0
4	11	16.5	1	0	0 0

-How many different piecewise linear, (PWL), characteristics are required

```
  20
-List the data required for the connection characteristics,
 PWL, the piece-wise linear function no., IBP, the no. of Break Points in each
 PWL, Ordinate, lb or lb-in, over abscissa, in or rad, at each Break Point
 N.B. (1) Extension is assumed to be positive for both ordinate and abscissa
     (2) 0.0 for the first break point indicates symmetry about the origin
PWL   IBP   Ordinates over Abscissae
 1     3  -1.00E06  0.00E00  0.00E00  (platform-bolster vert. stiff)
         -1.00000  0.0000   1.00000
 2     2  -1.00E03  1.00E03          (platform-bolster vert. dampn)
         -1.0      1.0
 3     2  -1.00E06  1.00E06          (primary -long & lat. stiffne)
         -1.0      1.0
 4     2  -1.00E03  1.00E03          (primary -long & lat. damping)
         -1.0      1.0
 5     4  -1.50E05 -1.00E05  0.0      0.0   (secondary vert. stiff)
         -3.5     -3.45     0.0      1.0
 6     4  -5.0E04  -5.0E04    5.0E04   5.0E04 (center plate yaw damp)
         -1.0     -0.01     0.01     1.0
 7     4  -1.33E05 -5.20E03 -2.80E03  -2.80E03 (side bearing vert. stif)
         -1.3125  -0.3125   0.0      1.0
 8     4  -0.00E00 -0.00E00  0.00E00  0.00E00
         -1.0     -0.4      0.4      1.0
 9     4  -8.83E03 -3.83E03  3.83E03  8.83E03 (second. lat. stiffness)
         -0.38    -0.375    0.375    0.38
10     2  -1.62E03  1.62E03             (second. lat. damping  )
         -1.0      1.0
11     3  -1.00E06  0.00E06  0.00E06        (primary vert. stiffnes)
         -1.0      0.0      1.0
12     2  -1.00E03  1.00E03             (primary vert. damping )
         -1.0      1.0
13     4  -2.40E03 -2.40E03  2.40E03  2.40E03 (second. ver.  damping )
         -1.0     -0.01     0.01     1.0
14     4  -1.60E03 -1.60E03  1.60E03  1.60E03
         -1.0     -0.01     0.01     1.0
15     2   0.0      1.00E05             (track vert. stiffness )
          0.0      1.0
16     2   0.0      1.00E03             (track vert. damping   )
          0.0      1.0
17     4  -1.78E06 -8.92E05  8.92E05   1.78E06 (second. yaw stiffness)
        -0.057   -0.052    0.052    0.057
18     4  -0.30E04 -0.30E04  0.30E04   0.30E04 (second. yaw damping  )
         -1.0     -0.1      0.1      1.0
19     2   0.0      1.0E06
          0.0      1.0
20     2   0.0      1.0E03
          0.0      1.0
```

```
-SYSTEM FILE (.SYS) for the program NUCARS Version 1.0
 N.B. Parameters are in lb., in. & sec. unless otherwise stated.
-Enter a title up to 80 characters long between the lines,
--------------------------------------------------------------------------------
 Articulated Flt Cars, Loaded, Three Platforms
--------------------------------------------------------------------------------
-FOR THE BODIES
-Provide the number of heavy bodies including axles (IMM), and the number
 of input or light bodies (IBIN, used for input degrees of freedom )
   IMM   IBIN
    23   16
-List the number, name, in single quotes up to 15 characters long, and position
 of each body, (and axle body), relative to a datum on the system center,
 in inches, followed by the number of degrees of freedom required,
 followed by a list of the degrees of freedom for each, in turn,
 from  1=x, 2=y, 3=z, 4=phi, 5=theta, 6=psi, 7=epsx, 8=epsy, 9=epsz.
 The 4 degrees of freedom required for each axle are  2 3 4 6
 Body #  ' 15 CHAR NAME  '  Posn in X, Y & Z  No. & list of DoF's
   1   'First Platform '  -327.3   0.0  36.0   5   2 3 4 5 6
   2   'second Platform'  -917.5   0.0  36.0   5   2 3 4 5 6
   3   'Third Platform '  -1535.5  0.0  36.0   5   2 3 4 5 6
   4   '1st Bolster    '   -34.0   0.0  16.5   4   2 3 4 6
   5   '2nd Bolster    '  -612.5   0.0  16.5   4   2 3 4 6
   6   '3rd Bolster    '  -1230.5  0.0  16.5   4   2 3 4 6
   7   '4th Bolster    '  -1848.5  0.0  16.5   4   2 3 4 6
   8   '1st Lft  Sframe'   -34.0   39.0 16.5   5   1 2 3 5 6
   9   '1st Rgt  Sframe'   -34.0  -39.0 16.5   5   1 2 3 5 6
  10   '2nd Lft  Sframe'  -612.5   39.0 16.5   5   1 2 3 5 6
  11   '2nd Rgt  Sframe'  -612.5  -39.0 16.5   5   1 2 3 5 6
  12   '3rd Lft  Sframe'  -1230.5  39.0 16.5   5   1 2 3 5 6
  13   '3rd Rgt  Sframe'  -1230.5 -39.0 16.5   5   1 2 3 5 6
  14   '4th Lft  Sframe'  -1848.5  39.0 16.5   5   1 2 3 5 6
  15   '4th Rgt  Sframe'  -1848.5 -39.0 16.5   5   1 2 3 5 6
  16   'Axle number 1  '     0.0   0.0  16.5   4   2 3 4 6
  17   'Axle number 2  '    -68.0   0.0  16.5   4   2 3 4 6
  18   'Axle number 3  '   -578.5   0.0  16.5   4   2 3 4 6
  19   'Axle number 4  '   -646.5   0.0  16.5   4   2 3 4 6
  20   'Axle number 5  '  -1196.5   0.0  16.5   4   2 3 4 6
  21   'Axle number 6  '  -1264.5   0.0  16.5   4   2 3 4 6
  22   'Axle number 7  '  -1814.5   0.0  16.5   4   2 3 4 6
  23   'Axle number 8  '  -1882.5   0.0  16.5   4   2 3 4 6
continue the body list with the number and position of each input body,
relative to the same datum, in inches, followed by the number of input
degrees of freedom required, followed by a list of the degrees of freedom,
from  1=x, 2=y, 3=z, 4=phi, 5=theta, 6=psi, the number of the input history
for each degree of freedom, in turn, followed by a choice of input phase lag
for the input to this body, 0 = no, 1 = yes.
Body #  ' 15 CHAR NAME  '  Posn in X, Y & Z  No. & DoF list  Input list  Lag
  24   'Lft Rail Axle 1'    0.0  29.75  0.0   2   2 3    1 3      1
  25   'Rgt Rail Axle 1'    0.0 -29.75  0.0   2   2 3    2 4      1
```

```
 26  'Lft Rail Axle 2'  -68.0  29.75  0.0   2   2 3    1 3     1
 27  'Rgt Rail Axle 2'  -68.0 -29.75  0.0   2   2 3    2 4     1
 28  'Lft Rail Axle 3' -578.5  29.75  0.0.  2   2 3    1 3     1
 29  'Rgt Rail Axle 3' -578.5 -29.75  0.0   2   2 3    2 4     1
 30  'Lft Rail Axle 4' -646.5  29.75  0.0   2   2 3    1 3     1
 31  'Rgt Rail Axle 4' -646.5 -29.75  0.0   2   2 3    2 4     1
 32  'Lft Rail Axle 5' -1196.5 29.75  0.0   2   2 3    1 3     1
 33  'Rgt Rail Axle 5' -1196.5 -29.75 0.0   2   2 3    2 4     1
 34  'Lft Rail Axle 6' -1264.5 29.75  0.0   2   2 3    1 3     1
 35  'Rgt Rail Axle 6' -1264.5 -29.75 0.0   2   2 3    2 4     1
 36  'Lft Rail Axle 7' -1814.5 29.75  0.0   2   2 3    1 3     1
 37  'Rgt Rail Axle 7' -1814.5 -29.75 0.0   2   2 3    2 4     1
 38  'Lft Rail Axle 8' -1882.5 29.75  0.0   2   2 3    1 3     1
 39  'Rgt Rail Axle 8' -1882.5 -29.75 0.0   2   2 3    2 4     1
```

-For all heavy bodies with flexible modes, give the position of each body geometric center, in the X direction from the datum, backward is -ve, its length in inches, the natural frequencies, in Hz., and the damping ratios in twist, vertical & lateral bending, as required.

Body # X-Posn X-Length Nat Frequencies(Hz.) Damping Ratios

-List the mass, roll, pitch and yaw inertias, in order, for each heavy body, including axles,

```
229.00  1.17E05  7.99E06  8.03E06
218.22  1.09E05  6.85E06  6.90E06
218.22  1.09E05  6.85E06  6.90E06
  3.78  2.76E03  0.0     2.76E03
  3.78  2.76E03  0.0     2.76E03
  3.78  2.76E03  0.0     2.76E03
  3.78  2.76E03  0.0     2.76E03
  2.85  0.0      1.31E03  1.31E03
  2.85  0.0      1.31E03  1.31E03
  2.85  0.0      1.31E03  1.31E03
  2.85  0.0      1.31E03  1.31E03
  2.85  0.0      1.31E03  1.31E03
  2.85  0.0      1.31E03  1.31E03
  2.85  0.0      1.31E03  1.31E03
  2.85  0.0      1.31E03  1.31E03
  6.47  4.93E03  1.26E03  4.93E03
  6.47  4.93E03  1.26E03  4.93E03
  6.47  4.93E03  1.26E03  4.93E03
  6.47  4.93E03  1.26E03  4.93E03
  6.47  4.93E03  1.26E03  4.93E03
  6.47  4.93E03  1.26E03  4.93E03
  6.47  4.93E03  1.26E03  4.93E03
  6.47  4.93E03  1.26E03  4.93E03
```

-FOR THE CONNECTIONS (including suspensions)
Identify the following parameters,
-Number of connections:

```
IALLC
 170
```

-Complete the following tables for each connection, identifying:
a name, in single quotes up to 20 characters long;
its position relative to the chosen datum in x, y, z inches;
the number of the body at each end, 0 for an earth in local track coords.;
a number indicating the degree(s) of freedom, translational 1,2,3 or
rotational 4,5,6; in x,y,z resp., including 2 for lateral wheel motion;
the type 1 - parallel pair of spring and damper characteristics
2 - series pair of spring and damper characteristics
3 - device with hysteresis between 2 PWL characteristics,
e.g. carriage spring or load sensitive suspension
4 - lateral/longitudinal suspension of the wheel on rail
in the track plane
5 - connection force as a history of the distance moved
and the identification number for each of type 1, 2 and 3;
axle number for type 4; input function number for type 5.
Note - single characteristics are treated as parallel pairs with the
missing characteristic set to zero in the subsequent table.
-Complete for all connections in turn,

Conn #	' 20 CHARACTER NAME '	Posn in X, Y & Z			Body1	Body2	DoF.	Type Number
1	'Axl 1 & Sfm Lft LON'	0.0	39.0	16.5	8	16	1	1 2
2	'Axl 1 & Sfm Rgt LON'	0.0	-39.0	16.5	9	16	1	1 2
3	'Axl 2 & Smf Lft LON'	-68.0	39.0	16.5	8	17	1	1 2
4	'Axl 2 & Smf Rgt LON'	-68.0	-39.0	16.5	9	17	1	1 2
5	'Axl 3 & Sfm Lft LON'	-578.5	39.0	16.5	10	18	1	1 2
6	'Axl 3 & Sfm Rgt LON'	-578.5	-39.0	16.5	11	18	1	1 2
7	'Axl 4 & Sfm Lft LON'	-646.5	39.0	16.5	10	19	1	1 2
8	'Axl 4 & Sfm Rgt LON'	-646.5	-39.0	16.5	11	19	1	1 2
9	'Axl 5 & Sfm Lft LON'	-1196.5	39.0	16.5	12	20	1	1 2
10	'Axl 5 & Sfm Rgt LON'	-1196.5	-39.0	16.5	13	20	1	1 2
11	'Axl 6 & Sfm Lft LON'	-1264.5	39.0	16.5	12	21	1	1 2
12	'Axl 6 & Sfm Rgt LON'	-1264.5	-39.0	16.5	13	21	1	1 2
13	'Axl 7 & Sfm Lft LON'	-1814.5	39.0	16.5	14	22	1	1 2
14	'Axl 7 & Sfm Rgt LON'	-1814.5	-39.0	16.5	15	22	1	1 2
15	'Axl 8 & Sfm Lft LON'	-1882.5	39.0	16.5	14	23	1	1 2
16	'Axl 8 & Sfm Rgt LON'	-1882.5	-39.0	16.5	15	23	1	1 2
17	'1st Cen. Plt. Lat'	-34.0	0.0	25.5	1	4	2	1 2
18	'2nd Cen. Plt. Lat'	-612.5	0.0	25.5	1	5	2	1 2
19	'Artcld 1-2 Pltfm Lat'	-612.5	0.0	33.5	2	5	2	1 2
20	'3rd Cen. Plt. Lat'	-1230.5	0.0	25.5	2	6	2	1 2
21	'Artcld 2-3 Pltfm Lat'	-1230.5	0.0	33.5	3	6	2	1 2
22	'4th Cen. Plt. Lat'	-1848.5	0.0	25.5	3	7	2	1 2
23	'1st Blst Sfm Lft Lat'	-34.0	39.0	16.5	4	8	2	1 4
24	'1st Blst Sfm Rgt Lat'	-34.0	-39.0	16.5	4	9	2	1 4
25	'2nd Blst Sfm Lft Lat'	-612.5	39.0	16.5	5	10	2	1 4
26	'2nd Blst Sfm Rgt Lat'	-612.5	-39.0	16.5	5	11	2	1 4
27	'3rd Blst Sfm Lft Lat'	-1230.5	39.0	16.5	6	12	2	1 4
28	'3rd Blst Sfm Rgt Lat'	-1230.5	-39.0	16.5	6	13	2	1 4
29	'4th Blst Sfm Lft Lat'	-1848.5	39.0	16.5	7	14	2	1 4
30	'4th Blst Sfm Rgt Lat'	-1848.5	-39.0	16.5	7	15	2	1 4

```
31  'Axl 1 & Sfm  Lft Lat'    0.0  39.0  16.5   8  16  2  1  2
32  'Axl 1 & Sfm  Rgt Lat'    0.0 -39.0  16.5   9  16  2  1  2
33  'Axl 2 & Sfm  Lft Lat'  -68.0  39.0  16.5   8  17  2  1  2
34  'Axl 2 & Sfm  Rgt Lat'  -68.0 -39.0  16.5   9  17  2  1  2
35  'Axl 3 & Sfm  Lft Lat' -578.5  39.0  16.5  10  18  2  1  2
36  'Axl 3 & Sfm  Rgt Lat' -578.5 -39.0  16.5  11  18  2  1  2
37  'Axl 4 & Sfm  Lft Lat' -646.5  39.0  16.5  10  19  2  1  2
38  'Axl 4 & Smf  Rgt Lat' -646.5 -39.0  16.5  11  19  2  1  2
39  'Axl 5 & Sfm  Lft Lat' -1196.5  39.0  16.5  12  20  2  1  2
40  'Axl 5 & Sfm  Rgt Lat' -1196.5 -39.0  16.5  13  20  2  1  2
41  'Axl 6 & Sfm  Lft Lat' -1264.5  39.0  16.5  12  21  2  1  2
42  'Axl 6 & Sfm  Rgt Lat' -1264.5 -39.0  16.5  13  21  2  1  2
43  'Axl 7 & Sfm  Lft Lat' -1814.5  39.0  16.5  14  22  2  1  2
44  'Axl 7 & Sfm  Rgt Lat' -1814.5 -39.0  16.5  15  22  2  1  2
45  'Axl 8 & Sfm  Lft Lat' -1882.5  39.0  16.5  14  23  2  1  2
46  'Axl 8 & Sfm  Rgt Lat' -1882.5 -39.0  16.5  15  23  2  1  2
47  'Carl CenPlt1 Lft Ver'  -34.0   7.0  25.5   1   4  3  1  1
48  'Carl CenPlt1 Rgt Ver'  -34.0  -7.0  25.5   1   4  3  1  1
49  'Carl CenPlt2 Lft Ver' -612.5   7.0  25.5   1   5  3  1  1
50  'Carl CenPlt2 Rgt Ver' -612.5  -7.0  25.5   1   5  3  1  1
51  'Carl & Car 2 Mdl Ver' -612.5   0.0  33.5   2   1  3  1  15
52  'Car2 CenPlt3 Lft Ver' -1230.5  7.0  25.5   2   6  3  1  1
53  'Car2 CenPlt3 Rgt Ver' -1230.5 -7.0  25.5   2   6  3  1  1
54  'Car2 & Car 3 Mdl Ver' -1230.5  0.0  33.5   3   2  3  1  15
55  'Car3 CenPlt4 Lft Ver' -1848.5  7.0  25.5   3   7  3  1  1
56  'Car4 CenPlt4 Rgt Ver' -1848.5 -7.0  25.5   3   7  3  1  1
57  'Ptfm1 & CenPlt 1 Yaw'  -34.0   0.0  25.5   1   4  6  1  7
58  'Ptfm1 & CenPlt 2 Yaw' -612.5   0.0  25.5   1   5  6  1  11
59  'Ptfm 1 & Ptfm 2  Yaw' -612.5   0.0  33.5   1   2  6  1  14
60  'Ptfm2 & CenPlt 3 Yaw' -1230.5  0.0  25.5   2   6  6  1  12
61  'Ptfm 2 & Ptfm 3  Yaw' -1230.5  0.0  33.5   2   3  6  1  14
62  'Ptfm3 & CenPlt 4 Yaw' -1848.5  0.0  25.5   3   7  6  1  13
63  '1st Sdbr    Lft Ver'  -34.0  29.8  25.5   1   4  3  1  3
64  '1st Sdbr    Rgt Ver'  -34.0 -29.8  25.5   1   4  3  1  3
65  '2nd inr Sdbr Lft Ver' -612.5  20.0  25.5   2   5  3  1  3
66  '2nd inr Sdbr Rgt Ver' -612.5 -20.0  25.5   2   5  3  1  3
67  '2nd otr Sdbr Lft Ver' -612.5  29.8  25.5   1   5  3  1  3
68  '2nd otr Sdbr Rgt Ver' -612.5 -29.8  25.5   1   5  3  1  3
69  '3rd inr Sdbr Lft Ver' -1230.5  20.0  25.5   3   6  3  1  3
70  '3rd inr Sdbr Rgt Ver' -1230.5 -20.0  25.5   3   6  3  1  3
71  '3rd otr Sdbr Lft Ver' -1230.5  29.8  25.5   2   6  3  1  3
72  '3rd otr Sdbr Rgt Ver' -1230.5 -29.8  25.5   2   6  3  1  3
73  '4th Sdbr    Lft Ver' -1848.5  29.8  25.5   3   7  3  1  3
74  '4th Sdbr    Rgt Ver' -1848.5 -29.8  25.5   3   7  3  1  3
75  '1st Blst Sfm Lft Ver'  -34.0  39.0  16.5   4   8  3  1  8
76  '1st Blst Sfm Rgt Ver'  -34.0 -39.0  16.5   4   9  3  1  8
77  '2nd Blst Sfm Lft Ver' -612.5  39.0  16.5   5  10  3  1  8
78  '2nd Blst Sfm Rgt Ver' -612.5 -39.0  16.5   5  11  3  1  8
79  '3rd Blst Sfm Lft Ver' -1230.5  39.0  16.5   6  12  3  1  8
80  '3rd Blst Sfm Rgt Ver' -1230.5 -39.0  16.5   6  13  3  1  8
```

```
 81  '4th Blst Sfm Lft Ver' -1848.5  39.0 16.5  7 14 3 1 8
 82  '4th Blst Sfm Rgt Ver' -1848.5 -39.0 16.5  7 15 3 1 8
 83  '1st Blst Sfm Lft Yaw'  -34.0  39.0 16.5  4  8 6 1 9
 84  '1st Blst Sfm Rgt Yaw'  -34.0 -39.0 16.5  4  9 6 1 9
 85  '2nd Blst Sfm Lft Yaw' -612.5  39.0 16.5  5 10 6 1 9
 86  '2nd Blst Sfm Rgt Yaw' -612.5 -39.0 16.5  5 11 6 1 9
 87  '3rd Blst Sfm Lft Yaw' -1230.5  39.0 16.5  6 12 6 1 9
 88  '3rd Blst Sfm Rgt Yaw' -1230.5 -39.0 16.5  6 13 6 1 9
 89  '4th Blst Sfm Lft Yaw' -1848.5  39.0 16.5  7 14 6 1 9
 90  '4th Blst Sfm Rgt Yaw' -1848.5 -39.0 16.5  7 15 6 1 9
 91  'Axl 1 & Sfm  Lft Ver'    0.0  39.0 16.5  8 16 3 1 5
 92  'Axl 1 & Sfm  Rgt Ver'    0.0 -39.0 16.5  9 16 3 1 5
 93  'Axl 2 & Sfm  Lft Ver'  -68.0  39.0 16.5  8 17 3 1 5
 94  'Axl 2 & Sfm  Rgt Ver'  -68.0 -39.0 16.5  9 17 3 1 5
 95  'Axl 3 & Sfm  Lft Ver' -578.5  39.0 16.5 10 18 3 1 5
 96  'Axl 3 & Sfm  Rgt Ver' -578.5 -39.0 16.5 11 18 3 1 5
 97  'Axl 4 & Sfm  Lft Ver' -646.5  39.0 16.5 10 19 3 1 5
 98  'Axl 4 & Sfm  Rgt Ver' -646.5 -39.0 16.5 11 19 3 1 5
 99  'Axl 5 & Sfm  Lft Ver' -1196.5  39.0 16.5 12 20 3 1 5
100  'Axl 5 & Sfm  Rgt Ver' -1196.5 -39.0 16.5 13 20 3 1 5
101  'Axl 6 & Sfm  Lft Ver' -1264.5  39.0 16.5 12 21 3 1 5
102  'Axl 6 & Sfm  Rgt Ver' -1264.5 -39.0 16.5 13 21 3 1 5
103  'Axl 7 & Sfm  Lft Ver' -1814.5  39.0 16.5 14 22 3 1 5
104  'Axl 7 & Sfm  Rgt Ver' -1814.5 -39.0 16.5 15 22 3 1 5
105  'Axl 8 & Sfm  Lft Ver' -1882.5  39.0 16.5 14 23 3 1 5
106  'Axl 8 & Sfm  Rgt Ver' -1882.5 -39.0 16.5 15 23 3 1 5
107  'Axl 1 W/R  Lft Lat'    0.0  29.75 0.0 16 24 2 4 1
108  'Axl 1 W/R  Rgt Lat'    0.0 -29.75 0.0 16 25 2 4 1
109  'Axl 2 W/R  Lft Lat'  -68.0  29.75 0.0 17 26 2 4 2
110  'Axl 2 W/R  Rgt Lat'  -68.0 -29.75 0.0 17 27 2 4 2
111  'Axl 3 W/R  Lft Lat' -578.5  29.75 0.0 18 28 2 4 3
112  'Axl 3 W/R  Rgt Lat' -578.5 -29.75 0.0 18 29 2 4 3
113  'Axl 4 W/R  Lft Lat' -646.5  29.75 0.0 19 30 2 4 4
114  'Axl 4 W/R  Rgt Lat' -646.5 -29.75 0.0 19 31 2 4 4
115  'Axl 5 W/R  Lft Lat' -1196.5  29.75 0.0 20 32 2 4 5
116  'Axl 5 W/R  Rgt Lat' -1196.5 -29.75 0.0 20 33 2 4 5
117  'Axl 6 W/R  Lft Lat' -1264.5  29.75 0.0 21 34 2 4 6
118  'Axl 6 W/R  Rgt Lat' -1264.5 -29.75 0.0 21 35 2 4 6
119  'Axl 7 W/R  Lft Lat' -1814.5  29.75 0.0 22 36 2 4 7
120  'Axl 7 W/R  Rgt Lat' -1814.5 -29.75 0.0 22 37 2 4 7
121  'Axl 8 W/R  Lft Lat' -1882.5  29.75 0.0 23 38 2 4 8
122  'Axl 8 W/R  Rgt Lat' -1882.5 -29.75 0.0 23 39 2 4 8
123  'Axl 1 W/R  Lft Ver'    0.0  29.75 0.0 16 24 3 1 6
124  'Axl 1 W/R  Rgt Ver'    0.0 -29.75 0.0 16 25 3 1 6
125  'Axl 2 W/R  Lft Ver'  -68.0  29.75 0.0 17 26 3 1 6
126  'Axl 2 W/R  Rgt Ver'  -68.0 -29.75 0.0 17 27 3 1 6
127  'Axl 3 W/R  Lft Ver' -578.5  29.75 0.0 18 28 3 1 6
128  'Axl 3 W/R  Rgt Ver' -578.5 -29.75 0.0 18 29 3 1 6
129  'Axl 4 W/R  Lft Ver' -646.5  29.75 0.0 19 30 3 1 6
130  'Axl 4 W/R  Rgt Ver' -646.5 -29.75 0.0 19 31 3 1 6
```

```
131  'Axl 5 W/R   Lft Ver' -1196.5  29.75 0.0 20 32 3 1 6
132  'Axl 5 W/R   Rgt Ver' -1196.5 -29.75 0.0 20 33 3 1 6
133  'Axl 6 W/R   Lft Ver' -1264.5  29.75 0.0 21 34 3 1 6
134  'Axl 6 W/R   Rgt Ver' -1264.5 -29.75 0.0 21 35 3 1 6
135  'Axl 7 W/R   Lft Ver' -1814.5  29.75 0.0 22 36 3 1 6
136  'Axl 7 W/R   Rgt Ver' -1814.5 -29.75 0.0 22 37 3 1 6
137  'Axl 8 W/R   Lft Ver' -1882.5  29.75 0.0 23 38 3 1 6
138  'Axl 8 W/R   Rgt Ver' -1882.5 -29.75 0.0 23 39 3 1 6
139  '1st Blst Sfm Lft Lon'  -34.0  39.0 16.5  4  8 1 1 10
140  '1st Blst Sfm Rgt Lon'  -34.0 -39.0 16.5  4  9 1 1 10
141  '2nd Blst Sfm Lft Lon' -612.5  39.0 16.5  5 10 1 1 10
142  '2nd Blst Sfm Rgt Lon' -612.5 -39.0 16.5  5 11 1 1 10
143  '3rd Blst Sfm Lft Lon' -1230.5  39.0 16.5  6 12 1 1 10
144  '3rd Blst Sfm Rgt Lon' -1230.5 -39.0 16.5  6 13 1 1 10
145  '4th Blst Sfm Lft Lon' -1848.5  39.0 16.5  7 14 1 1 10
146  '4th Blst Sfm Rgt Lon' -1848.5 -39.0 16.5  7 15 1 1 10
147  '1st Sdbr    Lft Lat'  -34.0  29.8 25.5  1  4 2 1 16
148  '1st Sdbr    Rgt Lat'  -34.0 -29.8 25.5  1  4 2 1 16
149  '2nd inr Sdbr Lft Lat' -612.5  20.0 25.5  2  5 2 1 16
150  '2nd inr Sdbr Rgt Lat' -612.5 -20.0 25.5  2  5 2 1 16
151  '2nd otr Sdbr Lft Lat' -612.5  29.8 25.5  1  5 2 1 16
152  '2nd otr Sdbr Rgt Lat' -612.5 -29.8 25.5  1  5 2 1 16
153  '3rd inr Sdbr Lft Lat' -1230.5  20.0 25.5  3  6 2 1 16
154  '3rd inr Sdbr Rgt Lat' -1230.5 -20.0 25.5  3  6 2 1 16
155  '3rd otr Sdbr Lft Lat' -1230.5  29.8 25.5  2  6 2 1 16
156  '3rd otr Sdbr Rgt Lat' -1230.5 -29.8 25.5  2  6 2 1 16
157  '4th Sdbr    Lft Lat' -1848.5  29.8 25.5  3  7 2 1 16
158  '4th Sdbr    Rgt Lat' -1848.5 -29.8 25.5  3  7 2 1 16
159  '1st Sdbr    Lft Lon'  -34.0  29.8 25.5  1  4 1 1 16
160  '1st Sdbr    Rgt Lon'  -34.0 -29.8 25.5  1  4 1 1 16
161  '2nd inr Sdbr Lft Lon' -612.5  20.0 25.5  2  5 1 1 16
162  '2nd inr Sdbr Rgt Lon' -612.5 -20.0 25.5  2  5 1 1 16
163  '2nd otr Sdbr Lft Lon' -612.5  29.8 25.5  1  5 1 1 16
164  '2nd otr Sdbr Rgt Lon' -612.5 -29.8 25.5  1  5 1 1 16
165  '3rd inr Sdbr Lft Lon' -1230.5  20.0 25.5  3  6 1 1 16
166  '3rd inr Sdbr Rgt Lon' -1230.5 -20.0 25.5  3  6 1 1 16
167  '3rd otr Sdbr Lft Lon' -1230.5  29.8 25.5  2  6 1 1 16
168  '3rd otr Sdbr Rgt Lon' -1230.5 -29.8 25.5  2  6 1 1 16
169  '4th Sdbr    Lft Lon' -1848.5  29.8 25.5  3  7 1 1 16
170  '4th Sdbr    Rgt Lon' -1848.5 -29.8 25.5  3  7 1 1 16
```

-List for each pair of type 1 - parallel connections, its number followed by
the identification numbers of the piecewise linear characteristics
for the stiffness and damping respectively, zero if absent, and
the combined force or moment limit in extn & compn, lb or lb-in.,
0.0 in extension at the vertical rail/wheel conn. allows valid wheel lift.
(If no limit exists, set the F-values outside the expected range.)

Pair #	Stiff PWL	Damp PWL	F-extn.	F-compn.
1	1	2	1.0E08	-1.0E08
2	3	4	1.0E08	-1.0E08
3	7	8	0.0E08	-1.0E08

4	9	10	1.0E08	-1.0E08
5	11	12	1.0E08	-1.0E08
6	14	15	0.0E08	-1.0E08
7	8	6	1.0E08	-1.0E08
8	5	13	1.0E08	-1.0E08
9	16	17	1.0E08	-1.0E08
10	18	19	1.0E08	-1.0E08
11	8	20	1.0E08	-1.0E08
12	8	21	1.0E08	-1.0E08
13	8	22	1.0E08	-1.0E08
14	8	23	1.0E08	-1.0E08
15	24	2	1.0E08	-1.0E08
16	8	25	1.0E08	-1.0E08

-List for each pair of type 2 - series connections, its number, followed by the identification numbers of the piecewise linear characteristics for the stiffness and damping respectively, and the stroke limit in extension & compression for the pair, in or rad, and the stiffness of the stop at the limit in lb/in or lb-in/rad.
(If no limit exists, set the S-values outside the expected range.)

Pair # Stiff PWL Damp PWL S-extn. S-compn. Stop K

-List the type 3 - hysteresis loop characteristics, giving to each a number, the identification numbers of the piecewise linear characteristics and a linear viscous bandwidth and force limits during extn and compn.

Loop # Extn PWL Comp PWL LVB width F-extn F-compn

-List the type 4 - axle to track characteristics, the general lateral rail stiffness and damping coefficient, and, for each axle, IAX, an identification number, IBDAX, its general body number, WRAD, the nominal wheel radius and INDWH, a wheel rotation index, 1 for solid, 2 for independent wheels, and ITRQ, traction torque input nos. for left and right wheels, 0 for none.

Lateral Rail Stiffness lb/in Lateral Rail Damping lb-sec/in

0.3E05 1.0E03

IAX	IBDAX	WRAD	INDWH	ITRQ-L	ITRQ-R
1	16	16.5	1	0	0 0 0
2	17	16.5	1	0	0 0 0
3	18	16.5	1	0	0 0 0
4	19	16.5	1	0	0 0 0
5	20	16.5	1	0	0 0 0
6	21	16.5	1	0	0 0 0
7	22	16.5	1	0	0 0 0
8	23	16.5	1	0	0 0 0

-How many different piecewise linear, (PWL), characteristics are required
25

-List the data required for the connection characteristics,
PWL, the piece-wise linear function no., IBP, the no. of Break Points in each PWL, Ordinate, lb or lb-in, over abscissa, in or rad, at each Break Point
N.B. (1) Extension is assumed to be positive for both ordinate and abscissa
(2) 0.0 for the first break point indicates symmetry about the origin

PWL IBP Ordinates over Abscissae

```
1    3  -1.00E06  0.00     0.00
       -1.0      0.0      1.0
2    2  -1.00E03  1.00E03
       -1.0      1.0
3    2  -1.00E06  1.00E06
       -1.0      1.0
4    2  -1.00E03  1.00E03
       -1.0      1.0
5    4  -1.33E05 -8.27E04  0.0      0.0
       -3.7375   -3.6875   0.0      1.0
6    4  -8220.0 -8220.0   8220.0   8220.0
       -1.0      -0.001    0.001    1.0
7    5  -2.50E05 -5.20E03 -2.80E03  0.0      0.0
       -1.3125   -0.3125   0.0      0.001    2.0
8    2   0.0       0.0
         0.0      10.0
9    4  -8.83E03 -3.83E03  3.83E03  8.83E03
       -0.38     -0.375    0.375    0.38
10   2  -1.62E03  1.62E03
       -1.0      1.0
11   3  -1.00E06  0.00E00  0.00E00
       -1.0      0.00     1.0
12   2  -1.00E03  1.00E03
       -1.0      1.0
13[1] 4  -3.32E03  -3.32E03  3.32E03  3.32E03 (see note at end
       -1.0      -0.01     0.01     1.0      at end of section)
14   2   0.0       1.00E05
         0.0      1.0
15   2   0.0       1.00E03
         0.0      1.0
16   4  -1.78E06 -8.92E05  8.92E05  1.78E06
       -0.057    -0.052    0.052    0.057
17   4  -0.30E04 -0.30E04  0.30E04  0.30E04
       -1.0      -0.1      0.1      1.0
18   2   0.0       1.00E06
         0.0      1.0
19   2   0.0       1.00E03
         0.0      1.0
20   4  -14982.0 -14982.0  14982.0  14982.0
       -1.0      -0.001    0.001    1.0
21   4  -13524.0 -13524.0  13524.0  13524.0
       -1.0      -0.001    0.001    1.0
22   4  -6762.0  -6762.0   6762.0   6762.0
       -1.0      -0.001    0.001    1.0
23   4  -4830.0  -4830.0   4830.0   4830.0
       -1.0      -0.001    0.001    1.0
24   3  -1.00E06  0.00     0.00
       -1.0      0.0      1.0
25   4  -900.00  -960.0    960.00   900.0
       -10.      -0.001    0.001    10.0
```

1 The connection characteristic for the damping elements in the secondary suspensions of the articulated flat car were originially defined:
-3.32E03 3.32E03
-1.0 1.0
but this is an overdamped system. The damping ratio for the second and third truck suspension was 1.47 and for the first and fourth 2.1. Two alternatives were considered:

The first was to define an equivalent viscous damping constant. From Den Hartog (1934), an equivalent damping constant can be defined

$$C_{eq} = \frac{4f}{\pi \omega X}$$

Where f is the colomb friction constant (3,320 lbs), ω is the frequency of oscillation, and X is the amplitude of oscillation. Letting ω equal the natural frequency (19.79 1/sec) and X equal one-half the suspension spring travel (1.844 in), C_{eq} is 232 lb-in/sec. This gives a damping ratio of 0.05 on the middle two trucks and 0.07 on the end trucks.

The other definition of damping considered was to represent the damping as a piece-wise linear element similar in form as the definition in the paintspotter car model.

Results from NUCARS runs using the two forms showed that a larger time step could be used with the linearized damping constant, but that the results between the two runs were quite different. Simulating the car traversing one inch amplitude sinusoids at a speed corresponding to the bounce natural frequency, the linearized damping model predicted a peak bolster load of 348 kips. The piece-wise linear model predicted a peak bolster load of 401 kips. Because the loads predicted by the paintspotter car model were close to the actual loads recorded on the paintspotter car, it was decided to use this representation of the damping for the articulated flat car.

Den Hartog, J.P., "Mechanical Vibration," 4th ed., Dover Publications, New York, 1985.

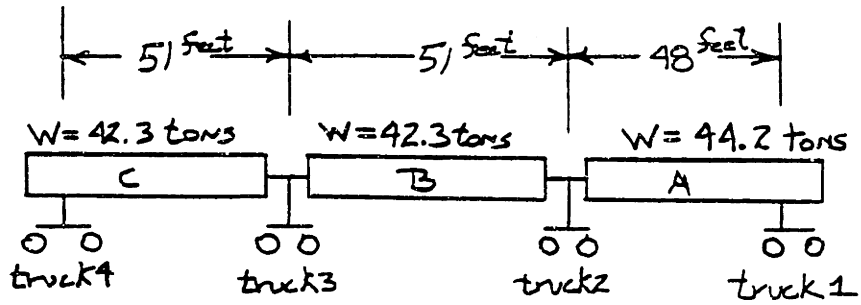

K_i = suspension stiffness on truck i

m_i = static mass on truck i

f_{n_i} = linearized natural frequency for truck i

$$= \sqrt{\frac{m_i}{k_i}}$$

$K_1 = K_2 = K_3 = K_4 = K = 44.9$ kips/inch

$m_1 = 114.5$ lb-sec^2/in

$m_2 = 224$ lb-sec^2/in

$m_3 = 219$ lb-sec^2/in

$m_4 = 109.5$ lb-sec^2/in

$f_{n_1} = f_{n_4} = 3.2$ Hz

$f_{n_2} = f_{n_3} = 2.3$ Hz

THREE PLATFORM ARTICULATED FLAT CAR, SCHEMATIC AND SELECTED PARAMETERS

Appendix D:

Anomaly information and peak bolster loads predicted in NUCARS simulations

Table 1: Case study 1: Paintspotter car and three miles of track data. Anomaly amplitudes and peak bolster load predictions for Criteria A (0.7, 71%, 39)

Anomaly name	Anomaly Amplitude (inches p/p)	Peak bolster load (kips) at 60mph	Peak bolster load (kips) at 80mph
Montj4	0.712	123.4	125.1
Margo1	0.722	128.7	146.7
Margo6	0.725	127.1	127.6
Margo4	0.755	134.9	140.7
Margo5	0.770	129.2	137.3
Margo2	0.817	116.8	123.7
River1	0.848	135.4	138.7
Montj1	0.850	148.1	139.5
Montj2	0.850	131.5	125.5
Montj3	0.897	152.6	151.6
River2	1.020	153.4	148.4
Margo3	1.115	181.1	154.9

Table 2: Case study 1: Paintspotter car and three miles of track data. Comparison of peak bolster loads on track anomalies identified by both criteria at 60 and 80 mph.

		Peak Bolster Load (kips) 60MPH		Peak Bolster Load (kips) 80MPH	
Criteria A (.7")	Criteria B (.5")	Criteria A	Criteria B	Criteria A	Criteria B
Margo1	MA9	128.7	128.7	146.7	146.7
Margo2	MA11	116.8	116.3	123.7	123.5
Margo3	**MA16**	**181.1**	**173.2**	**154.9**	**159.8**
Margo4	MA17	134.9	143.1	140.7	140.2
Margo5	MA18	129.2	129.2	137.3	137.1
Margo6	MA19	127.1	126.9	127.6	127.8
River1	RI1	135.4	136.6		
River2	RI2	153.4	155.1		

Table 3: Case study 1: Paintspotter car and three miles of track data. Anomaly Amplitudes and Peak Bolster Loads for Margo segment with Criteria B (0.5, 100%, 39)

Anomaly number MA..	Anomaly Amplitude (inches p/p)	Peak bolster load (kips) at 60mph	Peak bolster load (kips) at 80mph
6	0.503	108.2	112.1
10	0.517	115.7	118.5
4	0.528	111.1	119.6
15	0.528	120.3	121.1
12	0.536	117.4	120.9
5	0.549	113.6	117.6
7	0.562	111.2	111.8
1	0.564	121.6	127.9
8	0.565	117.2	121.1
3	0.601	120.8	122.5
2	0.602	120.6	123.7
14	0.636	128.1	130.7
13	0.678	111.3	119.4
19 (*6*)*	0.725	126.9	127.8
17 (*4*)	0.755	134.1	140.2
18 (*5*)	0.770	129.2	137.1
9 (*1*)	0.772	128.7	146.7
11 (*2*)	0.817	116.3	123.5
16 (*3*)	1.115	173.2	159.8

*The numbers appearing in parenthesis are the correspoding Margo() anomaly anomaly identified by Criteria A on this segment.

Table 4: Case study 1: Paintspotter car and three miles of track data. Anomaly amplitudes for Montjoli segment with Criteria B (0.5, 100%, 39)

Anomaly number	Anomaly Amplitude (inches p/p)	Peak bolster load (kips) at 60mph	Peak bolster load (kips) at 80mph
14	0.501	114.1	115.6
3	0.512	113.1	119.3
6	0.517	109.8	115.4
16	0.517	118.8	116.3
15	0.526	113.0	117.6
13	0.544	122.8	122.6
2	0.549	110.8	116.0
7	0.565	114.4	113.6
18	0.566	134.6	125.5
4	0.569	125.1	130.6
8	0.575	110.7	111.9
24	0.603	117.4	118.6
1	0.607	120.3	115.3
5	0.628	123.2	121.0
22	0.630	122.5	128.3
23	0.631	127.0	126.9
19	0.633	117.9	119.3
9	0.644	134.6	125.5
11	0.678	129.9	131.6
12	0.683	132.8	129.3
21 (*4*)	0.712	127.2	127.3
10 (*1*)	0.850	146.0	141.7
17 (*2*)	0.850	132.3	145.9
20 (*3*)	0.897	152.6	151.4

*The numbers appearing in parenthesis are the corresponding Montj() anomaly anomaly identified by Criteria A on this segment.

Table 5: Case study 2: Paintspotter car and 20 miles of track data using Criteria B (0.5, 100%, 39)

Anomaly number	Amplitude (inches p/p)	Peak bolster load (kips) at 60mph	Peak bolster load (kips) at 80mph
1	0.538	117.7	120.4
2	0.582	108.0	109.4
3	0.597	113.9	122.7
4	0.598	110.2	113.1
5	0.710	120.2	129.1
6	0.877	120.1	118.8

Table 6: Case study 3: Articulated flat car and 305 miles of track data. Outlier anomalies and peak load factors at 78, 60 and 40 mph.

Anomaly number	Amplitude (inches p/p)	Number of Peaks	Peak load ratio 78mph	Peak load ratio 60mph	Peak load ratio 40mph
1	0.548	3	1.27	1.21	1.18
2	0.585	3	1.26	1.21	1.17
3	0.569	3	1.30	1.19	1,18
4	0.591	4	1.32	1.34	1.22
5	0.564	4	1.32	1.29	1.17
6	0.599	5	1.32	1.28	1.24
7	0.582	6	1.29	1.26	1.18
8	0.604	5	1.24	1.27	1.19
9	0.661	5	1.26	1.23	1.19
10	0.640	6	1.35	1.32	1.20
11	0.630	7	1.37	1.29	1.19
12	0.604	7	1.28	1.33	1.20
13	0.651	8	1.28	1.27	1.18

Table 7: Case study 3: Articulated flat car and 305 miles of track data. Anomalies 1-28 of the 69 anomalies with amplitudes greater than 0.7 inch and peak load factors at 78 mph.
Anomalies with 1 or 2 peaks and amplitudes between 0.7 and 0.8 inch

Anomaly number	Amplitude (inches p/p)	Number of Peaks	Peak load ratio
1	0.753	1	1.32
2	0.749	1	1.38
3	0.749	1	1.42
4	0.779	1	1.46 (1.49)
5	0.757	1	1.41
6	0.752	1	1.36
7	0.765	1	1.31
8	0.788	1	1.42
9	0.743	1	1.43
10	0.787	1	1.22
11	0.781	1	1.39
12	0.715	1	1.31
13	0.727	1	1.37
14	0.748	1	1.48 (1.54)
15	0.752	1	1.39
16	0.703	1	1.25
17	0.702	1	1.35
18	0.785	1	1.36
19	0.725	1	1.40
20	0.706	1	1.41
21	0.763	1	1.39
22	0.792	1	1.46
23	0.704	1	1.39
24	0.767	1	1.41
25	0.760	2	1.36
26	0.727	2	1.28
27	0.730	2	1.44
28	0.758	2	1.29

Table 8: Case study 3: Articulated flat car and 305 miles of track data. Anomalies 29-43 of the 69 anomalies with amplitudes greater than 0.7 inch and peak load factors at 78 mph. And the eight additional anomalies extracted from the 2 peak, 0.8-0.9 inch group

Anomaly number	Amplitude (inches p/p)	Number of Peaks	Peak load ratio
29	0.825	1	1.41
30	0.839	1	1.31
31	0.853	1	1.36
32	0.829	1	1.39
33	0.818	1	1.27
34	0.843	1	1.37
35	0.860	1	1.26
36	0.803	1	1.46
37	0.842	1	1.44
38	0.833	1	1.31
39	**0.874**	**2**	**1.54**
40	0.854	2	1.31
41	**0.832**	**2**	**1.50**
42	0.838	2	1.40
43	**0.833**	**2**	**1.58**
E1	0.838	2	1.37
E2	**0.868**	**2**	**1.57**
E3	0.813	2	1.49
E4	0.853	2	1.31
E5	0.876	2	1.46
E6	0.869	2	1.27
E7	**0.896**	**2**	**1.53**
E8	**0.876**	**2**	**1.63**

Table 9: Case study 3: Articulated flat car and 305 miles of track data. Anomalies 44-69 of the 69 anomalies with amplitudes greater than 0.7 inch and peak load factors at 78 mph

Anomaly number	Amplitude (inches p/p)	Number of Peaks	Peak load ratio
44	0.937	1	1.39
45	0.952	1	1.45
46	0.981	1	1.28
47	0.919	1	1.47
48	**0.798**	**3**	**1.51**
49	0.795	3	1.37
50	0.825	4	1.33
51	0.925	2	1.29
52	0.925	2	1.44
53	0.943	2	1.32
54	0.978	2	1.41
55	**0.924**	**2**	**1.63**
56	0.954	3	1.40
57	0.970	4	1.30
58	0.988	4	1.47
59	**1.046**	**1**	**1.57**
60	1.000	1	1.48
61	**1.024**	**2**	**1.60**
62	1.056	2	1.44
63	1.034	2	1.41
64	1.019	3	1.43
65	**1.086**	**4**	**1.55**
66	1.006	5	1.44
67	**1.238**	**3**	**1.74**
68	**1.248**	**3**	**1.61**
69	1.355	6	1.44